공학박사학위논문

A study on the optical property and thermal stability of highly soluble dyes and their application on liquid crystal display color filters

액정 디스플레이 컬러필터용 고용해성 염료의 광학적 특성 및 열 안정성에 대한 연구

2014년 2월

서울대학교 대학원

재료공학부

최 준

A study on the optical property and thermal stability of highly soluble dyes and their application on liquid crystal display color filters

액정 디스플레이 컬러필터용 고용해성 염료의 광학적 특성 및 열안정성에 대한 연구

지도교수 김 재 필

이 논문을 공학박사학위논문으로 제출함

2014년 2월

서울대학교 대학원

재료공학부

최 준

최준의 박사학위논문을 인준함

2014년 2월

위 원 장 _____ (인)

부 위 원 장 _____ (인)

위 원 _____ (인)

위 원 _____ (인)

위 원 _____ (인)

Abstract

A study on the optical property and thermal stability of highly soluble dyes and their application on liquid crystal display color filters

Choi Jun

Department of Materials Science and Engineering

The Graduate School

Seoul National University

Liquid crystal display (LCD) modules are used widely in a variety of electronic displays, such as computers and TVs. Among the elements of LCD modules, the color filter, which converts the white backlight into red (R), green

(G) and blue (B) colored lights, is a vital component. Currently, the pigment dispersion method to form RGB patterned pixels using photo lithography has been adopted widely to produce color filters because color filters with superior stability can be achieved. It is also advantageous to scale up the panel size while maintaining its pixel uniformity. Although color filters produced by this method have good thermal and photo-chemical stability, they have low chromatic properties due to the aggregation behavior of pigment particles used as colorants. Dyes can be an attractive alternative to overcome this limitation due to the reduced light scattering because they are dissolved in the media and exist in molecular form. However, in order for the dyes to be applied successfully to an LCD manufacturing process, their low thermal stability needs to be improved. In this study, several series of dyes highly soluble to the industrial solvents were synthesized and then used to fabricate color filters by a spin-coating technique. The spectral and thermal properties of the dye-based color filters were investigated in comparison with those of pigment-based color filters. The optical and chromatic properties of some dye-based color filters were superior and their thermal stabilities were similar to those of the pigment-based color filters.

In order to improve the optical performance of red color filters, several perylene dyes were designed and synthesized. Among them, dyes with bulky

functional substituents at the bay and terminal positions were highly soluble in cyclohexanone, the industrial solvent currently used in the pigment dispersion method. The prepared color filters with these dyes exhibited superior spectral properties due to the smaller particle size of the dyes. However, their thermal stability varied with the dye structures, and only the dyes mono-substituted at the bay position had sufficient thermal stability.

In order to be used as high performance yellow compensating dyes, novel coronene derivatives were synthesized from *N,N'*-bis(2,6-diisopropylphenyl)-1,7-dibromo perylene-3,4,9,10-tetracarboxdiimide via a one-step reaction. The suggested synthetic route is the simplest and most economical among the methods to extend the aromatic systems along the short molecular axis of perylene. The synthesized molecules exhibited superior stability and color strength as yellow chromophores. They were characterized by significant hypsochromic shifts of the absorption compared to perylene tetracarboxdiimide and high fluorescence quantum yields.

In order to improve the optical performance of green color filters, several phthalocyanine dyes were designed and synthesized. The solubility, spectral properties, and thermal stability of the prepared six phthalocyanine dyes varied depending on their isomeric structures and core metals. They were dissolved in industrial solvent–binder composites and spin coated with yellow compensating

coronene dye into dye-based LCD color filters. The prepared color filters exhibited superior optical properties compared to conventional pigment-based ones due to the fluorescence of coronene dye and less light scattering resulting from the smaller particle size of the phthalocyanine dyes.

Three novel triazatetrabenzcorrole dyes were synthesized via a ring-contraction reaction to be applied as colorants for dye-based color filter and black matrix. The absorption peaks of the synthesized dyes showed a red-shifted Soret band and a blue-shifted Q-band compared to phthalocyanine dyes, and this can be extremely beneficial when applied for liquid crystal display color filter and black matrix. These dyes exhibited enhanced solubility in the industrial solvents by the introduction of bulky axial substituents. The spin-coated films prepared with these dyes exhibited superior optical and chromatic properties compared to the phthalocyanine-based or pigment-based ones for green color filter, even without the addition of a yellow compensating dye. In addition, they showed satisfactory dielectric properties for the black matrix of color filter on array mode.

Four novel yellow quinophthalone dyes were designed and synthesized in order to examine the influence of aggregation behavior on the optical and thermal properties of LCD color filters. When the synthesized dyes were spin-coated onto a glass substrate, re-aggregation or migration of the dye molecules

were shown in the field emission scanning electron microscopy images after the baking processes. These behaviors of dye molecules can be the main reason for the deterioration of the optical and thermal properties of dye-based color filters, but the degree of deterioration could be reduced by the modification of the dye structures.

KEYWORDS: LCD, Color filter, Black matrix, Photo lithography, Perylene dye, Coronene dye, Phthalocyanine dye, Triazatetrabenzcorrole dye, Quinophthalone dye, Transmittance, Color gamut, Contrast ratio, Thermal stability, Aggregation

Student Number: 2008-20692

Contents

perylene dyes for dye-based LCD color filters

Chapter 3

Facile synthesis and characterization of novel coronene chromophores and their application to LCD color filters

Chapter 4

Synthesis and Characterization of Thermally Stable Dyes with Improved Optical Properties for Dye-based LCD Color Filters

Chapter 5

Synthesis and Characterization of Novel Triazatetra

benzcorrole Dyes for LCD Color Filter and Black Matrix

Chapter 6
The Influence of Aggregation Behavior of Novel Quinophthalone Dyes on Optical and Thermal Properties of LCD Color Filters

List of Tables

List of Schemes

List of Figures

Figure 6.7 The change of the absorption peaks of dye-based color filters with increasing postbaking temperature.

Chapter 1

Introduction

1.1 Structure of LCD color filters

Displays are the most important media in this information age. Since the late 20th century, flat-panel displays have replaced the market share of CRTs (Cathode Ray Tubes) [1,2]. Among the flat-panel displays, LCDs, electronically modulated optical devices made up of many segments filled with liquid crystals and arrayed in front of a light source (backlight) to produce images in color, hold the greatest market share due to the many advantages such as low cost, low power consumption, and flexibility. The color filter, which converts the white backlight into red (R), green (G), and blue (B) colored lights, is the key component in the growth of display technology since it has the greatest potential to enhance picture quality [1,2]. The fundamental structures of LCD and LCD color filter are magnified in Figure 1.1 and 1.2. A color filter consists of glass substrate, black matrix, color filter layer (RGB colors), Indium Tin Oxide (ITO) film. The black matrix material is coated on clear substrate in the

optically inactive areas to prevent light leakage and provide a light shield for the amorphous silicon transistors. The black matrix material should have a low reflectance to optimize contrast ratio. Black matrix material should not interfere with the electrical signals of thin film transistor (TFT) to be applied for color filter on array (COA) mode that color filter is patterned right onto the TFT array. Therefore, extensive investigation is currently being performed on colorants with low dielectric constants such as dyes, so that they can replace the carbon black with high dielectric constant [3,4]. The RGB colors are fabricated which contain red, green, and blue colors from either dyes or pigments. After the color layer is formed, protection overcoat layer is deposited. The purpose of overcoat layer is the reduction of color pattern's thickness variation, durability against sputtering, and chemical resistance. A column spacer is a material used to maintain a uniform cell gap between the TFT and the color filter glass.

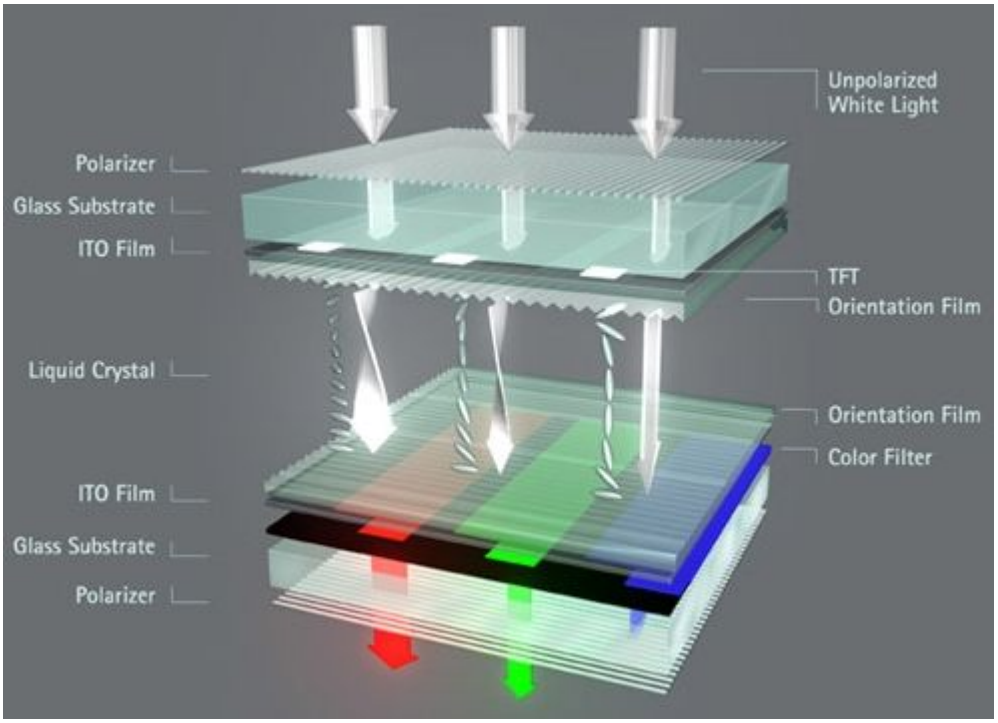

Figure 1.1 Basic structure of liquid crystal display (LCD).

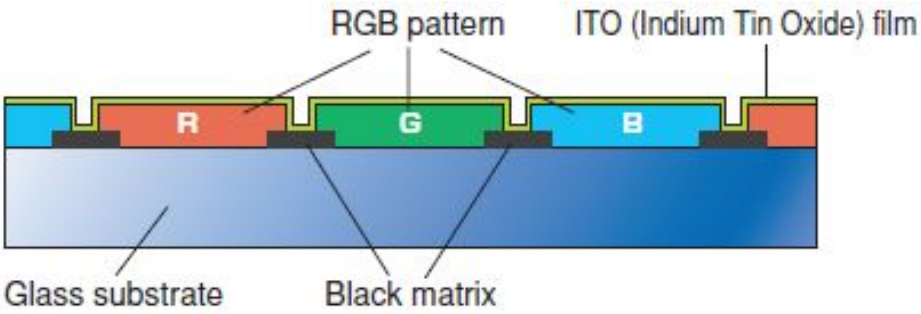

Figure 1.2 Basic structure of LCD color filter.

1.2 Manufacturing of LCD color filters

1.2.1 Color photo-resist (PR)

A photo-resist (PR) is a light-sensitive material used in several industrial processes, such as photolithography and photoengraving to form a patterned coating on a surface. Photo-resist are classified into two groups: positive and negative-tone resists.

- ✓ A positive-tone photo-resist is a type of photo-resist in which the portion of the photo-resist that is exposed to light becomes soluble to the photo-resist developer. The portion of the photo-resist that is unexposed remains insoluble to the photo-resist developer.
- ✓ A negative-tone photo-resist is a type of photo-resist in which the portion of the photo-resist that is exposed to light becomes insoluble to the photo-resist developer. The portion of the photo-resist that is unexposed dissolved by the photo-resist developer.

The color photo-resist is negative-tone photo-resist which is made up of coloring material, dispersant, photo-sensitive binder, multi-functional monomer, photo-initiator, and additives such as leveling agent and coupling agent.

Colorant system is consisted of pigment and dispersant which is pigment-derivative dispersant. In particular, considering of spectral property, chromaticity and stability, the colorants are limited to eleven pigments as shown in Table 1.1.

Table 1.1 Conventional colorants for LCD color filters.

Color	Color Index Number	Structure
Red	C.I. Pigment Red 177	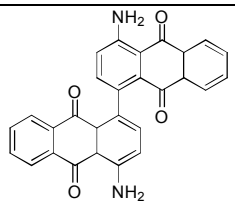
	C.I. Pigment Red 254	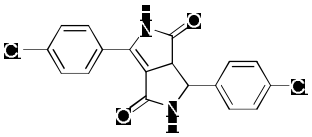
Green	C.I. Pigment Green 7	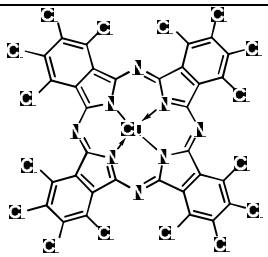

	C.I. Pigment Green 36	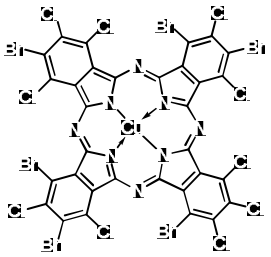
	C.I. Pigment Green 58	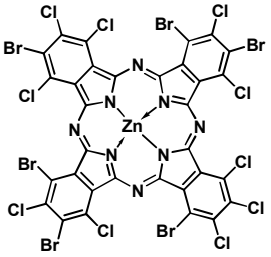
Blue	C.I. Pigment Blue 15:6	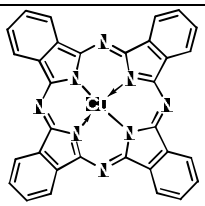
	C.I. Pigment Blue 60	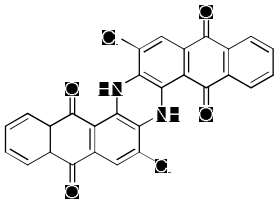
Violet	C.I. Pigment Violet 23	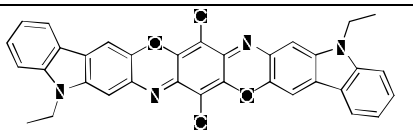

Yellow	C.I. Pigment Yellow 138	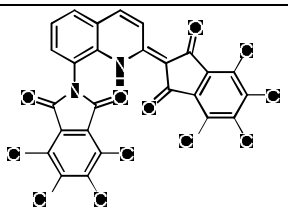
	C.I. Pigment Yellow 139	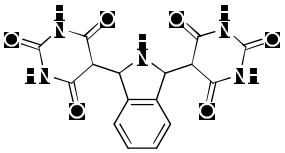
	C.I. Pigment Yellow 150	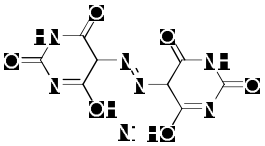

1.2.2 Fabrication of RGB color pattern

The fabrication process of color filters is following photolithographic method using color photo-resist as shown in Figure 1.3 [1,2].

1. Black matrix formation;

A black matrix is formed first in order to prevent any leakage of backlight and the RGB color mixture.

2. Color resist coating;

Color photo-resist is coated on the entire glass substrate.

3. Exposure;

To make the pattern insoluble, it is UV cured by exposure through a photo-mask.

4. Development & baking;

After the removal of unnecessary portions of the color resist by the developing solution, the pattern is cured through baking. The above processes from step 2 to 4 are repeated three times (for RGB).

5. ITO film formation;

ITO film (transparent conductive film) is formed by the spattering method.

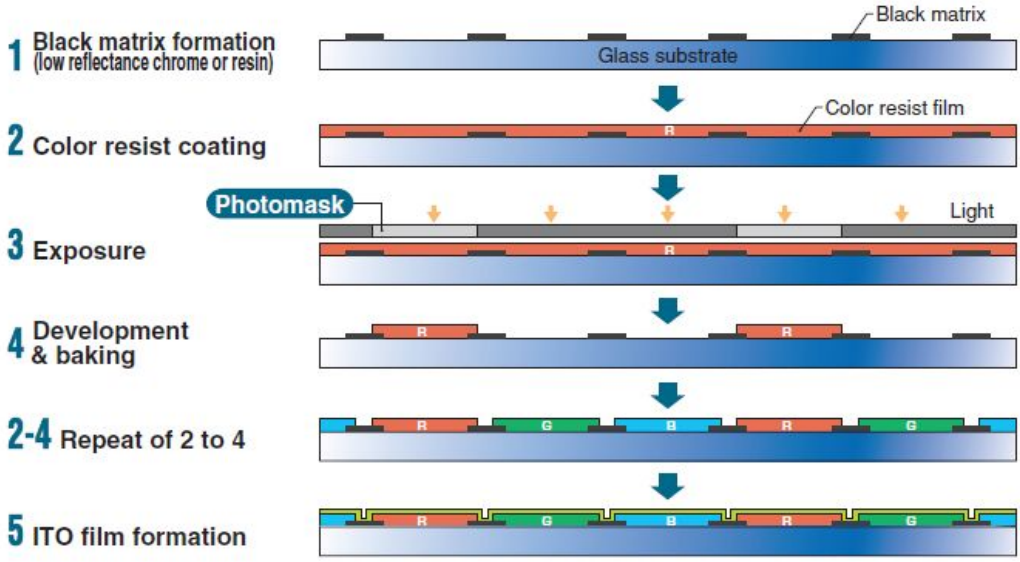

Figure 1.3 Color filter manufacturing process by the photolithographic method.

1.3 Requirements of color filters

1.3.1 High color purity and high transmittance

In order to have both high quality color picture and brightness in TV, laptop and monitor, the LCD panel is required to have high color purity and high transmittance. Therefore, the selection of the colorants such as pigments and dyes should be based on sharp spectrum eliminating unnecessary wavelengths and retaining only the necessary light [5-7]. Besides, the surface roughness of

colored pattern caused by pigments can affect the color characteristics of the filter. The roughness is produced by the pigment particles lying on the surface of the coloring layer. The surface of a colored pattern becomes cloudy and thereby decreases the transmittance [8,9]. This drawback can be controlled by adding leveling agents or optimizing conditions of manufacturing process such as soft-bake and development.

1.3.2 High contrast

The color filter contrast is defined as the ratio of transmissive light intensity of setting two polarizers parallel to intensity of setting them across, setting the color filter between two polarizer sheets. High contrast characteristic is necessary for high color purity and good legibility [5]. The depolarization effect is the most important optical characteristics of the color filter. It occurs when the light linearly polarized by passing through a polarizer plate is disturbed in the film due to the scattering and birefringence of pigment particles. It causes a reduction in the contrast ratio. The low contrast ratio of the film may cause a serious problem with active matrix liquid crystal displays (AMLED). This problem can be overcome by decreasing the particle size and improving the stability of dispersion.

1.3.3 Low reflection

Reflectivity of TFT-LCD module is mainly determined by black matrix material on color filter. Chromium, chrome oxide or black resins have been widely used for STN-LCD and TFT-LCD because of light shielding ability and low reflection. High resistivity, high optical density (OD), high light shielding, high resolution, low reflectance and low cost black matrix is preferred for LCD applications.

1.3.4 High stability against heat, light and chemical

The color filters must exhibit high heat resistance without thermal flow and chromatic changes during the alignment layer formation step. The chromatic changes (ΔE_{ab}) should be less than 3 after heating at 250°C for 1 h [8,9]. The light stability of the pixels is important because these pixels are illuminated with back light of LCDs. The color filters are exposed to a mercury-xenon lamp with ultraviolet (UV) filter for more than two million lux hours. The chromatic changes (ΔE_{ab}) after exposure should be less than 3 [1,2]. The chemical stability is a key factor since color filters are exposed to solvents, acids, and bases

during the LCD fabrication process. The cured film must be resistant towards alignment layer solvents such as NMP and γ-butyrolactone, towards acids during etching of the ITO or towards bases used in the development system [1,2].

1.4 Previous researches and research purpose

The color filter, which converts the white backlight into red (R), green (G), and blue (B) colored lights, is the key component in the growth of display technology since it has the greatest potential to enhance picture quality. Only 6.3% of the backlight can pass through the whole panel, which includes a polarizing filter, TFT-array, LC cell, and color filter. In particular, the transmittance through the color filter is the lowest (30%). Therefore, developing high transmittance color filters is essential for saving energy consumption as well as improving picture-quality of displays. Currently, the pigment dispersion method to form RGB patterned pixels using photolithography has been widely adopted to produce color filters because color filters with superior stability can be achieved [10]. It is also advantageous to scale up the panel size while maintaining its pixel uniformity. Although color filters produced by this method have good thermal and photo-chemical stability, they have low chromatic

properties due to the aggregation behavior of pigment particles used as colorants [11].

In a previous report of our research group (Prof. J.P. Kim group), water soluble dyes were successfully applied to ink-jetted color filters [12,13], but researches on Ink-jet printing method are not active nowadays because of the difficulty in scale up and low pixel uniformity. Therefore, the investigation on changing colorant materials in the photolithography process is necessary for high performance LCD color filters. Dyes can be attractive alternatives to overcome chromatic limitation due to the reduced light scattering resulting from the fact that they are dissolved in the media and exist in molecular form. However, in order for the dyes to be applied successfully to the LCD manufacturing process, their low thermal stability needs to be improved [6]. Moreover, they should be highly soluble in industrial solvents and have sharp absorption peaks for superior optical properties.

In this study, various series of red, yellow, and green thermally stable dyes with high solubility were designed and synthesized. Their characteristics were investigated and some of them were successfully applied to the dye-based color filter pixels. In particular, a series of triazatetrabenzcorrole dyes were applied to the LCD color filter system without compensating dye and also applied to the LCD black matrix.

Although the aggregation tendency of dyes is much lower than that of the pigments, it can be the main reason for the deterioration of the optical properties of color filters. There was a previous research on the relationship between the dye aggregation and their spectral properties [14]. In this study, the influence of aggregation behavior of dyes on optical and thermal properties of LCD color filters was investigated.

1.5 References

[1] Tsuda K. Color filters for LCDs. Displays 1993;14:115-24.

[2] Sabnis RW. Color filter technology for liquid crystal displays. Displays 1999;20:119-29.

[3] Tani M, Ito S, Sakagawa M, Sugiura T. A photoresist for black matrix on TFT arrays. Soc Inform Display Dig 1997;28:969-72.

[4] Hirayama H, Hidaka K, Imai N, Ibaraki N. Integrated black matrix on TFT arrays composed on newly developed Bi-SiOx ceramic thin film. Soc Inform Display Dig 1997;28:180-3.

[5] Yeh P, Gu C. Optics of liquid crystal displays. New York: John Wiley & Sons, Inc.; 1999 p. 198-272.

[6] Sugiura T. Dyed color filters for liquid-crystal displays. Journal of the SID

1993;1:177-180.

[7] Kim YD, Kim JP, Kwon OS, Cho IH. The synthesis and application of thermally stable dyes for ink-jet printed LCD color filters. Dyes Pigm 2009;81:45-52.

[8] Choi J, Sakong C, Choi JH, Yoon C, Kim JP. Synthesis and characterization of some perylene dyes for dye-based LCD color filters. Dyes Pigm 2011;90:82-88.

[9] Sakong C, Kim YD, Choi JH, Yoon C, Kim JP. The synthesis of thermally-stable red dyes for LCD color filters and analysis of their aggregation and spectral properties. Dyes Pigm 2011;88:166-173.

[10] Takanori K, Yuki N, Yuko N, Hidemasa Y, Kang WB, Pawlowski PG. Polymer optimization of pigmented photoresists for color filter production. Jpn J Appl Phys 1998;37:1010-6.

[11] Na DY, Jung IB, Nam SY, Yoo CW, Choi YJ. The rheological behavior and dispersion properties of millbase for LCD colorfilters. J Korean Inst Electr Electron Mater Eng 2007;20:450-5.

[12] Kim YD, Kim JP, Kwon OS, Cho IH. The synthesis and application of thermally stable dyes for ink-jet printed LCD color filters. Dyes Pigm 2009;81:45-52.

[13] Kim YD, Cho JH, Park CR, Choi JH, Yoon C, Kim JP. Synthesis,

application and investigation of structure–thermal stability relationships of thermally stable water-soluble azo naphthalene dyes for LCD red color filters. Dyes Pigm 2011;89:1-8.

[14] Sakong C, Kim YD, Choi JH, Yoon C, Kim JP. The synthesis of thermally-stable red dyes for LCD color filters and analysis of their aggregation and spectral properties. Dyes Pigm 2011;88:166-73.

Chapter 2

Synthesis and characterization of some perylene dyes for dye-based LCD color filters

2.1 Introduction

Liquid crystal display (LCD) modules are used widely in a variety of electronic displays, such as computers and TVs. Among the elements of LCD modules, the color filter, which converts the white backlight into red (R), green (G) and blue (B) colored lights, is a vital component **[1,2]**.

Currently, the pigment dispersion method to form RGB patterned pixels using photo lithography has been adopted widely to produce color filters because color filters with superior stability can be achieved **[3]**. It is also advantageous to scale up the panel size while maintaining its pixel uniformity. Although color filters produced by this method have good thermal and photo-chemical stability, they have low chromatic properties due to the aggregation behavior of pigment particles used as colorants **[4]**. Dyes can be an attractive alternative to overcome this limitation due to the reduced light scattering

because they are dissolved in the media and exist in molecular form. However, in order for the dyes to be applied successfully to a LCD manufacturing process, their low thermal stability needs to be improved **[5]**.

In a previous report **[6]**, water soluble dyes were applied to ink-jetted color filters, but there are few reports on the application of dyes on the currently used photo lithography process.

In this study, a range of highly soluble red perylene dyes were designed and synthesized for dye-based LCD color filters. Perylene-3,4,9,10-tetracarboxylic diimide derivatives show excellent thermal stability originating from their very high resonance stabilization energy **[7]** and π-π interactions due to the planar molecular structure **[8,9]**. In addition, they have very strong and sharp absorption at approximately 530 nm **[10]**. However, they have low solubility in common industrial solvents, such as cyclohexanone, which limits their applications **[11]**. In this study, the solubility of the dyes was increased by substituting various bulky functional groups at the bay and terminal positions. The absorbance, solubility and thermal stability of the dyes substituted at one or both of the bay positions were examined and compared. Dye-based color filters were fabricated using both type of dyes, and their chromatic properties and thermal stability were analyzed.

2.2 Experimental

2.2.1 Materials and instrumentation

Perylene-3,4,9,10-tetracarboxylic dianhydride, 2,6diisopropylaniline, m-cresol, iodine, sulfuric acid, bromine, acetic acid, potassium carbonate anhydrous, phenol, 4-tert-butylphenol, and 4-tert-octylphenol purchased from Sigma Aldrich, and isoquinoline purchased from TCI were used as received. All the other reagents and solvents were of reagent-grade quality and obtained from commercial suppliers. Transparent glass substrates were provided by Paul Marienfeld GmbH & Co. KG. Commercial pigment-based color filter and acrylic binder LC20160 were supplied by SAMSUNG Cheil industries Inc. ^{1}H-NMR spectra were recorded on a Bruker Avance 500 spectrometer at 500 MHz using chloroform-d and TMS, as the solvent and internal standard, respectively. Matrix Assisted Laser Desorption/Ionization Time Of Flight (MALDI-TOF) mass spectra were collected on a Voyager-DE STR Biospectrometry Workstation with a-cyano-4-hydroxy-cynamic acid (CHCA) as the matrix. Absorption and transmittance spectra were measured using a HP 8452A spectrophotometer. Chromatic characteristics of the color filters were analyzed on a Scinco color spectrophotometer. Thermogravimetric analysis (TGA) was

conducted under nitrogen at a heating rate of 10 °C min^{-1} using a TA Instruments Thermogravimetric Analyzer 2050. The thickness of the color filters was measured using a Nano System Nanoview E-1000.

2.2.2 Synthesis

The dyes **2, 4a, 4b, 6a, 6b** are already known structures, and we have modified and detailed the synthesis of them in this paper. The dyes **5a, 5b, 5c** are new structures.

2.2.2.1 N,N'-Bis(2,6-diisopropylphenyl)-perylene-3,4,9,10-tetracarboxydiimide (2)

A mixture of perylene-3,4,9,10-tetracarboxylic dianhydride (3.92 g, 0.01 mol), 2,6 diisopropylaniline (5.65 ml, 0.03mol), m-cresol (60 ml) and isoquinoline (6 ml) was stirred at 50 °C for 2 h. The temperature of the mixture was raised to 200 °C and kept for 12 h. The warm solution was poured into 60 ml of acetone, and the precipitate was filtered out. The collected solution was poured into 1200 ml of n-Hexane and temperature of the mixture solution was dropped to 0~5 °C and kept for 24 h. The precipitate was filtered out and dried

at 80 °C under vacuum. The crude product was purified by column chromatography on silica gel using CH_2Cl_2/MeOH (40:1) as the eluent to obtain **2** as red solid.

Yield 56.4% ; ^{1}H NMR (CDCl3, ppm) : 8.80 (d, 4H), 8.75 (d, 4H), 7.50 (t, 2H), 7.36 (d, 4H), 2.75 (septet, 4H), 1.19 (d, 24H) ; MALDI-TOF MS : m/z 712.10 (100%, $[M+2K]^+$).

2.2.2.2 N,N'-Bis(2,6-diisopropylphenyl)-1,7-dibromoperylene-3,4,9,10-tetracarboxy diimide (4b)

Perylene-3,4,9,10-tetracarboxylic dianhydride (16.0 g, 40.7 mmol), iodine (0.39 g, 1.52 mmol), and sulfuric acid (98%, 225 ml) were mixed and stirred for 2 h at room temperature. The reaction temperature was set at 80 °C, and bromine (3.58 ml, 70 mmol) was added dropwise over 2h. The mixture was reacted further at 80 °C for 16 h, cooled to room temperature, and the excess bromine gas was displaced by nitrogen gas. The precipitate obtained after adding ice-water to the mixture was collected by suction filtration. The precipitate was washed with water several times until the aqueous layer became neutral to yield dibromo dianhydride as crude product. The crude product was then dried at 100 °C under reduced pressure and used for the next step without

further purification.

The crude 1,7-dibromoperylene-3,4,9,10-tetracarboxylic dianhydride (8.0 g, 14.5 mmol), 2,6-diisopropylaniline (8.8 ml, 46.7 mmol), and acetic acid (4.6 ml) were mixed and heated at 120 °C in N-Methyl-2-pyrrolidone (NMP) (100ml) under the nitrogen atmosphere for 96 h. The precipitate obtained after adding water to the mixture was collected by suction filtration. The crude product was washed with water, dried, and purified by column chromatography on silica gel using CH_2Cl_2 as the eluent. The band containing tribrominated diimide could be separated firstly. Then, the second band containing a mixture of dibrominated isomeric diimides was collected. The mixture was washed with EtOH and toluene and heated at 80 °C for 12 h in toluene (50ml). The pure diimide, red compound **4b**, was recrystallized from the hot toluene solution **[12]**. Yield 42.8% ; ^{1}H NMR ($CDCl_3$, ppm) : 9.56 (d, 2H), 9.01 (d, 2H), 8.80 (d, 2H), 7.52 (t, 2H), 7.36 (d, 4H), 2.74 (septet, 4H), 1.18 (d, 24H) ; MALDI-TOF MS : m/z 869.83 (100%, $[M+2K]^+$).

2.2.2.3 N,N'-Bis(2,6-diisopropylphenyl)-1-bromoperylene-3,4,9,10-tetracarboxy diimide (4a)

4a could be separated by column chromatography from the same crude

product of **4b**. After obtaining a mixture of dibrominated isomeric diimides, **4a** was obtained as the third eluted compound. The product **4a** was used for the next step without further purification because there was no isomer.

Yield 36.7% ; ^{1}H NMR ($CDCl_3$, ppm) : 9.85 (d, 1H), 9.03 (s, 1H), 8.80 (m, 3H), 8.72 (d, 1H), 8.71 (d, 1H), 7.51 (t, 2H), 7.36 (d, 4H), 2.76 (septet, 4H), 1.18 (d, 24H) ; MALDI-TOF MS : m/z 790.96 (100%, $[M+2K]^+$).

2.2.2.4 N,N'-Bis(2,6-diisopropylphenyl)-1-phenoxy-perylene-3,4,9,10-tetracarboxy diimide (5a)

5a (1 g, 1.27 mmol) was mixed with potassium carbonate anhydrous (0.7 g), phenol (0.14 g, 1.50 mmol), and NMP (70ml). The mixture was heated to 120 °C under argon and was stirred at this temperature for 24 h. The reaction mixture was cooled to room temperature and poured into 5% HCl (250ml). The precipitate was filtered, repeatedly washed with water, and dried in a vacuum at 70 °C. The crude product was purified by column chromatography on silica gel using CH_2Cl_2 as the eluent to obtain **5a** as red solid.

Yield 85.8% ; ^{1}H NMR ($CDCl_3$, ppm) : 9.65 (d, 1H), 8.81 (m, 2H), 8.75 (m, 3H), 8.40 (s, 1H), 7.47 (m, 4H), 7.33 (m, 4H), 7.26 (t, 1H), 7.19 (d, 2H), 2.73 (septet, 4H), 1.16 (d, 24H) ; MALDI-TOF MS : m/z 804.37 (100%, $[M+2K]^+$).

2.2.2.5 N,N'-Bis(2,6-diisopropylphenyl)-1-p-tert-butylphenoxy-perylene-3,4,9,10-tetracarboxydiimide (5b)

5b was synthesized in the same manner with **5a** using **4a** (1 g, 1.27 mmol), potassium carbonate anhydrous (0.7 g), and 4-tert-butylphenol (0.23 g, 1.50 mmol).

Yield 86.1% ; ^{1}H NMR ($CDCl_3$, ppm) : 9.68 (d, 1H), 8.82 (m, 2H), 8.75 (m, 3H), 8.42 (s, 1H), 7.48 (m, 4H), 7.33 (m, 4H), 7.13 (d, 2H), 2.74 (septet, 4H), 1.36 (s, 9H), 1.16 (d, 24H) ; MALDI-TOF MS : m/z 860.28 (100%, $[M+2K]^{+}$).

2.2.2.6 N,N'-Bis(2,6-diisopropylphenyl)-1-p-tert-octylphenoxy-perylene-3,4,9,10-tetracarboxydiimide (5c)

5c was synthesized in the same manner with **5a** using **4a** (1 g, 1.27 mmol), potassium carbonate anhydrous (0.7 g), and 4-tert-octylphenol (0.31 g, 1.50 mmol).

Yield 87.8% ; ^{1}H NMR ($CDCl_3$, ppm) : 9.68 (d, 1H), 8.81 (m, 2H), 8.75 (m, 3H), 8.39 (s, 1H), 7.46 (m, 4H), 7.34 (m, 4H), 7.11 (d, 2H), 2.73 (septet, 4H), 1.75 (s, 2H), 1.40 (s, 6H), 1.16 (d, 24H), 0.75 (s, 9H) ; MALDI-TOF MS : m/z

916.31 (100%, $[M+2K]^+$).

2.2.2.7 N,N'-Bis(2,6-diisopropylphenyl)-1,7-dilphenoxy-perylene-3,4,9,10-tetracarboxydiimide (6a)

6a was synthesized in the same manner with **5a** using **4b** (1 g, 1.15 mmol), potassium carbonate anhydrous (0.7 g), and phenol (0.24 g, 2.50 mmol).
Yield 83.1% ; ^{1}H NMR ($CDCl_3$, ppm) : 9.64 (d, 2H), 8.70 (d, 2H), 8.43 (s, 2H), 7.46 (m, 6H), 7.31 (d, 4H), 7.24 (t, 2H), 7.18 (d, 4H), 2.70 (septet, 4H), 1.14 (d, 24H) ; MALDI-TOF MS : m/z 896.31 (100%, $[M+2K]^+$).

2.2.2.8 N,N'-Bis(2,6-diisopropylphenyl)-1,7-bis(p-tert-butylphenoxy)-perylene-3,4,9,10-tetracarboxydiimide (6b)

6b was synthesized in the same manner with **6a** using **4b** (1 g, 1.15 mmol), potassium carbonate anhydrous (0.7 g), and 4-tert-butylphenol (0.38 g, 2.50 mmol).
Yield 81.9% ; ^{1}H NMR ($CDCl_3$, ppm) : 9.66 (d, 2H), 8.71 (d, 2H), 8.45 (s, 2H), 7.46 (m, 6H), 7.31 (d, 4H), 7.12 (d, 4H), 2.71 (septet, 4H), 1.35 (s, 18H), 1.15 (d, 24H) ; MALDI-TOF MS : m/z 1008.49 (100%, $[M+2K]^+$).

2.2.3 Preparation of dye-based inks and color filters

The red ink for a color filter was composed of the dye (0.1g), cyclohexanone (3.2g), and LC20160 (1.4g) as a binder based on acrylate.

The prepared dye-based inks were coated on a transparent glass substrate using a MIDAS System SPIN-1200D spin coater. The coating speed was initially 100 rpm for 5 s, which was then increased to 300 rpm and kept constant for 20 s. The wet dye-coated color filters were then dried at 80 °C for 20 min, prebaked at 150 °C for 10 min, and postbaked at 230 °C for 1h. After each step, the coordinate values of the color filters were measured. All spin coated dye-based color filters were 1.6μm thick.

2.2.4 Investigation of solubility

The solubility of the synthesized dyes in CH_2Cl_2 and cyclohexanone were examined to determine the effects of substituents at the bay and terminal positions. The prepared dyes were added to the solvents at various concentrations, and the solutions were sonicated for 5 min using an ultrasonic cleaner ME6500E. The solutions were left to stand for 48 h at room temperature,

and checked for precipitation to determine the solubility of the dyes.

2.2.5 Measurement of spectral and chromatic properties

Absorption spectra of the synthesized dyes and the transmittance spectra of pigment-based and dye-based color filters were measured using a UV-vis spectrophotometer. The chromatic values were recorded on a color spectrophotometer (Scinco colormate).

2.2.6 Measurement of thermal stability

The thermal stability of the synthesized dyes was evaluated by thermogravimetry (TGA). The prepared dyes were heated to 110 °C and held at that temperature for 10 min to remove the residual water and solvents. The dye was then, heated to 220 °C and held at that temperature for 30 min to simulate the processing thermal conditions of color filter manufacturing. The dyes were finally heated to 400 °C to determine their degradation temperature. The heating was carried out at the rate of 10 °C min^{-1} under nitrogen atmosphere **[6, 13]**.

To check the thermal stability of the dyes in color filters, the fabricated

color filters were heated to 230 ℃ for 1 h in a forced convection oven (OF-02GW Jeiotech Co., Ltd.). The color difference values (ΔE_{ab}) before and after heating were measured on a color spectrophotometer (Scinco colormate) in CIE L*a*b* mode.

2.2.7 Geometry optimization of the synthesized dyes

The difference of thermal stability due to the structural differences in the dyes were analyzed by optimizing the dye structures using the Gaussian 03 program, and examining the core twist angles that affect the intermolecular interaction. The optimized geometries of the dye structures were calculated at the B3LYP/6-31G* level.

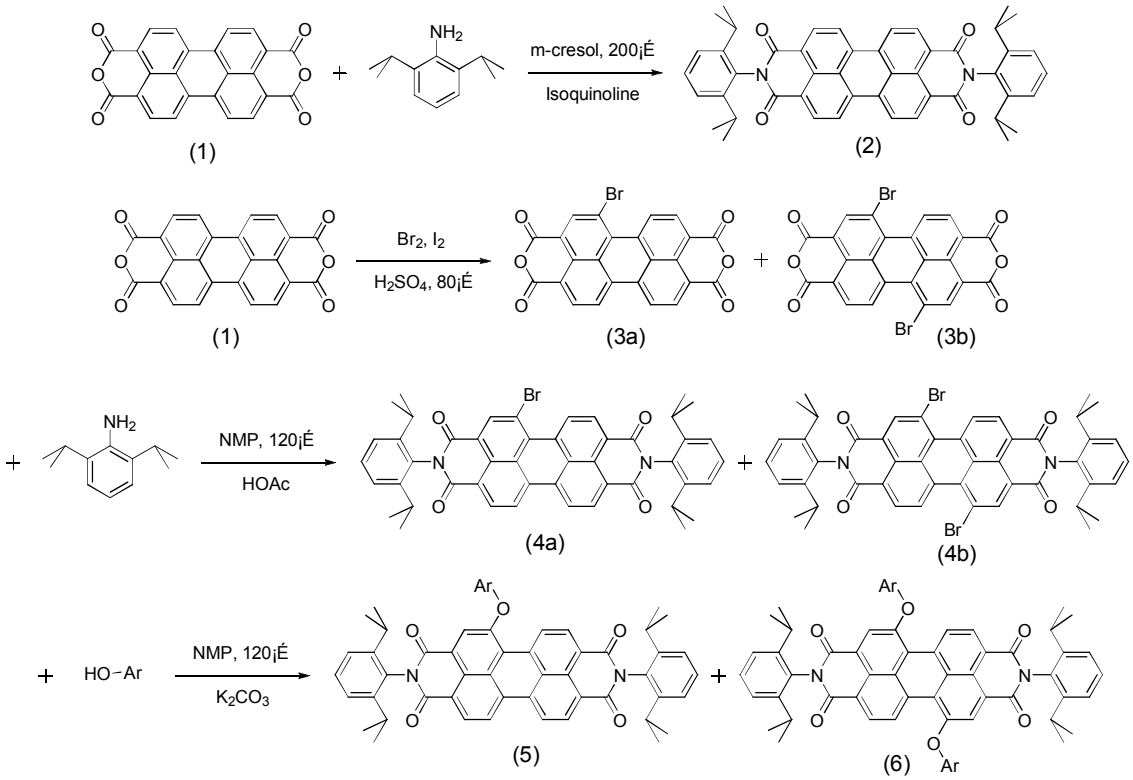

5a : Ar = phenyl

5b : Ar = 4-tert-butyl phenyl

5c : Ar = 4-tert-octyl phenyl

6a : Ar = phenyl

6b : Ar = 4-tert-butyl phenyl

Scheme 2.1 Synthesis of perylene dyes.

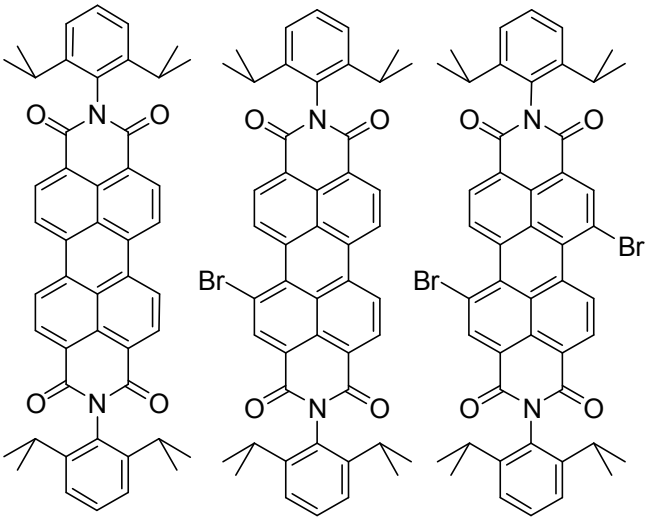

2 **4a** **4b**

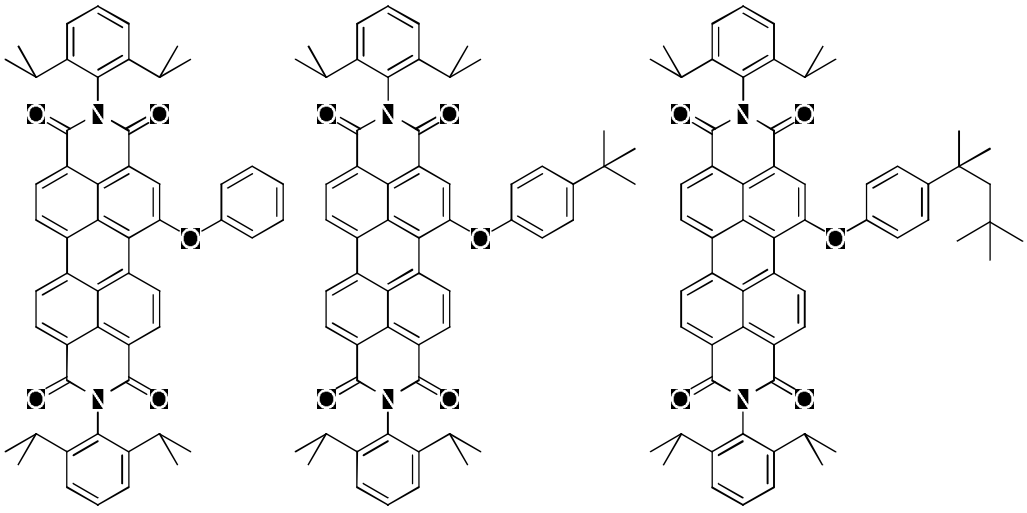

5a **5b** **5c**

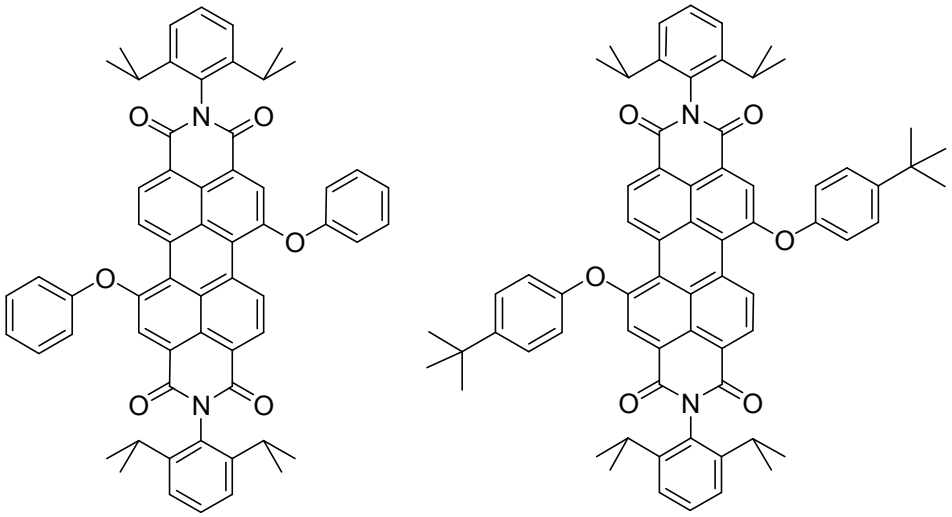

6a **6b**

Figure 2.1 Synthesized dyes.

2.3. Results and discussion

2.3.1. Design concept of dyes

The steric restriction caused by the imidization of bulky aryl groups at the terminal positions of Perylene-3,4,9,10-tetracarboxylic dianhydride decreases the crystal packing density of the dyes, which in turn increases their solubility **[14]**. In particular, *ortho*-alkyl-substituted aromatics maximize this effect.

However, substitution at the terminal position does not affect the UV-Vis absorption spectra significantly because the conjugation nodes along the long axis of the molecule limit the electronic interactions between the main body of the molecule and corresponding substituents **[15,16]**.

Although the solubility of dye **2** in common organic solvents, such as CH_2Cl_2, was increased significantly, it was not soluble enough in industrial solvents, such as cyclohexanone, to be suitable as a color filter. (Table 2.1) Additional bulky substituents were introduced at their bay positions to further improve their solubility. The solubility was increased remarkably when the bulky aryl groups were substituted at the bay positions because they deviated from the plane of the molecule and the planarity of the main body was broken **[14]**.

The introduction of substituents at the bay positions was demonstrated to alter the UV-Vis absorption spectra of dyes significantly **[17]**. Substituents with an ether linkage group were chosen to minimize the bathochromic shift in the absorption spectra and have high affinity with industrial solvents. In particular, phenoxy substituents were considered to be superior to alkoxy ones due to the lower bathochromic shift **[18]** and greater steric hindrance for high solubility.

2.3.2 Solubility of dyes

The dyes need to be dissolved in industrial solvents to a concentration of at least 4~5wt% to be suitable for LCD color filters. Table 2.1 lists the solubility data of the four representative dyes. Without the appropriate modification of the molecular structure, perylene derivatives have low solubility due to the planar structure, which facilitates the formation of crystals with high lattice energy **[14]**.

The solubility of dye **2** in CH_2Cl_2 was significantly higher than Perylene-3,4,9,10-tetracarboxylic dianhydride due to the terminal bulky aryl groups that rotate 90° out of the plane of the molecule. However, the solubility of dye **2** in cyclohexanone was still very low. The molecular structure of dye **4b** is no longer planar due to the presence of Br atoms at the bay positions, which in turn decrease the crystal packing density **[19]**. Therefore, the solubility of dye **4b** in CH_2Cl_2 and cyclohexanone was higher than that of dye 1 but was still insufficient for use in LCD color filters.

There were significant improvements in the solubility of dye **5b** and **6b** when the Br atoms were replaced with bulky phenoxy substituents that induce further twisting of the two naphthalene subunits in the perylene core **[20]**. The core twisting effect of the mono-substituted dye was less than 1,7-di(substituted) dye (Figure 2.7). Consequently, dye **5b** would have higher

crystallinity than dye **6b**, but the asymmetric molecular structure of dye **5b** could offset this effect. Therefore, the solubility of both dyes was similar in both solvents and sufficient for use in LCD color filters. In particular, their high solubility in cyclohexanone was attributed to the affinity between the ether linkage of the dyes and solvent molecules.

Table 2.1 Solubility of the dyes at 20 °C.

	2	**4b**	**5b**	**6b**
CH_2Cl_2	+	++	+++	+++
Cyclo hexanone	-	+	+++	+++

+++ : $5.0 \times 10^4 \sim 1.0 \times 10^5$ mg litre^{-1}

++ : $5.0 \times 10^3 \sim 5.0 \times 10^4$ mg litre^{-1}

+ : $5.0 \times 10^2 \sim 5.0 \times 10^3$ mg litre^{-1}

- : $< 5.0 \times 10^2$ mg litre^{-1}

2.3.3 Spectral and chromatic properties of dyes and dye-based color filters

Fig. 2.2 and Table 2.2 shows the absorption spectra of dyes **5** and **6** in CH_2Cl_2. To apply a dye to LCD red color filters, the dye needs to have a strong and sharp absorption maximum in the 525~550 nm range. The absorption maxima of the above dyes with various phenoxy substituents at the bay positions were slightly bathochromic compared to Perylene-3,4,9,10-tetracarboxylic dianhydride (λ_{max} = 526 nm) due to the electron donating effect of the substituents **[21]**. The bathochromic shifts in the mono-substituted dyes (**5a~c**) were less than those of 1,7-di(substituted) dyes (**6a~b**) because such an effect of substituents diminishes. As can be seen from the spectral data of **5a~c** and **6a~c**, the bulkier alkyl group at the *para* position produces a larger red-shift in λ_{max} due to the increse in donating power.

The above dyes show spectral-broadening compared to Perylene-3,4,9,10-tetracarboxylic dianhydride but still have satisfactory spectral sharpness for use in LCD color filters. This spectral-broadening was attributed to the increase in conjugation between the substituents and perylene core, as well as to twisting of the perylene core by the substituents **[12]**.

The molar extinction coefficients of the synthesized dyes were quite high and varied with the dye structure. Therefore, the dye-based color filters could have higher tinctorial strength compared to the pigment-based one with considerably lower dye content. The molar extinction coefficients of the mono-

substituted dyes were higher than the 1,7-di(substituted) dyes because their structural planarity was less distorted. However, the molar extinction coefficient of dye **5c** was lower than that of dyes **6a** and **6b**, probably due to the steric effect of the tert-octyl group.

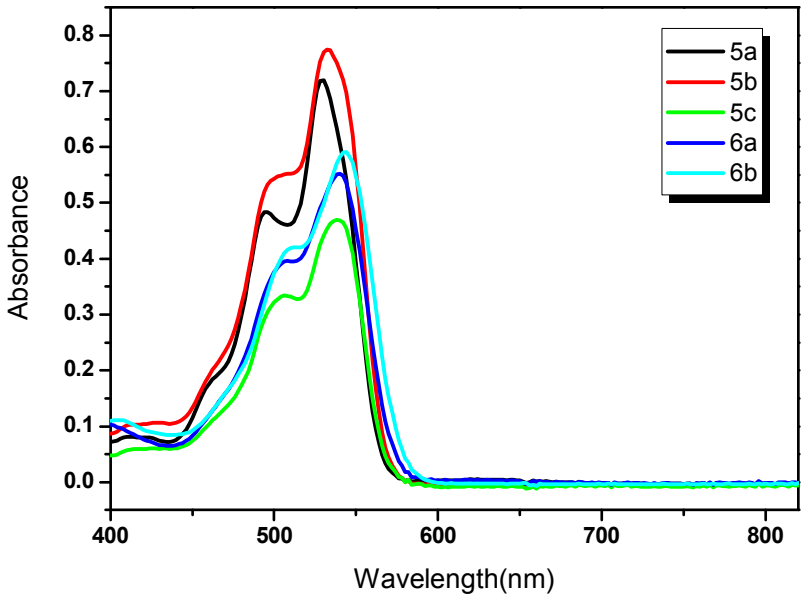

Figure 2.2 Absorption spectra in CH_2Cl_2 (10^{-5}mol liter^{-1}).

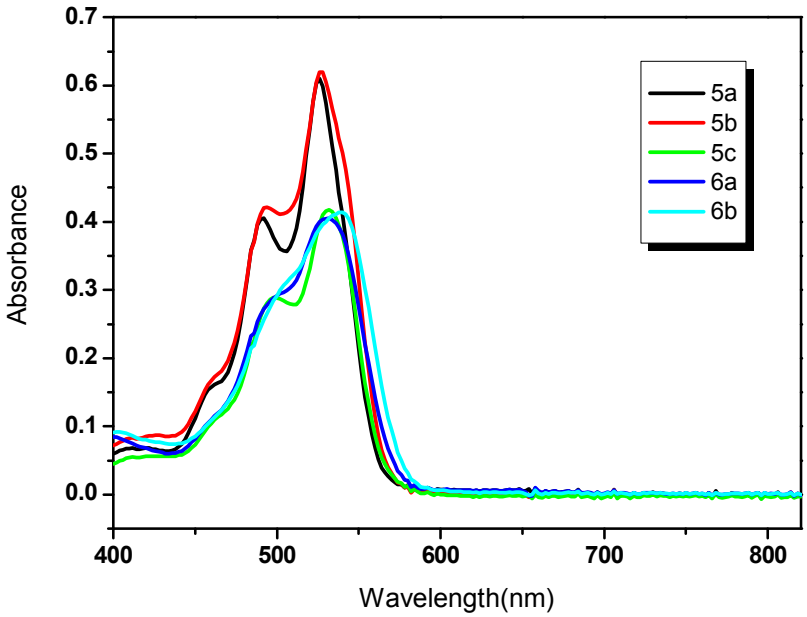

Figure 2.3 Absorption spectra in Cyclohexanone (10^{-5}mol liter^{-1}).

Table 2.2 Absorption spectra of the prepared dyes in CH_2Cl_2.

Dye	λ_{max} (nm)	ε_{max} (L mol-1 cm-1)	$\Delta\lambda_{1/2}$ (nm)
5a	**530**	**72000**	**67**
5b	**532**	**77000**	**70**
5c	**538**	**47000**	**68**

6a	**540**	**55000**	**71**
6b	**544**	**59000**	**71**

Table 2.3 Absorption spectra of the prepared dyes in Cyclohexanone.

Dye	**λ_{max} (nm)**	**ε_{max} (L mol-1 cm-1)**	**$\Delta\lambda_{1/2}$ (nm)**
5a	**526**	**61000**	**65**
5b	**528**	**62000**	**68**
5c	**532**	**42000**	**67**
6a	**532**	**41000**	**74**
6b	**538**	**41000**	**78**

Fig. 2.3 and Table 2.3 shows the absorption spectra of dyes **5** and **6** in cyclohexanone, the industrial solvent of LCD color filters. There were some differences between the absorption spectra in cyclohexanone and CH_2Cl_2. When the dyes were dissolved in cyclohexanone, the absorption maxima were hypsochromic by approximately 4~6nm and the molar extinction coefficients decreased by approximately 10000~20000 compared to those in CH_2Cl_2. This

would be attributed to the difference in affinity between the dyes and solvents.

Fig. 2.4 shows the transmittance spectra of the pigment-based color filter and the fabricated dye-based color filters with dyes **5** and **6**. All the dye-based color filters had similar or superior transmittance spectra compared to the pigment-based one because dyes dissolved in the media have a smaller particle size, which leads to less light scattering **[6, 22]**. In particular, the synthesized perylene dyes can maintain a well-dissolved state because of their high molar extinction coefficients so that only small amounts of dyes are needed for LCD color filters. The color filter with dye **6b** showed the highest transmittance over 625nm because of its two bulky tert-butyl phenoxy substituents, which lead to less aggregation of dye molecules. Table 2.4 shows the transmittance of the pigment-based and dye-based color filters at 650nm; the dye-based color filters had higher transmittance. However, all the dye-based color filters had undesirable transmittance at 400-500nm, as shown in Fig. 2.4, and yellow color compensating dyes are needed to cut off these undesirable transmittance.

Table 2.5 lists the coordinate values of the pigment-based color filter and fabricated dye-based color filters with dyes **5** and **6**. Although dye-based color filters had a lower colorant content, they could have a similar color gamut with a pigment-based one due to the high molar extinction coefficients. In particular, the color filters with dyes **5a** and **5b**, which have higher molar extinction

coefficients, had larger x values. However, the x, y values of the color filters with dyes **6a** and **6b** decreased after postbaking due to their low thermal stability, as shown in Fig. 2.5 and Table 2.5. Compared to the pigment-based color filter, the dye-based ones had smaller y values, which are advantageous for a wide color gamut. In particular, the color filters with more bathochromic dyes had smaller y values. The dye-based color filters also had higher brightness (Y) values than the pigment-based one due to their higher transmittance **[6]**.

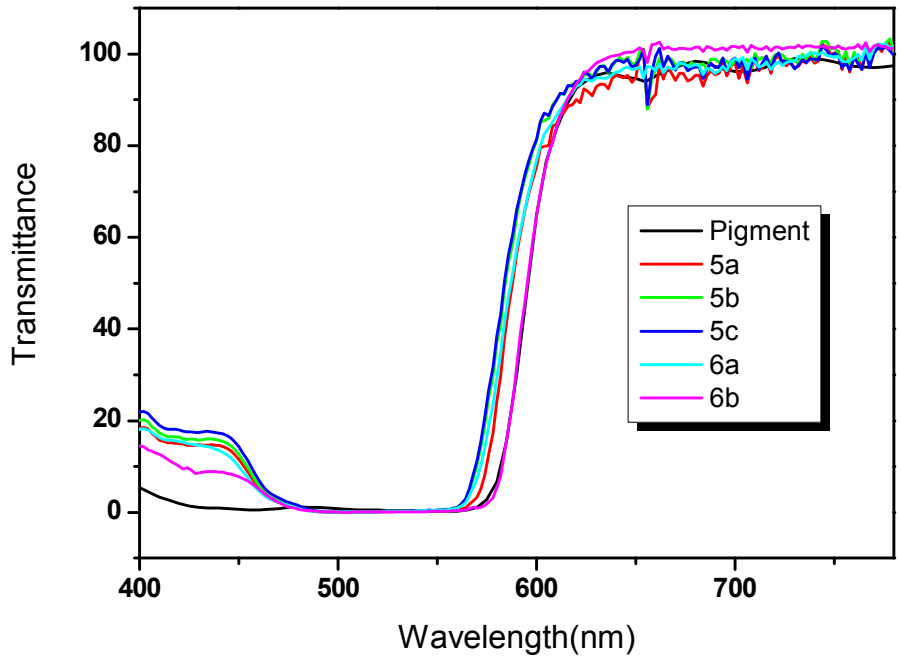

Figure 2.4 Transmittance spectra of the spin-coated color filters.

Table 2.4 Transmittance of the spin-coated color filters at 650nm.

Color filter	Transmittance (%) at 650nm
Pigment	**94.5997**
5a	**94.8496**
5b	**97.7593**
5c	**97.5466**
6a	**96.7853**
6b	**100**

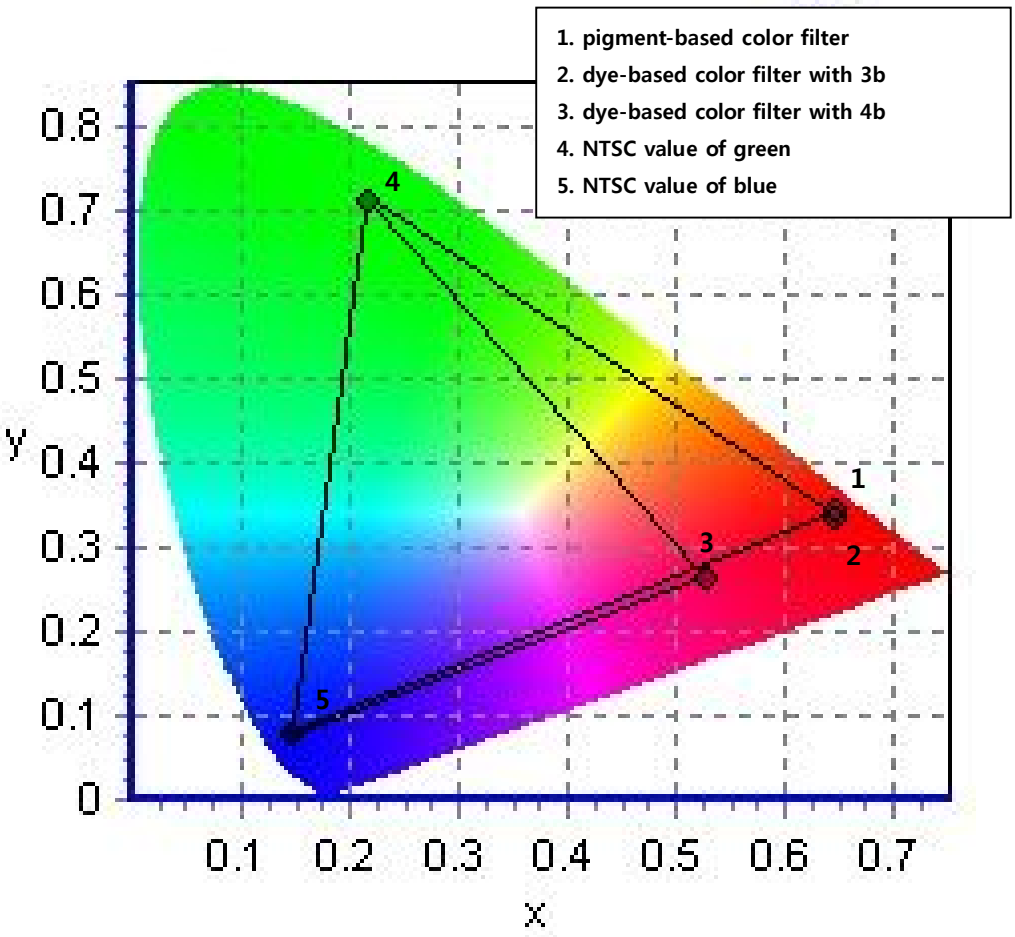

Figure 2.5 CIE 1931 chromaticity diagram of the pigment-based and dye-based color filters.

Table 2.5 The coordinate values corresponding to the CIE 1931 chromaticity diagram of the pigment based and dye-based color filters.

Color filter		x*	y*	Y**
Pigment	**prebake**	**0.644**	**0.345**	**22.10**
	postbake	**0.641**	**0.343**	**22.16**
5a	**prebake**	**0.639**	**0.337**	**23.01**
	postbake	**0.635**	**0.335**	**23.28**
5b	**prebake**	**0.642**	**0.335**	**24.69**
	postbake	**0.640**	**0.334**	**25.01**
5c	**prebake**	**0.623**	**0.311**	**25.25**
	postbake	**0.615**	**0.309**	**26.20**
6a	**prebake**	**0.634**	**0.304**	**24.72**
	postbake	**0.528**	**0.262**	**30.06**
6b	**prebake**	**0.626**	**0.303**	**24.49**
	postbake	**0.527**	**0.269**	**29.67**

* x, y : The coordinate values of CIE 1931 chromaticity diagram

** Y : brightness value

2.3.4 Thermal stability of dyes and dye-based color filters

Dye molecules should have a strong intermolecular interaction and form compact aggregates to have the high thermal stability **[23-25]**. The synthesized perylene dyes contain many aromatic rings and have a relatively flat molecular structure that contributes to the strong π-π stacked interactions **[8,9]**. In addition, their high molecular weight and polar substituents at the bay positions are advantageous for intermolecular interactions, such as van der Waals force and dipole-dipole interaction **[6]**.

For dyes to be used as color filters, they should endure temperatures of 220 °C, which is the highest temperature in the LCD manufacturing process, without significant weight loss **[26,27]**. Mono-substituted dyes **5a** and **5b** showed less than 1% weight loss after 30 min at 220 °C and were stable up to 250 °C, whereas the 1,7-di(substituted) dyes **6a** and **6b** showed approximately 5% weight loss, as shown in Fig. 2.6. This was attributed to the lower core twisting and less anti-aggregation effect of the substituents of the mono-substituted dyes, which leads to close packing of the dye molecules for high thermal stability. In a previous report, field emission scanning electron microscopy (FE-SEM) studies of various dyes showed that the dye with less steric hindrance had the bigger aggregate size that led to superior thermal

stability **[28]**. Therefore, the thermal stability of 1,7-di(substituted) dyes is insufficient for use in LCD color filters, even though they exhibited excellent spectral properties. The mono-substituted dye **5c** showed less weight loss than dyes **6a** and **6b** but more weight loss than dyes **5a** and **5b** due to the low thermal stability caused by the tert-octyl alkyl chain.

The ΔE_{ab} values of the color filters should be less than 3 after heating for one hour at 230 °C for commercial applications. The color filters with the mono-substituted dyes had satisfactory ΔE_{ab} values that varied according to their structures, as shown in Table 2.6. In contrast, the color filters with the 1,7-di(substituted) dyes had ΔE_{ab} values bigger than 3, which means that their thermal stability is insufficient.

As shown in Table 2.5, the x, y coordinate values of the color filters with the 1,7-di(substituted) dyes decreased and their brightness (Y) values increased after post baking. This suggests that their original red color faded due to degradation of their molecular structure. However, the thermal stability of dye-based color filters can be improved if the commercial binder used for the pigments can be adjusted.

The difference in thermal stability between the two types of dyes was analyzed partially by geometry calculations. Fig. 2.7 shows the optimized geometries of dyes **5b** and **6b**, which showed molecular core twisting due to the bulky

phenoxy substituents at the bay positions **[29]**. The approximate dihedral angle between the two naphthalene subunits attached to the central benzene ring was 8.6° and 26.2° for dyes **5b** and **6b**, respectively. Therefore, the core twisting that decreases π-π stacked interaction was more severe in the 1,7-di(substituted) dye, which in turn led to lower thermal stability.

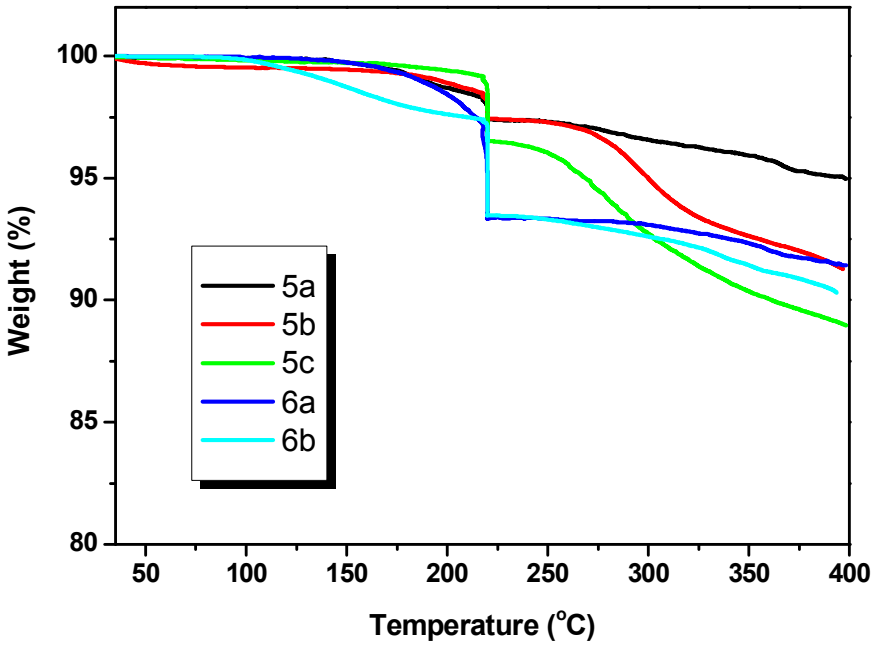

Figure 2.6 Thermogravimetric analysis (TGA) of the prepared dyes.

5b

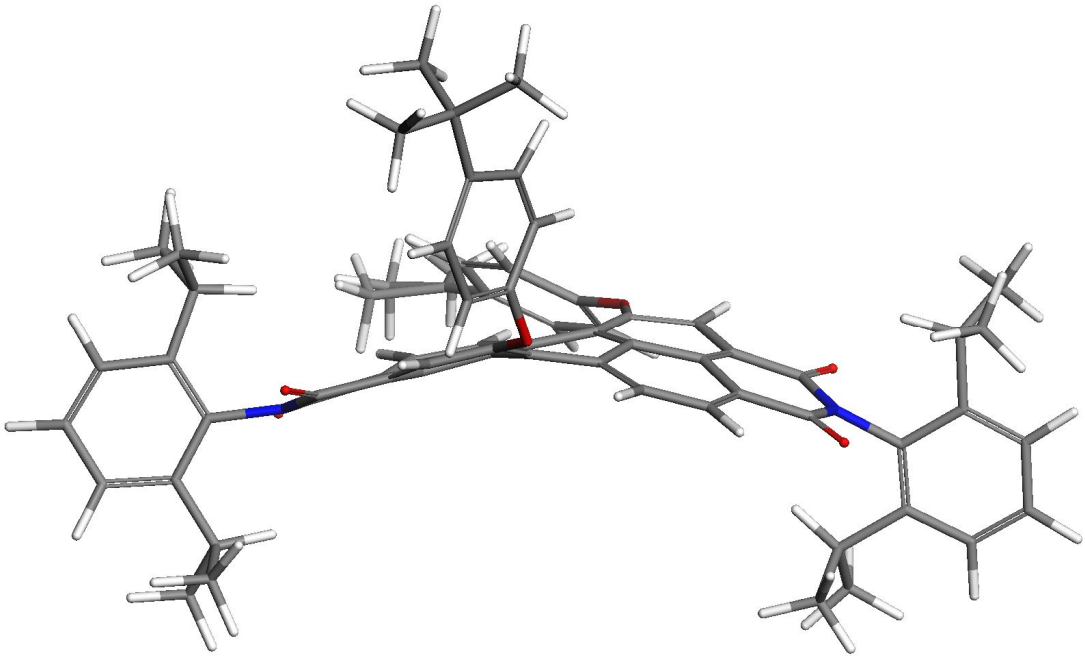

6b

Figure 2.7 Geometry-optimized structures of dyes 5b and 6b.

Table 2.6 Thermal stability of the dye-based and pigment-based color filters.

Color filter	ΔE_{ab}
Pigment	**0.248**
5a	**0.613**
5b	**0.752**
5c	**1.823**
6a	**9.873**
6b	**9.668**

2.4. Conclusions

Eight red perylene dyes were synthesized, and among them five solubility enhanced dyes were used in color filters. The difference in solubility of the

prepared dyes was attributed to the bulky functional substituents at the bay and terminal positions and the core twisting of the molecular structures.

All five dyes showed sharp absorption near 530nm, and the dye-based color filters could have a similar color gamut to the pigment-based one despite the much lower colorant content used due to their high molar extinction coefficients. In addition, the dye-based color filters with those dyes could have higher transmittance than the pigment-based one because they dissolved in the media, would exist in the molecular phase and could have a smaller particle size that leads to less light scattering.

The mono-substituted dyes had satisfactory thermal stability due to the properly controlled aggregation, whereas the 1,7-di(substituted) dyes did not meet the commercial criterion because their two bulky substituents at the bay positions made them thermally less stable.

2.5. References

[1] Tsuda K. Color filters for LCDs. Displays 1993;14:115-24.

[2] Sabnis RW. Color filter technology for liquid crystal displays. Displays 1999;20:119-29.

[3] Takanori K, Yuki N, Yuko N, Hidemasa Y, Kang WB, Pawlowski PG.

Polymer optimization of pigmented photoresists for color filter production. Jpn J Appl Phys 1998;37:1010-6.

[4] Na DY, Jung IB, Nam SY, Yoo CW, Choi YJ. The rheological behavior and dispersion properties of millbase for LCD colorfilters. J Korean Inst Electr Electron Mater Eng 2007;20:450-5.

[5] Sugiura T. Dyed color filters for liquid-crystal displays. J Soc Inf Disp 1993;1:177-80.

[6] Kim YD, Kim JP, Kwon OS, Cho IH. The synthesis and application of thermally stable dyes for ink-jet printed LCD color filters. Dyes and pigments 2009;81;45−52.

[7] Langhals H. Cyclic carboxylic imide structures as structure elements of high stability. Novel developments in perylene dye chemistry. Heterocycles 1995;40;477-500.

[8] Kim JH, Masaru M, Fukunishi K. Three dimensional molecular stacking and functionalities of aminonaphthoquinine by intermolecular hydrogen bondings and interlayer π-π interactions. Dyes and pigments 1998;40:53-7.

[9] Thetford D, Cherryman J, Chorlton AP, Docherty R. Theoretical molecular modeling calculations on the solid state structure of some organic pigments. Dyes and pigments 2004;63:259-76.

[10] Herbst W, Hunger K. Industrial organic pigments: production, properties,

applications: Third edition. Willey-VCH. pp. 476.

[11] Langhals H. Control of the interations in multichromophores: Novel concepts. Perylene bis-imides as components for larger functional units. Helvetica chimica acta 2005;88:1309-43.

[12] Chao CC, Leung M. Photophysical and Electrochemical Properties of 1,7-Diaryl-Substituted Perylene Diimides. J. Org. Chem. 2005;70;4323-31.

[13] Guerrero DJ, DiMenna B, Flaim T, Mercado R, Sun S, Dyed red, green, and blue photoresist for manufacture of high-resolution color filter arrays for image sensors. Proc Soc Photo Opt Instrum Eng 2003;5017:298-306.

[14] Seybold G, Wagenblast G. New perylene and violanthrone dyestuffs for fluorescent collectors. Dyes and pigments 1989;11;303-17.

[15] Chen Z, Debije MG, Debaerdemaeker T, Osswald P, Würthner F. Tetrachloro-substituted Perylene Bisimide Dyes as Promising n-Type Organic Semiconductors: Studies on Structural, Electrochemical and Charge Transport Properties. Chem. Phys. Chem. 2004;5;137-40.

[16] Lee SK, Zu Y, Herrmann A, Geerts Y, Müllen K, Bard AJ. Electrochemistry, Spectroscopy and Electrogenerated Chemiluminescence of Perylene, Terrylene, and Quaterrylene Diimides in Aprotic Solution. J. Am. Chem. Soc. 1999;121;3513-20.

[17] Langhals H, Blanke P. An approach to novel NIR dyes utilising a-effect

donor groups. Dyes and pigments 2003;59;109−116.

[18] Zhao C, Zhang Y, Li R, Li X, Jiang J. Di(alkoxy)-and Di(alkylthio)-Substituted Perylene-3,4,9,10-tetracarboxy Diimides with Tunable Electrochemical and Photophysical Properties. J. Org. Chem. 2007;72;2402-10.

[19] Ma YS, Wang CH, Zhao YJ, Yu Y, Han CX, Qiu XJ, Shi Z. Perylene diimide dyes aggregates: Optical properties and packing behavior in solution and solid state. Supramolecular chemistry 2007;19:141-9.

[20] Würthner F, Sautter A, Thalacker C. Substituted Diazadibenzoperylenes: New functional building blocks for supramolecular chemistry. Angew. Chem. 2000;112;1298-1301; Angew. Chem. Int. Ed. 2000;39;1243-45.

[21] Sun B, Zhao Y, Qiu X, Han C, Yu Y, Shi Z. Substitution effect of 1,7-asymmetrically substituted 3,4:9,10-perylenebis(dicarboximide) dyes. Supramolecular chemistry 2008;20:537-544.

[22] Tilley RJD. Colour and optical properties of materials. Chichester: John Wiley & Sons Inc.; 2000. pp. 108-10.

[23] Giles CH, Duff DG, Sinclair RS. The relationship between dye structure and fastness properties. Rev Prog Coloration 1982;12:58-65.

[24] Das S, Basu R, Minch M, Nandy P. Heat-induced structural changes in merocyanine dyes: X-ray and thermal studies. Dyes and pigments 1995;29:191-201.

[25] Chunlong Z, Nianchun M, Liyun L. An investigation of the thermal stability of some yellow and red azo pigments. Dyes and pigments 1993;23:13-23.

[26] Ohmi T. Manufacturing process of flat display. JSME Int J Ser B (Jpn Soc Mech Eng) 2004;47:422-8.

[27] Takamatsu T, Ogawa S, Ishii M. Color filter fabrication technology for LCDs. Sharp Tech J 1991;50:69-72.

[28] Sakong C, Kim YD, Choi JH, Yoon C, Kim JP. The synthesis of thermally-stable red dyes for LCD color filters and analysis of their aggregation and spectral properties. Accepted in Dyes and pigments 2011;88:166-73.

[29] Würthner F, Thalacker C, Diele S, Tschierske C. Fluorescent J-type aggregates and thermotropic columnar mesophases of perylene bisimide dyes. Chem Eur J 2001;7:2245-52.

Chapter 3

Facile synthesis and characterization of novel coronene chromophores and their application to LCD color filters

3.1. Introduction

Rylene tetracarboxdiimide derivatives including Perylene-3,4,9,10-tetracarboxdiimide are useful chromophores exhibiting exceptional chemical, thermal, and photochemical stability with high extinction coefficients **[1]**. They have a wide range of applications, such as reprographic processes **[2]**, photovoltaic cells **[3]**, fluorescent solar collectors **[4]**, energy relaying dyes for solar cells **[5]**, optoelectronic devices **[6]**, light emitting diodes **[7]** as well as usual colorant usage. Therefore, diverse methodologies to functionalize the aromatic core of perylene tetracarboxdiimide have been reported to extend the range of application of these chromophores as functional dyes **[8-13]**. The extension of the aromatic systems along the long molecular axis of perylene usually induced bathochromic shifts of the absorption spectra with increasing extinction coefficients **[8]**. However, their absorption maxima shifted

hypsochromically when the aromatic systems of those molecules were enlarged along the short molecular axis, such as coronenetetracarboxdiimides **1** (Fig. 3.1) **[9]**. These coronene derivatives can be extremely valuable because they are considerably stable and show high color strengths compared to other yellow chromophores. In general, stability and color strength of dye molecules often increase with increasing size of the aromatic system, which inevitably causes a bathochromic shift in absorption **[10]**.

Several synthetic routes from perylene to coronene have been reported. The core extension of perylenediimides using a Diels-Alder reaction with maleic anhydride **[11]** and synthesizing bisalkynyl substituted perylenediimides and their successive cyclization to coronene were reported **[9]**. In addition, the further core expanded structure, dibenzocoronene **2** (Fig. 3.1), was synthesized by palladium-catalyzed dehydrobromination after Suzuki coupling of 2-bromophenylboronic acid at the bay position of bromo-substituted perylene **[12]**. This is also possible by palladium-assisted cycloaddition of benzyne **[8]** or by the photocyclization of Suzuki-coupled phenylboronic acid **[13]**. However, all these synthetic methods were limited to some degree by the moderate yields, side reactions, and severe synthetic conditions.

In this study, new coronene derivatives were synthesized through a novel simple one step synthetic route and their characteristics were discussed as well.

In particular, their properties for yellow compensating dyes for color filters, which converts the white backlight into red (R), green (G) and blue (B) colored lights in LCD display panel, were investigated.

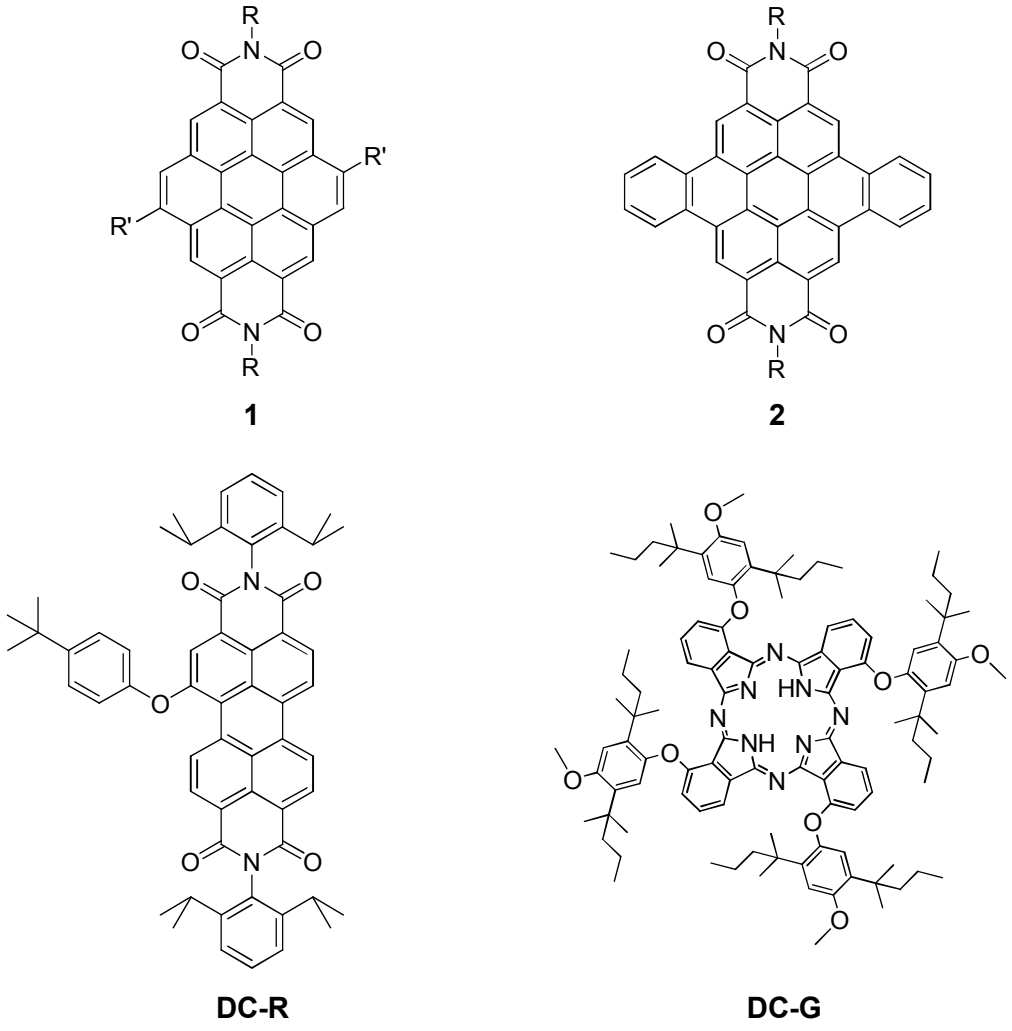

Figure 3.1 Coronene carboximide derivatives and prepared dyes for color filters.

3.2 Experimental

3.2.1 Materials and instrumentation

1-phenylvinylboronic acid, $Pd(PPh_3)_4$, and Na_2CO_3 purchased from Sigma-Aldrich were used as received. All the other reagents and solvents were of reagent-grade quality and obtained from commercial suppliers. Transparent glass substrates were provided by Paul Marienfeld GmbH & Co. KG. Commercial acrylic binder LC20160 was supplied by SAMSUNG Cheil industries Inc.

^{1}H NMR and ^{13}C NMR spectra were recorded on a Bruker Avance 500 spectrometer at 500MHz using chloroform-*d* and TMS, as the solvent and internal standard, respectively. Matrix Assisted Laser Desorption/Ionization Time Of Flight (MALDI-TOF) mass spectra were collected on a Voyager-DE STR Biospectrometry Workstation with α-cyano-4-hydroxy-cynamic acid (CHCA) as the matrix. Elemetal analysis was done on CE Instrument EA1112. Absorption and transmittance spectra were measured using a HP 8452A spectrophotometer. Fluorescence spectra were measured using a Shimadzu RF-5301PC spectrofluorometer. Chromatic characteristics of the color filters were

analyzed on a Scinco color spectrophotometer. Thermogravimetric analysis (TGA) was conducted under nitrogen at a heating rate of 10 °C min^{-1} using a TA Instruments Thermogravimetric Analyzer 2050.

3.*2.2. Synthesis*

N,N'-Bis(2,6-diisopropylphenyl)-1,7-dibromoperylene-3,4,9,10-tetracarboxdiimide **5**, *N,N'*-Bis(2,6-diisopropylphenyl)-1-bromoperylene-3,4,9,10-tetracarboxdiimide **5'**, and DC-R were synthesized according to the previously reported procedures **[14]**. DC-G was synthesized according to the procedures reported elsewhere **[15]**.

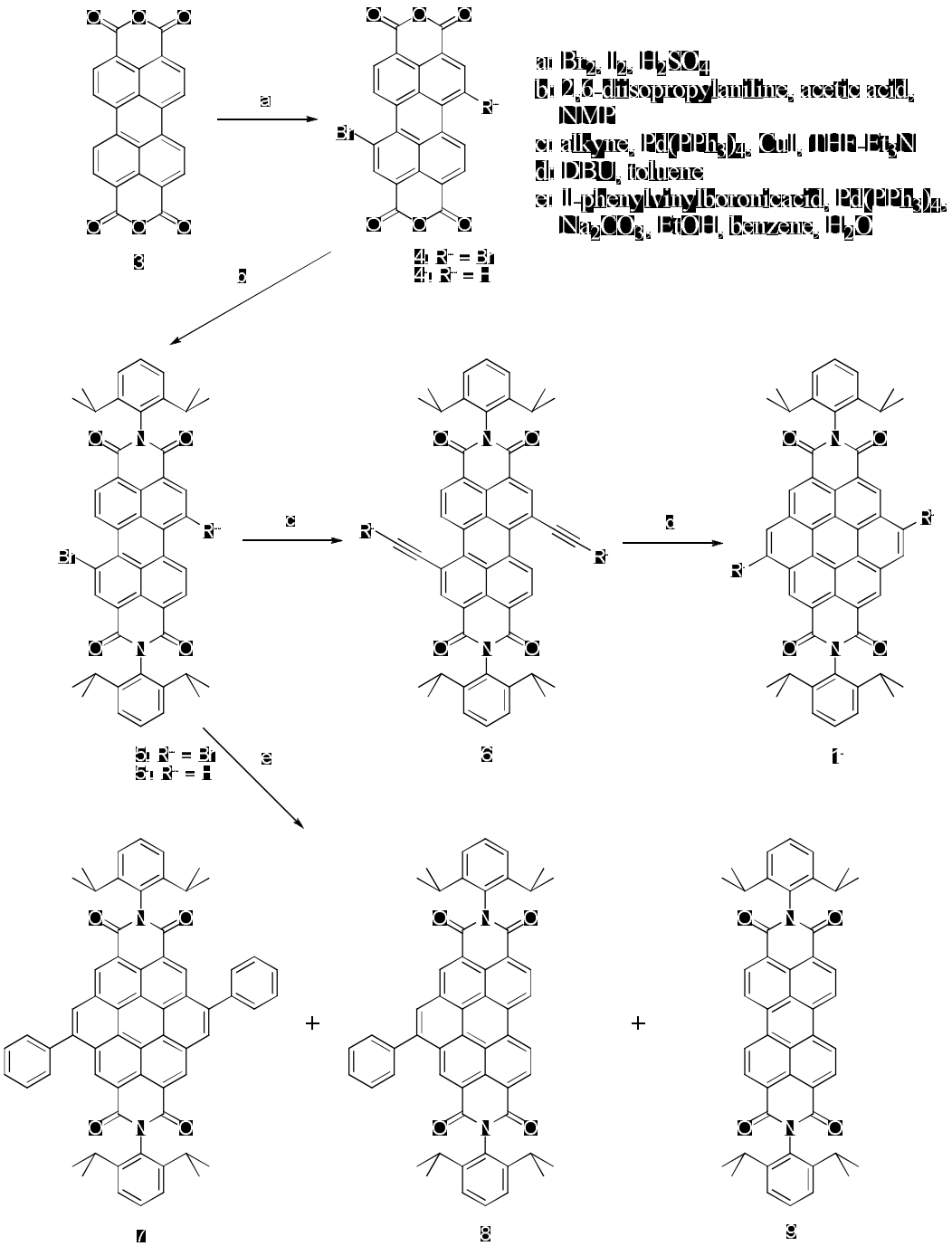
a: Br_2, I_2, H_2SO_4
b: 2,6-diisopropylaniline, acetic acid, NMP
c: alkyne, $Pd(PPh_3)_4$, CuI, THF-Et_3N
d: DBU, toluene
e: 4-phenylvinylboronic acid, $Pd(PPh_3)_4$, Na_2CO_3, EtOH, benzene, H_2O
3
4: R'' = Br
4': R'' = H
5: R'' = Br
5': R'' = H
6
7
8
9

Scheme 3.1 Synthesis of coronene carboximide derivatives.

3.2.2.1. N,N′-Bis(2,6-diisopropylphenyl)-5,11-diphenylcoronene-2,3,8,9-tetracarboxdiimides 7

A deaerated mixture of EtOH (5.79mL), benzene (33.12mL), H_2O (8.13mL) was added to a solid mixture of **5** (1.0 g, 1.15 mmol), 1-phenylvinylboronic acid (0.68 g, 4.6 mmol), $Pd(PPh_3)_4$ (66.57 mg, 5.0 mol%), and Na_2CO_3 (1.2 g, 11.5 mmol) under nitrogen. The mixture was reacted at 80 °C for 120 h. The reaction was quenched by the addition of water. The mixture was extracted with dichloromethane several times. The combined organic layer was dried over anhydrous $MgSO_4$ and concentrated under reduced pressure to provide a crude solid. The crude solid was further purified by column chromatography on silica gel using dichloromethane as the eluent. The band containing a trace of compounds synthesized from tribrominated diimide could be separated firstly. Then, the second band containing yellow compound **7** was collected.

Yield 52.1%; Mp > 300 °C (decomp.). ^{1}H NMR(500MHz, $CDCl_3$): δ = 1.24 (d, *J* = 6.5 Hz, 24H), 2.99 (septet, *J* = 40.0 Hz, 4H), 7.42 (d, *J* = 8.5 Hz, 4H), 7.54

(t, J = 9.2 Hz, 2H), 7.70 (t, J = 9.0 Hz, 2H), 7.76 (t, J = 13.5 Hz, 4H), 7.97 (t, J = 10.2 Hz, 4H), 9.27 (s, 2H), 10.17 (s, 2H), 10.22 (s, 2H); ^{13}C NMR(126MHz, $CDCl_3$): δ = 23.98, 24.34, 29.52, 29.92, 122.20, 122.38, 124.00, 124.26, 124.39, 124.49, 125.21, 129.03, 129.35, 129.42, 129.93, 130.05, 130.37, 130.44, 131.15, 131.21, 131.46, 131.76, 139.38, 139.49, 142.93, 143.13, 145.96, 146.07, 164.99, 165.13; MALDI-TOF MS: m/z 911.07 (100%, [M + H^+]); Found: C, 84.52; H, 5.45; N, 3.10%. Calc. for $C_{64}H_{50}N_2O_4$: C, 84.37; H, 5.53; N, 3.07%.

3.2.2.2. N,N′-Bis(2,6-diisopropylphenyl)-5-phenylbenzoperylene-2,3,8,9-tetracarboxdiimides 8

8 was synthesized in the same manner with **7** using **5'** (1.0 g, 1.27 mmol), 1-phenylvinylboronic acid (0.38 g, 2.54 mmol), $Pd(PPh_3)_4$ (66.57 mg, 5.0 mol%), and Na_2CO_3 (1.2 g, 11.5 mmol)

Yield 66.8%; Mp > 300 °C (decomp.). ^{1}H NMR(500MHz, $CDCl_3$): δ = 1.21 (d, J = 7.0 Hz, 24H), 2.84 (septet, J = 38.5 Hz, 4H), 7.38 (dd, J = 26.2 Hz, 4H), 7.52 (m, J = 18.4 Hz, 2H), 7.61 (t, J = 9.9 Hz, 1H), 7.67 (t, J = 14.5 Hz, 2H), 7.77 (t, J = 9.4 Hz, 2H), 8.81 (s, 1H), 9.22 (d, J = 8.2 Hz, 2H), 9.49 (d, J = 10.8 Hz, 2H), 9.56 (s, 1H), 9.63 (s, 1H); ^{13}C NMR(126MHz, $CDCl_3$): δ = 24.25,

24.32, 29.55, 29.92, 122.41, 122.60, 123.22, 123.62, 123.71, 124.30, 124.42, 124.49, 124.73, 124.88, 126.08, 128.02, 128.10, 128.93, 129.03, 129.31, 129.72, 129.86, 129.88, 130.00, 130.25, 130.75, 130.92, 130.96, 131.10, 133.50, 133.94, 134.29, 135.21, 138.91, 143.15, 145.91, 145.96, 164.17, 164.26, 164.35; MALDI-TOF MS: m/z 811.09 (100%, $[M + H^+]$); Found: C, 83.12; H, 5.58; N, 3.42%. Calc. for $C_{56}H_{46}N_2O_4$: C, 82.94; H, 5.72; N, 3.45%.

3.2.3 Preparation of dye-based inks and color filters

The dye-based ink for a color filter was composed of the cyclohexanone (3.2g), acrylic binder (1.4g), and dye (0.1g).

The prepared dye-based inks were coated on a transparent glass substrate using a MIDAS System SPIN-1200D spin coater. The coating speed was initially 100 rpm for 5 s, which was then increased to 500 rpm and kept constant for 20 s. The wet dye-coated color filters were then dried at 80 °C for 20 min, prebaked at 150 °C for 10 min, and postbaked at 230 °C for 1h. After each step, the coordinate values of the color filters were measured.

3.2.4 Measurement of thermal stability

Thermal stability of the synthesized dyes was evaluated by thermogravimetry (TGA). The prepared dyes were heated to 110 °C and held at that temperature for 10 min to remove residual water and solvents. The dyes were then, heated to 220 °C and held at that temperature for 30 min to simulate the processing thermal conditions of color filter manufacturing. The dyes were finally heated to 400 °C to determine their degradation temperature. The temperature was raised at the rate of 10 °C min^{-1} under nitrogen atmosphere.

To check the thermal stability of the dyes in color filters, the fabricated color filters were heated to 230 °C for 1 h in a forced convection oven (OF-02GW Jeiotech Co., Ltd.). The color difference values (ΔE_{ab}) before and after heating were measured on a color spectrophotometer (Scinco colormate) in CIE L'a'b' mode.

3.3 Results and discussion

3.3.1 Synthesis

Different types of linear alkyl chains were introduced selectively at the R' position of coronenetetracarboxdiimides **1** through reactions c and d of scheme 1 as described in literature **[9]**. In this reference, sterically demanding

substituents, such as *tert*-butyl or a phenyl group, could not be introduced because the bulky substituents at the C-C triple bond restricted the cyclization reaction. However, as shown in the experimental section of this paper, phenylvinylboronic acid, inherent with an aryl group, was reacted successfully with bromo-substituted perylenediimides **5**, and **5'** under similar conditions to Suzuki-coupling and spontaneously cyclized to afford two novel compounds diphenylcoronene tetracarboxdiimide **7** and monophenylbenzoperylene tetracarboxdiimide **8**. The conveniences of this synthesis are that the 1,6-isomer of 1,7-dibromoperylene tetracarboxdiimide **5** does not have to be removed because both isomers react with phenylvinylboronic acid to form the same desired product **7**, and 1,7-dibromoperylenediimide **5** and mono-bromoperylenediimide **5'** could be obtained from the same crude product after column chromatography **[14]**. The yield of monophenylbenzoperylene **8** (66.8%) was higher than that of diphenylcoronene **7** (52.1%) because there were more side products such as mono-substituted compound when diphenylcoronene **7** was synthesized. In column chromatography process of diphenylcoronene **7**, the first band of the eluent was carrying the impurity reacted from the trace of tribrominated diimide, and the second band was for diphenylcoronene **7**. Monophenylbenzoperylene **8** was also obtained as a side product at the fourth band of the eluent, and the sixth band was for N,N'-

bis(2,6-diisopropylphenyl)-perylene-3,4,9,10-tetracarboxdiimide **9**, all bromines were removed. The described synthetic route is the simplest and most economical method with a considerable yield under mild conditions.

3.3.2 Photophysical properties of dyes

Both coronene derivatives **7** and **8** are highly soluble in most organic solvents, such as dichloromethane, hexane, and toluene since the aggregation between dyes is suppressed by steric hindrance of the phenyl groups at the bay positions as well as the diisopropylphenyl groups at the terminal positions, which are distorted from the plane of the main body of the coronene derivatives **[14]**. Monophenylbenzoperylene **8** shows the main absorption maximum at 472nm (Fig. 3.2), which originated from the typical vibronic structure of perylene, giving this chromophore a very strong and vivid yellow color. The shape of this characteristic main peak is analogous to that of dibenzocoronene **2**, but hypsochromically shifted by approximately 22nm **[12]**. Monophenylbenzoperylene **8** is an ideal yellow chromophore since its main peak is very sharp and there is no absorption over 500nm. The extinction coefficient of monophenylbenzoperylene **8** at 472nm (ε = 66,000 M^{-1} cm^{-1}) is similar to that of dibenzocoronene **2** at 494nm (ε = 66,000 M^{-1} cm^{-1}) and higher

than that of coronene **1** at 428nm (ε = 62,000 M^{-1} cm^{-1}) **[12]**. Diphenylcoronene **7** shows its main absorption maximum at a much shorter wavelength (426nm, ε = 60,000 M^{-1} cm^{-1}) with minor absorption at approximately 512nm (Fig. 3.2). The shape of these absorption peaks is similar to that of coronene **1**, which has an alkyl chain introduced at the R' position, but the distance between the two absorption maxima is slightly different **[9]**. The minor absorption around 512nm gives diphenylcoronene **7** a somewhat dull color in solution compared to the much brighter and greener color of monophenylbenzoperylene **8**. The absorption spectra of these molecules make them very suitable as yellow compensating dyes for LCD color filters. In particular, monophenylbenzoperylene **8** can be used to cut off the undesirable transmittance in short wavelength range of red color, and extremely useful for making the green color with narrow half-band width **[16]**.

Diphenylcoronene **7** and monophenylbenzoperylene **8** show fluorescence maxima at 524 and 497nm, respectively (Fig. 3.2). Their quantum yields are 82 and 86%, respectively, which are much higher than other yellow fluorophores, e.g. acridine yellow, which has a fluorescence quantum yield of 47% **[17]**. In particular, diphenylcoronene **7** can be an excellent donor dye for DSSCs using Förster resonance energy transfer (FRET) because the emission of diphenylcoronene **7** is strong and barely overlaps with the absorption range **[18]**.

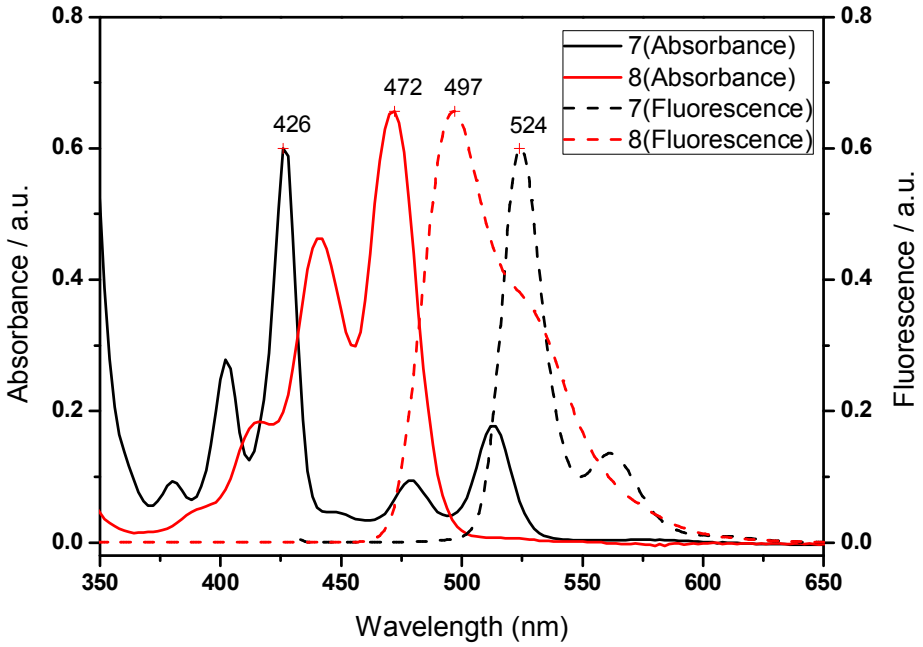

Figure 3.2 Absorption and fluorescence spectra of compounds 7 and 8 in CH_2Cl_2 (10^{-5}mol liter^{-1}).

3.3.3 Spectral and chromatic properties of spin coated color filters

Currently, dyes are extensively investigated to replace pigments in LCD manufacturing process since there are growing needs for enhancing the picture

quality **[14]**. The dye-based color filters have superior transmittance compared to the pigment-based one because dyes dissolved in the media have a smaller particle size, which leads to less light scattering **[19]**. Monophenylbenzoperylene **8** can make ideal transmittance spectra of red and green color filters when used as a yellow compensating dye, shown in Table 3.1, Fig. 3.3, and 3.4. The common red dyes, such as DC-R, which have undesirable transmittance under 500nm, as shown in Fig. 3.2, cannot be solely used to color filters without yellow compensating dye **[14]**. Monophenylbenzoperylene **8** absorbing under 500nm intensively without any residual absorption over 500nm can cut off undesirable transmittance of given red dye effectively with maintenance of the desired transmittance range. This kind of compensation effect is more prominent in green color. The main dyes for green color, such as DC-G, transmit wide range of wavelength to have dull bluish green color. However, the dye composite including monophenylbenzoperylene **8** exhibited sharp transmittance spectrum cut off under 500nm as shown in Fig. 3.4. Therefore, vivid and clear green color could be realized by blending monophenylbenzoperylene **8**. With less amount of the green dye in the mixture with the yellow dye, λ_{max} of the color filter red shifted about 20nm to be closer to the green color for conventional LCD color filters **[16]**.

Table 3.2 and Fig. 3.5 shows the coordinate values of spin coated color

filters. The coordinate values of DC-R were rarely affected by blending of monophenylbenzoperylene **8**, but the x value of DC-G was increased to be close to the conventional green coordinate (0.274, 0.572) of the LCD color filters.

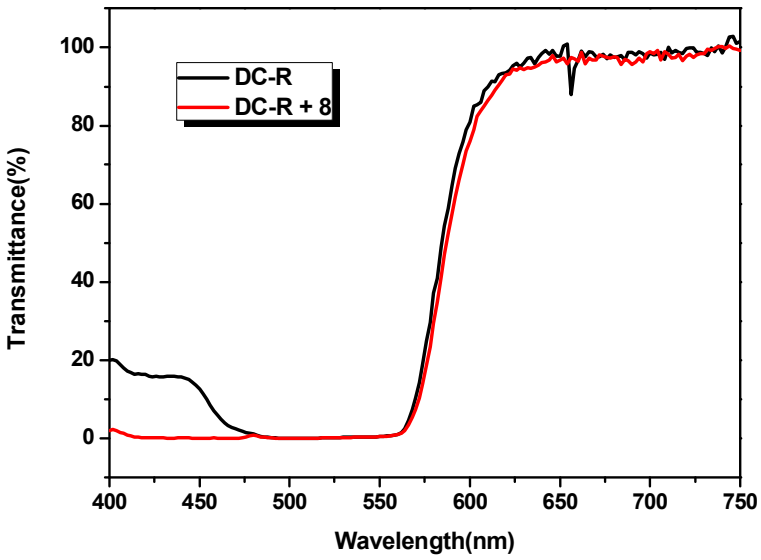

Figure 3.3 Transmittance spectra of red spin coated color filters.

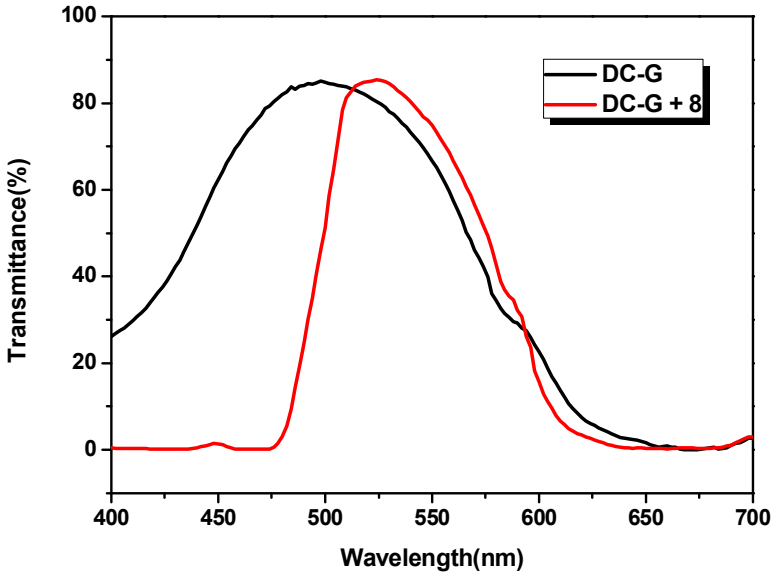

Figure 3.4 Transmittance spectra of green spin coated color filters.

Table 3.1 Transmittance of the spin-coated color filters.

Prepared dyes	λ_{max}(nm)	Transmittance(%)
DC-R	**626**	**95.89**
DC-R + 8	**628**	**94.78**
DC-G	**498**	**85.05**

DC-G + 8	**524**	**85.39**

Table 3.2 The coordinate values corresponding to the CIE 1931 chromaticity diagram and the color difference values of the spin coated color filters.

Prepared dyes	**Y**	**x**	**y**	**$\triangle E_{ab}$**
DC-R	**25.01**	**0.640**	**0.334**	**0.752**
DC-R + 8	**24.33**	**0.631**	**0.339**	**1.04**
DC-G	**54.28**	**0.205**	**0.572**	**1.69**
DC-G + 8	**58.54**	**0.286**	**0.563**	**1.77**

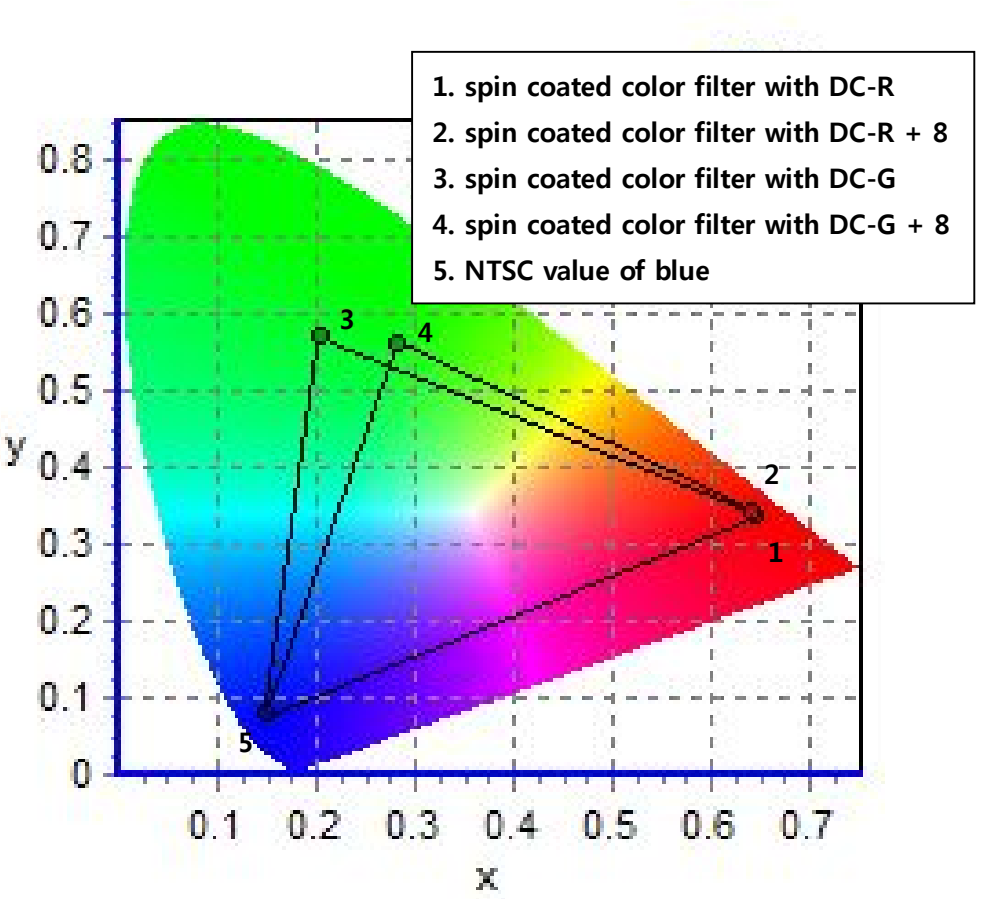

Figure 3.5 CIE 1931 chromaticity diagram of the spin coated color filters.

3.3.4 Thermal stability of dyes and spin coated color filters

Although the dyes have superior optical properties than the pigments, they were hardly applied for LCD color filters owing to their inferior thermal

stability. For dyes to be used as color filters, they should endure temperature of 220 °C, which is the current highest temperature in the LCD manufacturing process, without significant weight loss **[20, 21]**. The synthesized novel dyes 7 and 8 have more rigid structures than other yellow chromophores to be suitable for the colorants of LCD color filters. However, their thermal stabilities are somewhat different according to the degree of substitution. In our earlier report, the 1,7-di(substituted) perylene diimides exhibited lower thermal stability than the mono-substituted one due to the higher core twisting of their main body resulted from bulky aryl substituents at both side bay positions **[14]**. Similarly, whereas the monophenylbenzoperylene **8** showed less than 3% of weight loss in isothermal section which is sufficient for LCD color filters, diphenylcoronene **7** showed much more weight loss as shown in Fig. 3.6. The thermal stability of the spin coated color filters is estimated by the color difference (ΔE_{ab}) value. The ΔE_{ab} values of the color filters should be less than 3 after heating for one hour at 230 °C for commercial applications **[16]**. The ΔE_{ab} values of the color filters with monophenylbenzoperylene **8** were less than 3 desired for LCD manufacturing process, as shown in Table 3.2.

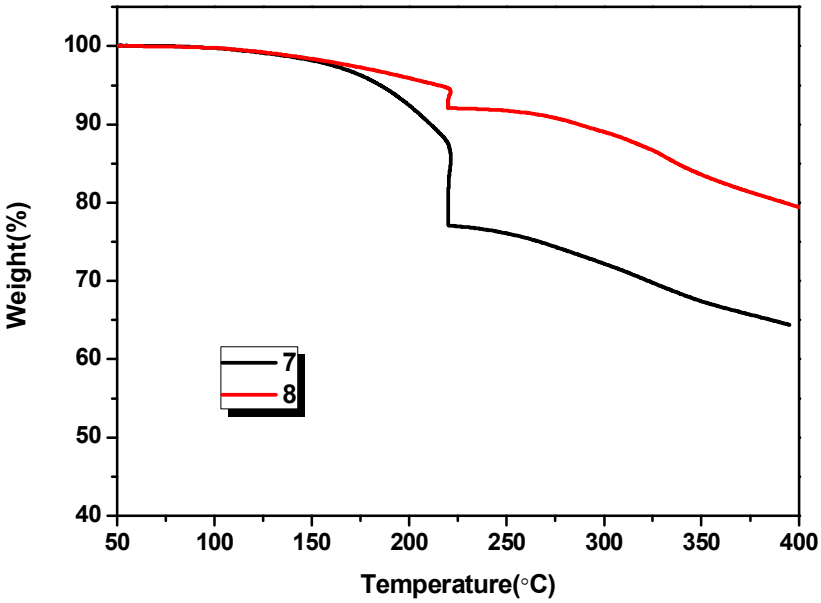

Figure 3.6 Thermogravimetric analysis (TGA) of the synthesized dyes.

3.4 Conclusions

In summary, we have successfully synthesized two novel compounds diphenylcoronene **7** and monophenylbenzoperylene **8** by a simple one-step reaction. These chromophores are stable, have largely hypsochromic shifted absorption peaks compared to perylene-3,4,9,10-tetracarboxdiimide and exhibit strong, bright emission. They can be used as good yellow chromophores or fluorophores for a wide range of applications according to their characteristic

range of absorption and emission peaks. While diphenylcoronene **7** draws attention to be applied for energy relaying dye of DSSC, monophenylbenzoperylene **8** was successfully applied as a yellow compensating dye for LCD color filters.

3.5 References

[1] Nagao Y, Misono T. Synthesis and properties of N-alkyl-N'-aryl-3,4:9,10-perylenebis(dicarboximide). Dyes Pigm 1984;5:171-88.

[2] Loufty HO, Hor AM, Kazmaler P, Tarn MJ. J Imaging Sci 1989;33:151-9.

[3] Schlettwein D, Wöhrle D, Kaarmann E, Melville U. Conduction type of substituted tetraazaporphyrins and perylene tetracarboxylic acid diimides as detected by thermoelectric power measurements. Chem Mater 1994;6:3-6.

[4] Seybold G, Wagenblast G. New perylene and violanthrone dyestuffs for fluorescent collectors. Dyes Pigm 1989;11:303-17.

[5] Hardin BE, Hoke ET, Armstrong PB, Yum JH. Increased light harvesting in dye-sensitized solar cells with energy relay dyes. Nat Photonics 2009;3:406-11.

[6] Hernando J, de Witte PAJ, van Dijk EMHP, Korterik J, Nolte RJM. Investigation of Perylene Photonic Wires by Combined Single-Molecule

Fluorescence and Atomic Force Microscopy. Angew Chem Int Edit 2004;43:4045-9.

[7] Angadi MA, Cosztola D, Wasielewski MR. Organic light emitting diodes using poly(phenylenevinylene) doped with perylenediimide electron acceptors. Mater Sci Eng B 1999;B63:191-4.

[8] Avlasevich Y, Müller S, Erk P, Müllen K. Novel Core-Expanded Rylenebis(Dicarboximide) Dyes Bearing Pentacene Units: Facile Synthesis and Photophysical Properties. Chem Eur J 2007;13:6555-61.

[9] Rohr U, Kohl C, Müllen K, van de Craats A, Warman J. Liquid crystalline coronene derivatives. J Mater Chem 2001;11:1789-99.

[10] Zollinger H. Color Chemistry, VCH Weinheim 1987.

[11] Langhals H, Kirner S. Novel fluorescent dyes by the extension of the core of perylene-tetracarboxylic bisimides. Eur J Org Chem 2000:365-80.

[12] Müller S, Müllen K. Facile synthetic approach to novel core-extended perylene carboximide dyes. Chem Commun (camb) 2005;32:4045-6.

[13] Li Y, Zheng H, Li Y, Wang S, Wu Z, Liu P, Gao Z, Liu H, Zhu D. Photonic logic gates based on control of FRET by a solvatochromic perylene bisimide. J Org Chem 2007;72:2878-85.

[14] Choi J, Sakong C, Choi JH, Yoon C, Kim JP. Synthesis and characterization of some perylene dyes for dye-based LCD color filters. Dyes Pigm

2011;90:82-8.

[15] Lee W, Yuk SB, Choi J, Jung DH, Choi SH, Park JS, Kim JP. Synthesis and characterization of solubility enhanced metal-free phthalocyanines for liquid crystal display black matrix of low dielectric constant. Dyes Pigm (DYPI 3432)

[16] Kim YD, Kim JP, Kwon OS, Cho IH. The synthesis and application of thermally stable dyes for ink-jet printed LCD color filters. Dyes Pigm 2009;81:45-52.

[17] Olmsted J. Calorimetric determinations of absolute fluorescence quantum yields. J Phys Chem 1979;83:2581-4.

[18] Basham JI, Mor GK, Grimes CA. Förster resonance energy transfer in dye-sensitized solar cells. ACS Nano 2010;4:1253-8.

[19] Tilley RJD. Colour and optical properties of materials. Chichester, John Wiley & Sons Inc 2000;108-10.

[20] Ohmi T. Manufacturing process of flat display. JSME Int J Ser B (Jpn Soc Mech Eng) 2004;47:422-8.

[21] Takamatsu T, Ogawa S, Ishii M. Color filter fabrication technology for LCDs. Sharp Tech J 1991;50:69-72.

Chapter 4

Synthesis and Characterization of Thermally Stable Dyes with Improved Optical Properties for Dye-based LCD Color Filters

4.1 Introduction

Displays are the most important media in the information age. Since the late-20th century, flat-panel displays have replaced the market share of CRTs (Cathode Ray Tubes) **[1,2]**. Among the flat-panel displays, LCDs, electronically modulated optical devices made up of many segments filled with liquid crystals and arrayed in front of a light source (backlight) to produce images in color, hold the greatest market share due to the many advantages such as low cost, low power consumption, and flexibility. The color filter, which converts the white backlight into red (R), green (G), and blue (B) colored lights, is the key component in the growth of display technology since it has the greatest potential to enhance picture quality **[1,2]**. Only 6.3% of the back light can pass

through the whole panel, which includes the polarizing filter, TFT-array, LC cell, and color filter. In particular, the transmittance through the color filter is the lowest (30%). Therefore, developing high transmittance color filters is essential for saving energy consumption as well as improving high-quality displays.

Currently, the pigment dispersion method to form RGB patterned pixels using photo lithography has been widely adopted to produce color filters, because color filters with superior stability can be achieved **[3]**. Although color filters produced by this method have good thermal and photo-chemical stability, they have low chromatic properties due to the aggregation behavior of pigment particles used as colorants **[4]**. Dyes can be attractive alternatives to overcome this limitation due to the reduced light scattering resulting from the fact that they are dissolved in the media and exist in molecular form. However, in order for the dyes to be applied successfully to the LCD manufacturing process, their low thermal stability needs to be improved **[5]**. Moreover, they should be highly soluble in industrial solvents and have sharp absorption peaks for superior optical properties.

Therefore, to replace pigments with dyes in LCD manufacturing, the remarkably stable molecule, phthalocyanine (PC), has been modified into six highly soluble dyes and blended with a yellow benzoperylene dye to exhibit appropriate green colors. To the best of the authors' knowledge, this is the first

report of applying 100% dyes to the green color resist for photo lithography process. The green color, which transmits light within the range of 520~550nm, has the greatest contribution to the optical property of color filters since it is the most sensitive to human eyes **[2]**. For this purpose, the thermal stability, optical properties, and solubility of PC and benzoperylene dyes as the colorant materials for color filters were investigated according to their characteristic structures. In addition, the transmittance and color gamut of the spin coated color filters with these dyes were examined and compared with the pigment-based color filter.

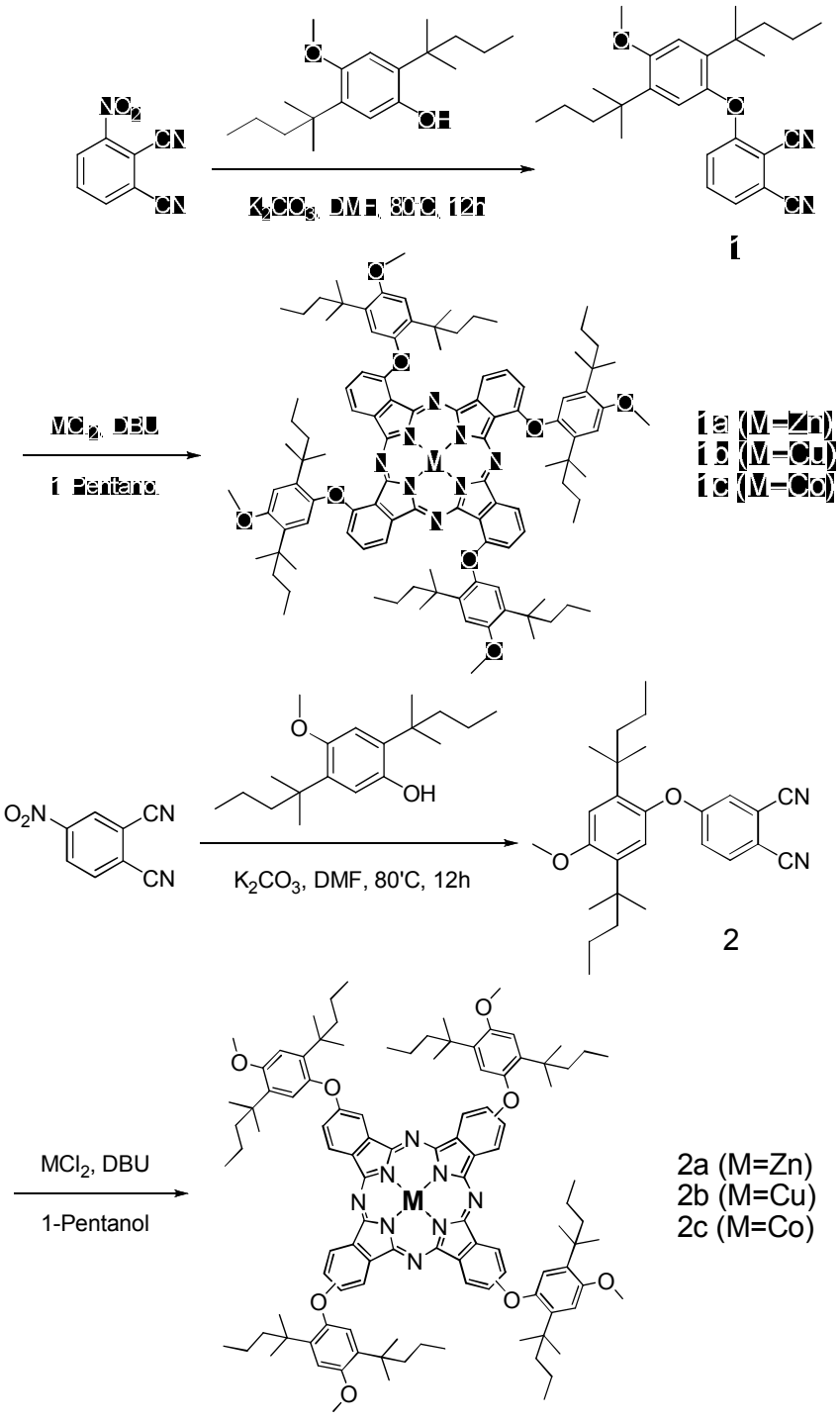
K_2CO_3, DMF, 80°C, 12h
1
MCl_2, DBU
1-Pentanol
1a (M=Zn)
1b (M=Cu)
1c (M=Co)
K_2CO_3, DMF, 80'C, 12h
2
MCl_2, DBU
1-Pentanol
2a (M=Zn)
2b (M=Cu)
2c (M=Co)

Scheme 4.1 Synthesis route of α-position and β-position substituted phthalocyanines.

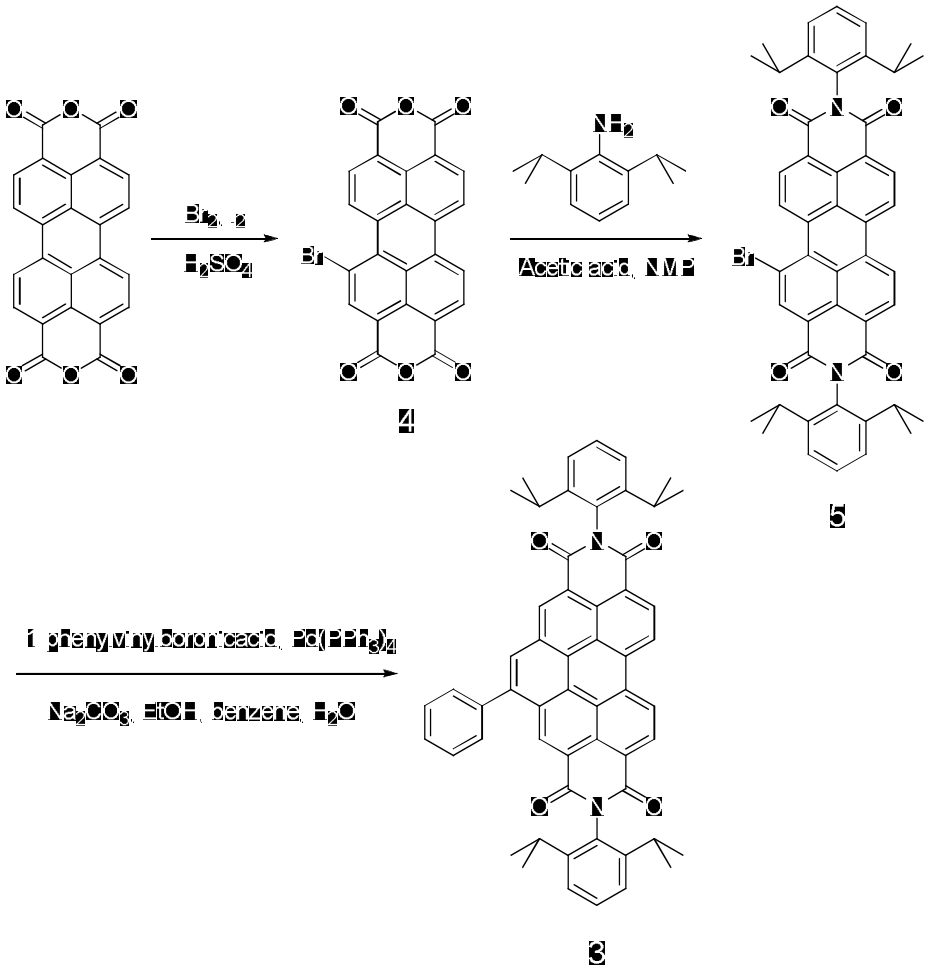

Scheme 4.2 Synthesis route of monophenylbenzoperylene.

4.2 Experimental

4.2.1 Materials and instrumentation

1,8-Diazabicyclo-7-undecene (DBU), 3(4)-nitrophthalonitrile, 2,5-bis-(1,1-dimethylbutyl)-methoxyphenol purchased from TCI, and $ZnCl_2$, $CuCl_2$, $CoCl_2$ purchased from Sigma-Aldrich were used as received. All the other reagents and solvents were of reagent-grade quality and obtained from commercial suppliers. Transparent glass substrates were provided by Paul Marienfeld GmbH & Co. KG. Commercial pigment-based color filter and acrylic binder were supplied by NDM Inc.

^{1}H NMR spectra were recorded on a Bruker Avance 500 spectrometer at 500MHz using chloroform-d and TMS, as the solvent and internal standard, respectively. Matrix Assisted Laser Desorption/Ionization Time Of Flight (MALDI-TOF) mass spectra were collected on a Voyager-DE STR Biospectrometry Workstation with a-cyano-4-hydroxy-cynamic acid (CHCA) as the matrix. Absorption and transmittance spectra were measured using a HP 8452A spectrophotometer. Fluorescence spectra were measured using a Shimadzu RF-5301PC spectrofluorometer. Chromatic characteristics of the

color filters were analyzed on a Scinco color spectrophotometer. Thermogravimetric analysis (TGA) was conducted under nitrogen at a heating rate of 10 °C min^{-1} using a TA Instruments Thermogravimetric Analyzer 2050. The thickness of the color filters was measured using a Nano System Nanoview E-1000.

4.2.2 Synthesis

4.2.2.1 3-(2,5-Bis(1,1-dimethylbutyl)-4-methoxyphenoxy)phthalonitrile (1)

3-nitrophthalonitrile(1g, 5.77mmol) and 2,5-bis-(1,1-dimethylbutyl)-methoxyphenol (1.68g, 5.77mmol) were dissolved in dry DMF(30ml) and anhydrous K_2CO_3(1.06g, 7.66mmol) was added in portions during 4h. The mixture was stirred at 80 °C for 10h under nitrogen atmosphere. After filtering the reaction mixture, the residue was extracted with CH_2Cl_2 and dried by rotary evaporation. After removal of the solvent, the crude product was purified on a silica gel column (CH_2Cl_2/hexane: 5/1) to afford the target compound as a light brown solid (1.98g, 82.22%). ^1H NMR (500MHz, $CDCl_3$, 25 °C, TMS): δ = 7.44 (t, 1H), 7.32 (d, 1H), 6.89 (d, 1H), 6.76 (1H, s), 6.60(1H, s), 3.78 (s, 3H, -O-CH_3), 1.64 (m, 2H), 1.54 (m, 2H), 1.20(d, 12H), 1.02 (m, 2H), 0.98 (m, 2H),

0.77 (t, 3H), 0.65 (t, 3H).

4.2.2.2 1(4)-Tetrakis(2,5-Bis(1,1-dimethylbutyl)-4-methoxyphenoxy)-phthalocyaninatozinc(II) (1a)

The solution of **1** (1.26g, 3mmol) in 1-pentanol (50ml) was refluxed under a nitrogen atmosphere and $ZnCl_2$ (0.41g, 3mmol) was added. After adding DBU (2.25ml, 15mmol), the solution was heated under reflux for 12h. After filtering the reaction mixture, the residue was purified on a silica gel column (CH_2Cl_2/MeOH: 50/1) to afford the target compound as a bluish green solid (0.76g, 58.35%). MALDI-TOF MS : m/z 1740.07 (100%, $[M+2K]^+$); Found: C, 74.36; H, 7.74; N, 6.37; O, 7.49%. Calc. for $C_{106}H_{132}N_8O_8Zn$: C, 74.38; H, 7.77; N, 6.55; O, 7.48%.

4.2.2.3 1(4)-Tetrakis(2,5-Bis(1,1-dimethylbutyl)-4-methoxyphenoxy)-phthalocyaninatocopper(II) (1b)

1b was synthesized following the same procedure for **1a** using **1** (1.26g, 3mmol), 1-pentanol (50ml), $CuCl_2$ (0.40g, 3mmol), and DBU (2.25ml, 15mmol). The crude product was purified on a silica gel column

(CH_2Cl_2/Hexane: 2/3) to afford the target compound as a dark bluish green solid (0.78g, 60.38%). MALDI-TOF MS : m/z 1737.86 (100%, $[M+2K]^+$); Found: C, 74.66; H, 8.18; N, 6.10; O, 7.61%. Calc. for $C_{106}H_{132}N_8O_8Zn$: C, 74.46; H, 7.78; N, 6.55; O, 7.49%.

4.2.2.4 1(4)-Tetrakis(2,5-Bis(1,1-dimethylbutyl)-4-methoxyphenoxy)-phthalocyaninatocobalt(II) (1c)

1c was synthesized following the same procedure for **1a** using **1** (1.26g, 3mmol), 1-pentanol (50ml), $CoCl_2$ (0.39g, 3mmol), and DBU (2.25ml, 15mmol). The crude product was purified on a silica gel column (CH_2Cl_2/Hexane: 1/1) to afford the target compound as a dark bluish green solid (0.68g, 51.71%). MALDI-TOF MS : m/z 1732.87 (100%, $[M+2K]^+$); Found: C, 74.77; H, 7.45; N, 6.55; O, 7.78%. Calc. for $C_{106}H_{132}N_8O_8Zn$: C, 74.66; H, 7.80; N, 6.57; O, 7.51%.

4.2.2.5 4-(2,5-Bis(1,1-dimethylbutyl)-4-methoxyphenoxy)phthalonitrile (2)

4-nitrophthalonitrile(1g, 5.77mmol) and 2,5-bis-(1,1-dimethylbutyl)-methoxyphenol(1.68g, 5.77mmol) were dissolved in dry DMF(30ml) and

anhydrous K_2CO_3(1.06g, 7.66mmol) was added in portions during 4h. The mixture was stirred at 80 °C for 8h under nitrogen atmosphere. After filtering the reaction mixture, the residue was extracted with CH_2Cl_2 and dried by rotary evaporation. After removal of the solvent, the crude product was purified on a silica gel column ($CHCl_3$) to afford the target compound as a light brown solid (2.13g, 88.47%). ^{1}H NMR (500MHz, $CDCl_3$, 25℃, TMS): δ = 7.69 (d, 1H), 7.22 (s, 1H), 7.14 (d, 1H), 6.82 (s, 1H), 6.63(s, 1H), 3.08 (s, 3H, -O-CH_3), 1.71 (m, 2H), 1.56 (m, 2H), 1.26(d, 12H), 1.04 (m, 2H), 0.96 (m, 2H), 0.81 (t, 3H), 0.71 (t, 3H).

4.2.2.6 2(3)-Tetrakis(2,5-Bis(1,1-dimethylbutyl)-4-methoxyphenoxy)-phthalocyaninatozinc(II) (2a)

2a was synthesized following the same procedure for **1a** using **2** (1.26g, 3mmol), 1-pentanol (50ml), $ZnCl_2$ (0.41g, 3mmol), and DBU (2.25ml, 15mmol). The crude product was purified on a silica gel column (CH_2Cl_2) to afford the target compound as a bluish green solid (0.89g, 67.89%). MALDI-TOF MS : m/z 1738.44 (100%, $[M+2K]^+$); Found: C, 74.61; H, 8.04; N, 6.59; O, 7.35%. Calc. for $C_{106}H_{132}N_8O_8Zn$: C, 74.38; H, 7.77; N, 6.55; O, 7.48%.

4.2.2.7 2(3)-Tetrakis(2,5-Bis(1,1-dimethylbutyl)-4-methoxyphenoxy)-phthalocyaninatocopper(II) (2b)

2b was synthesized following the same procedure for **1a** using **2** (1.26g, 3mmol), 1-pentanol (50ml), $CuCl_2$ (0.40g, 3mmol), and DBU (2.25ml, 15mmol). The crude product was purified on a silica gel column (CH_2Cl_2/Hexane: 1/1) to afford the target compound as a dark bluish green solid (0.85g, 65.57%). MALDI-TOF MS : m/z 1737.54 (100%, $[M+2K]^+$); Found: C, 74.50; H, 7.43; N, 6.80; O, 7.19%. Calc. for $C_{106}H_{132}N_8O_8Zn$: C, 74.46; H, 7.78; N, 6.55; O, 7.49%.

4.2.2.8 2(3)-Tetrakis(2,5-Bis(1,1-dimethylbutyl)-4-methoxyphenoxy)-phthalocyaninatocobalt(II) (2c)

2c was synthesized following the same procedure for **1a** using **2** (1.26g, 3mmol), 1-pentanol (50ml), $CoCl_2$ (0.39g, 3mmol), and DBU (2.25ml, 15mmol). The crude product was purified on a silica gel column (CH_2Cl_2/Hexane: 1/1) to afford the target compound as a dark bluish green solid (0.62g, 47.56%). MALDI-TOF MS : m/z 1732.52 (100%, $[M+2K]^+$); Found: C, 74.63; H, 7.99; N, 6.41; O, 7.46%. Calc. for $C_{106}H_{132}N_8O_8Zn$: C, 74.66; H, 7.80;

N, 6.57; O, 7.51%.

4.2.3 Preparation of dye-based inks and color filters

Green ink for a color filter was composed of the propylene glycol methyl ether acetate (PGMEA) (3.2g), acrylic binder (1.4g), and phthalocyanine dye (0.1g) or phthalocyanine dye (0.07g) with benzoperylene dye (0.03g).

The prepared dye-based inks were coated on a transparent glass substrate using a MIDAS System SPIN-1200D spin coater. The coating speed was initially 100 rpm for 5 s, which was then increased to 500 rpm and kept constant for 20 s. The wet dye-coated color filters were then dried at 80 °C for 20 min, prebaked at 150 °C for 10 min, and postbaked at 230 °C for 1h. After each step, the coordinate values of the color filters were measured. All spin coated dye-based color filters were 1.6μm thick.

4.2.4 Investigation of solubility

Solubility of the synthesized dyes in PGMEA were examined to determine the effects of substituents at the α and β positions. The prepared dyes were

added to the solvents at various concentrations, and the solutions were sonicated for 5 min using an ultrasonic cleaner ME6500E. The solutions were left to stand for 48 h at room temperature, and checked for precipitation to determine the solubility of the dyes.

4.2.5 Measurement of spectral and chromatic properties

Absorption spectra of the synthesized dyes and transmittance spectra of pigment-based and dye-based color filters were measured using a UV-vis spectrophotometer. Fluorescence spectrum of yellow compensating dye was measured using a Shimadzu RF-5301PC spectrofluorometer. Chromatic values were recorded on a color spectrophotometer (Scinco colormate).

4.2.6 Measurement of thermal stability

Thermal stability of the synthesized dyes was evaluated by TGA. The prepared dyes were heated to 110 °C and held at that temperature for 10 min to remove residual water and solvents. The dyes were then, heated to 220 °C and held at that temperature for 30 min to simulate the processing thermal

conditions of color filter manufacturing. The dyes were finally heated to 400 °C to determine their degradation temperature. The temperature was raised at the rate of 10 °C min^{-1} under nitrogen atmosphere.

To check the thermal stability of the dyes in color filters, the fabricated color filters were heated to 230 °C for 1 h in a forced convection oven (OF-02GW Jeiotech Co., Ltd.). The color difference values (ΔE_{ab}) before and after heating were measured on a color spectrophotometer (Scinco colormate) in CIE L'a'b' mode.

4.3. Results and discussion

4.3.1 Synthesis

The solubility enhanced six metal PCs tetra-substituted at the (β) peripheral and (α) non-peripheral position were designed and synthesized as shown in Scheme 4.1. Each precursor of them (**1, 2**) was synthesized through a nucleophilic aromatic substitution reaction between nitro phthalonitriles and phenols with functional groups having affinity with industrial solvent, PGMEA, and their structures were confirmed by ^{1}H NMR **[6]**.

The metal PCs (**1a~c**, **2a~c**) were synthesized by a cyclotetramerization reaction of the precursors and purified via column chromatography **[7]**. The PCs synthesized from monosubstituted phthalonitriles can theoretically have constitutional isomers, and their properties were observed without further attempts to separate these isomers in this work **[8]**. All metal PCs were obtained in relatively high yields and those with less sterically crowded β-position substituted had slightly higher yields. The structures of synthesized PCs were confirmed by MALDI-TOF spectroscopy and elemental analysis.

A novel compound, monophenylbenzoperylene tetracarbox-diimide **3**, that enlarges its aromatic system along the short molecular axis of perylene asymmetrically was synthesized by reaction between phenyl vinyl boronic acid and bromo-substituted perylenediimides **5** under similar conditions to Suzuki-coupling and spontaneous cyclization as shown in Scheme 4.2. In order to obtain mono-brominated precursor 1-bromoperylene-3,4:9,10-tetracarboxdiimide **4**, the bromination reaction was conducted under milder conditions than standard bromination of perylene, and the isomer 1,7-dibromoperylene-3,4:9,10-tetracarboxdiimide was separated by column chromatography **[9]**. The structure of Monophenyl-benzoperylene **3** was confirmed via ^{1}H NMR, ^{13}C NMR, MALDI-TOF spectroscopy, and elemental analysis.

Synthesized dyes		Solubility (g/100ml)
α-position	Zn (**1a**)	8.5
	Cu (**1b**)	8
	Co (**1c**)	8
β-position	Zn (**2a**)	7
	Cu (**2b**)	6
	Co (**2c**)	6
Yellow (**3**)		8

Table 4.1 Solubility of the synthesized dyes at 20 °C in PGMEA.

4.3.2 Characterization of dyes

4.3.2.1 Solubility of dyes

For dyes to be superior to pigments as colorants for LCD color filters they should exhibit high solubility in industrial solvents. Regardless of the

compatibility with binders, dye molecules should dissolve more than 5wt% in industrial solvents to have the desired optical properties without aggregation. The solubility of all synthesized dyes exceeded 5wt% in industrial solvents, PGMEA, as shown in Table 4.1. When it comes to PC dyes, the bulky functional groups substituted at the α, β-positions cause steric hindrance to reduce intermolecular aggregation and the ether linkages in their structures enhance their miscibility with PGMEA. They were tetra-substituted to have higher solubility than octa-substituted. Their higher solubility was induced from lower crystallinity owing to the isomers **[10,11]**. Dyes **1a~c** substituted at the more sterically crowded α positions showed higher solubility and in each group (**1a~c**, **2a~c**), zinc PCs **1a** and **2a** were more soluble in PGMEA **[12,13]**. Benzoperylene dye **3** also showed superb solubility in PGMEA since the bulky aryl groups substituted at the bay and terminal positions are twisted from the core body of the dye to prevent intermolecular π-π stacking **[14]**.

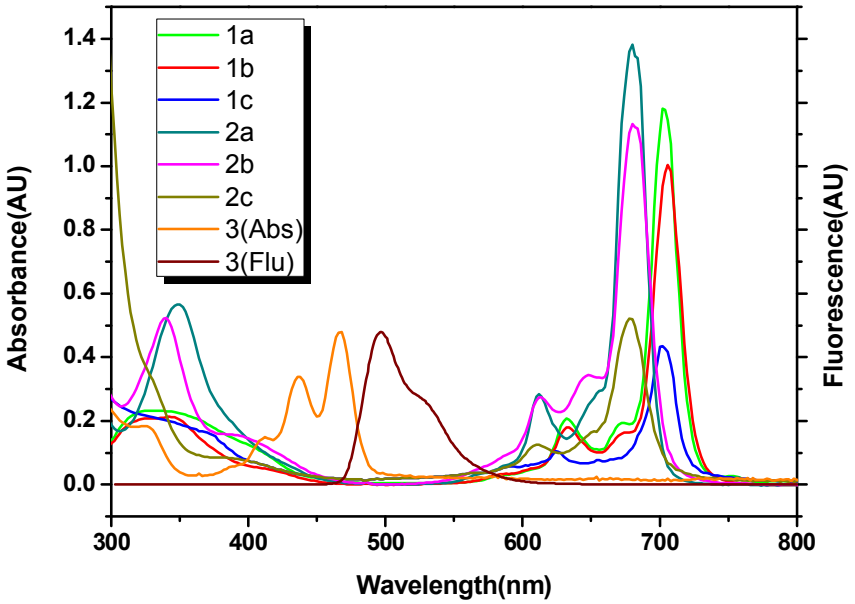

Figure 4.1 Absorption and fluorescence spectra of the synthesized dyes in PGMEA (5×10^{-6}mol liter^{-1} for dyes **1~2** and 10^{-5}mol liter^{-1} for dye 3).

Table 4.2 Absorption spectra of the synthesized dyes in PGMEA.

Synthesized dyes	λ_{max} (nm)	ε_{max} (L mol^{-1} cm^{-1})
1a	702	236000
1b	706	201000

1c	702	87000
2a	680	276000
2b	680	227000
2c	678	104000
3	468	48000

4.3.2.2 Spectral properties of dyes

The green dyes should strongly absorb the range above 630nm to be applied for dye-based LCD color filters effectively. In this aspect, the PCs have very good traits of their spectra for green color filters as well as their excellent stability. The absorption peaks of the six synthesized PC dyes started from 600nm and showed extremely strong and sharp maxima in the range of 680~710nm as shown in Fig. 4.1 The Q-bands of α-position substituted PCs (**1a~c**) were bathochromic shifted approximately 25nm compared to β-position substituted ones (**2a~c**) as shown in Table 4.2. When substituted at α-position, because of the increased electron donating effect of the substitutes, the linear combinations of atomic orbitals coefficients (LCAO) of HOMO levels are greater than those at the β-position, which leads to greater destabilization of

HOMO levels and hence the energy gap between HOMO and LUMO levels decreases **[7,15]**. The cyclic voltammetry curves and oxidation potential data of α, β-position substituted dyes (**1a**, **2a**) are provided in Fig. 4.9 and Table 4.5. Accordingly, β-position substituted PCs (**2a~c**) absorbing relatively more hypsochromic range showed hypsochromic-shifted transmittance compared to α-position substituted PCs (**1a~c**), and hence their transmittance peaks after yellow compensation appeared to be sharper as depicted in latter chapter. As described in the preceding chapter, α-position substituted PCs generally had higher solubility due to the heavily twisted structures which led to the decreased aggregation peak as shown in Fig. 4.1 **[16,17]**. The twisted structures of α-position substituted PCs made their extinction coefficients (ε) smaller than those of β-position substituted PCs, and this tendency was much more severe at the Soret band, as shown in Fig. 4.1. According to the core metals of PCs, the color strength decreased as Zn > Cu > Co.

In order to realize the ideal green colors for LCD display, the dyes should transmit only from 490 to 610nm selectively. Therefore, the yellow compensating dye should be added because this condition cannot be achieved only with PC dyes. The absorption peak of the synthesized benzoperylene diimide dye **3** was optimal for a yellow compensating dye, since it had a very strong absorption maximum at 468 nm, the absorption decreased steeply and

ended just before 500 nm. Moreover, dye **3** showed exceptionally strong color strength compared to other yellow chromophores. In general, stability and color strength of dye molecules often increase with increasing size of the aromatic system, which inevitably causes a bathochromic shift in absorption **[18]**. The fluorescence spectrum range of dye **3** was on the green region as shown in Fig. 4.1, which is advantageous for high transmittance of green color filters **[19]**. Therefore, dye **3** could be combined with PC dyes to make ideal green colors for LCD color filters.

4.3.2.3 Thermal stability of dyes

The dye molecules should have strong intermolecular interactions and form compact aggregates to have high thermal stabilities **[20-22]**. The metal PC dyes as main colorants for green color filters are known to be generally very stable. In particular, they have high thermal stability since they consist of extensive aromatic planar and symmetric systems which lead to one dimensional stacking like rolls of coins. They do not melt; Cu-PC is sublimed in an inert gas atmosphere at approximately 550 °C and ambient pressure **[23-25]**. The benzoperylene dye **3** as a yellow compensating dye is also known to be very stable compared to other yellow chromophores due to the strong π-π stacked

interaction resulting from an extensive aromatic system and a nearly flat molecular structure **[26]**. In particular, this dye can sustain the characteristic high thermal stability of perylene since only one side of the bay positions is substituted to keep the planarity of the perylene main body **[9]**. The high molecular weight and polar substituents of the synthesized green and yellow dyes are advantageous for intermolecular interactions, such as van der Waals force and dipole-dipole interaction **[27]**.

For dyes to be used as color filters, they should endure temperature of 220 °C, which is the current highest temperature in the LCD manufacturing process, without significant weight loss **[28,29]**. The β-position substituted PC dyes (**2a~c**) showed less than 1% weight loss after 30 min at 220 °C and were stable up to 400 °C, whereas the α-position substituted PC dyes except Zn-PC (**1b~c**) showed insufficient thermal stability as shown in TGA graph, Fig. 4.2. This gap in thermal stability is owing to the difference in aggregation tendency from the structural difference. Namely, the difference in the aggregating tendency of the two isomers was attributed to a steric constraint of the α-position isomer that restricts conformational freedom and, consequently, hinders formation of dimer and higher order complexes **[12]**. In the previous report, field emission scanning electron microscopy (FE-SEM) studies of various dyes showed that the dye with less steric hindrance had the bigger

aggregate size that led to superior thermal stability **[30]**. The yellow compensating dye **3** showed less than 3% weight loss in isothermal section as shown in Fig. 4.2, which is also sufficient for the LCD manufacturing process. The practical thermal stability of spin coated color filters needs to be discussed with color difference (ΔE_{ab}) values as expressed in latter chapter since it is affected by the compatibility with industrial solvents and binders as well as the inherent thermal stability of dye molecules.

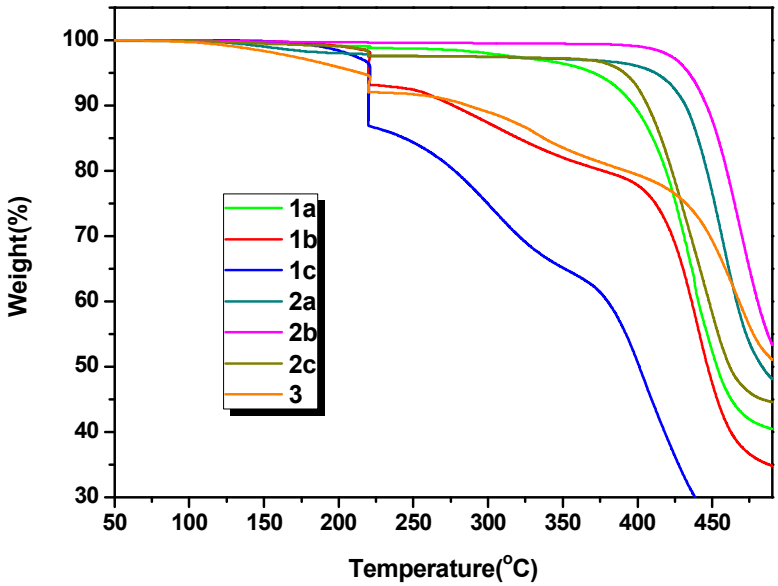

Figure 4.2 Thermogravimetric analysis (TGA) of the synthesized dyes.

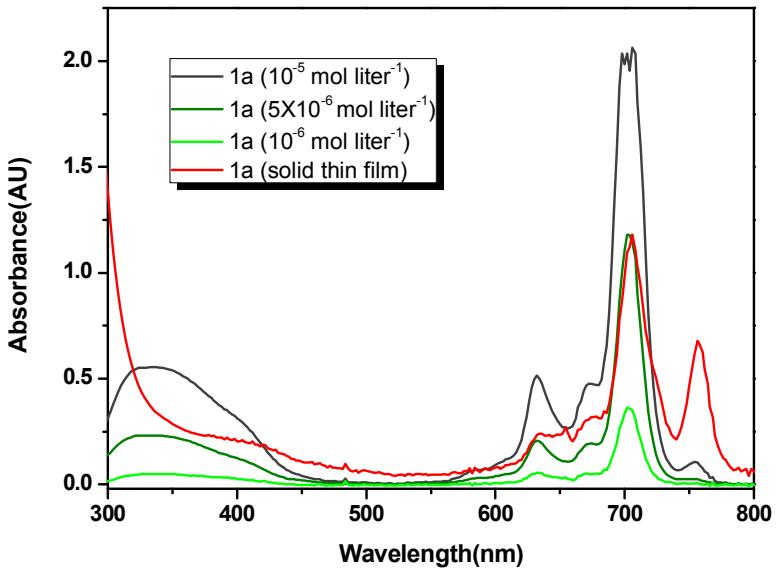

Figure 4.3 The UV/Vis absorption spectra of the synthesized dye, **1a**, at different concentrations in PGMEA and in the solid thin films.

4.3.3 Characterization of dye-based color filters

4.3.3.1 Spectral and chromatic properties of dye-based color filters

In order to make vivid and bright green color in LCD displays, the transmittance graphs of the color filters should be sharp and have transmission

maxima between 520~550nm. Fig. 4.4 and Fig. 4.5 show the transmittance graphs of the spin-coated color filters with synthesized green dyes. Each figure includes the spectra of green color filters before and after compensation with the yellow dye **3**, and a comparison is made between them and pigment-based color filter. The dye-based color filters had superior transmittance compared to pigment-based one because dyes dissolved in the media have a smaller particle size leading to less light scattering **[27,31]**. When the yellow compensating dye **3** is added to color resists, clearer green colors were obtained since the undesirable transmittance under 500nm was cut off and the wavelengths of maximum transmittance were red-shifted approximately 4~40nm. Therefore, the transmittances without yellow compensation had their maxima near 520nm, and the ones with yellow compensation had their maxima near 540nm as shown in Table 4.3. Before the yellow compensation, dye **2b** showed the highest maximum transmittance (94.85%) and after the yellow compensation, dye **1b** showed the highest maximum transmittance (94.47%). Except the dye **2b**, the maximum transmittances of the dyes increased after yellow compensation due to the fluorescence of the yellow dye 3 and the lowered contents of the green dyes **[19]**. In general, the color filters coated with α-position substituted PC dyes (**1a~c**) had slightly higher transmittance than those with β-position substituted ones (**2a~c**) due to the lower aggregating tendency. The α-position

substituted PC dyes are considered to show reduced light scattering after spin-coated onto the substrate which leads to the higher transmittance. Co-PC dyes (**1c**, **2c**) showed lower transmittance than other metal PC dyes on average.

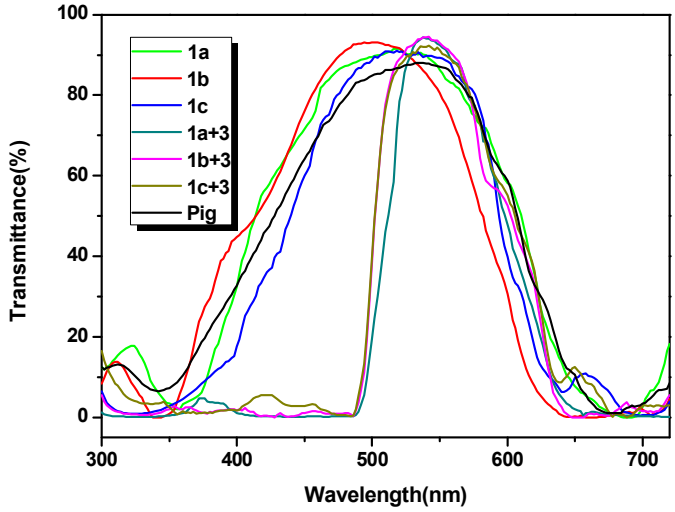

Figure 4.4 Transmittance spectra of the pigment-based and dye-based color filters.

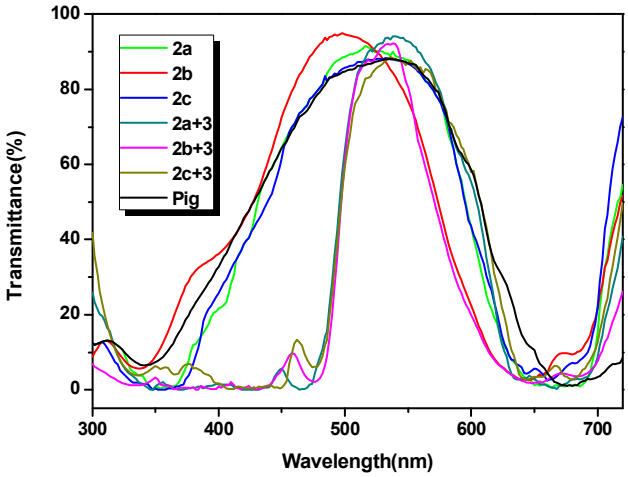

Figure 4.5 Transmittance spectra of the pigment-based and dye-based color filters.

Table 4.3 Transmittance of the pigment-based and dye-based color filters.

Spin-coated dyes	Transmittance at 520nm (%)	Transmittance at 540nm (%)	λ_{max}	$\Delta\lambda_{1/2}$
1a	91.56	89.96	520nm (91.56%)	204nm
1b	91.67	85.23	502nm (93.12%)	178nm
1c	90.76	89.79	518nm (90.97%)	161nm
2a	90.78	88.81	516nm (91.51%)	170nm

2b	91.49	83.32	498nm (94.85%)	152nm
2c	87.78	87.81	532nm (88.35%)	169nm
1a+3	78.52	94.05	538nm (94.38%)	92nm
1b+3	88.93	94.37	542nm (94.47%)	103nm
1c+3	87.50	91.97	542nm (92.34%)	106nm
2a+3	90.54	94.13	538nm (94.14%)	111nm
2b+3	87.42	92.07	538nm (92.24%)	78nm
2c+3	83.39	88.01	536nm (88.69%)	115nm
Pigment	86.78	87.91	536nm (88.11%)	193nm

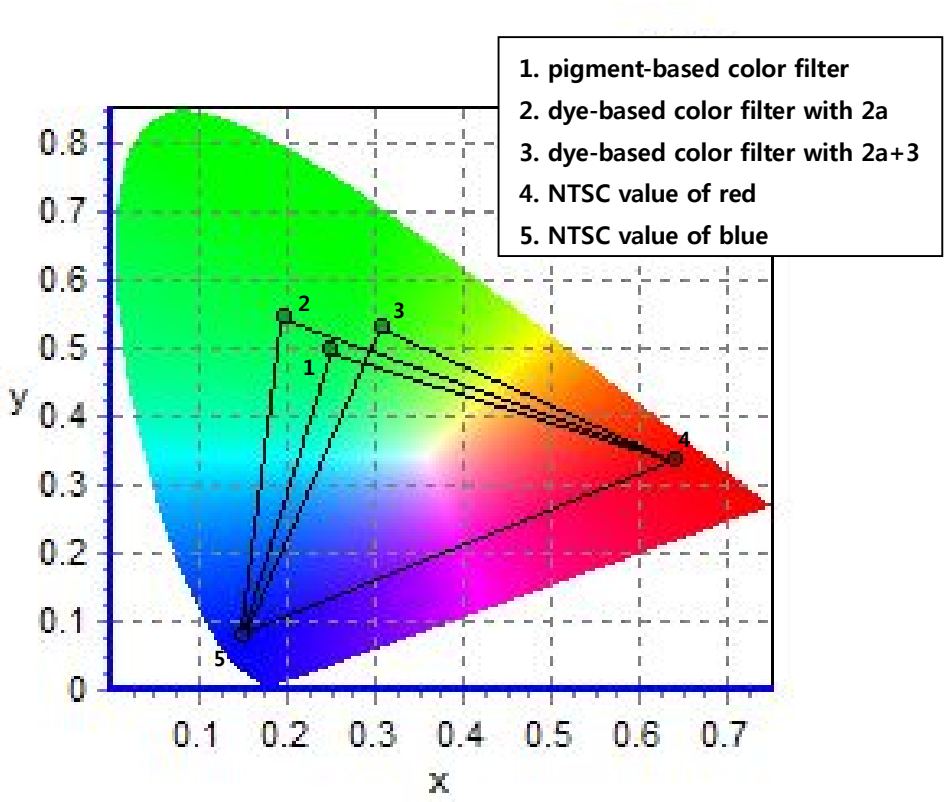

Figure 4.6 CIE 1931 chromaticity diagram of the pigment-based and dye-based color filters.

The coordinate values of the spin coated dye-based color filters are expressed in Table 4.4 and Fig. 4.6 with comparison to a pigment-based color filter. The all dye-based color filters are so economical that they showed similar or larger color gamuts in spite of the much lower colorant contents in the inks

due to the much higher tinctorial strength and the fluorescence of the compensating dye **[9,19]**. The color matching function of the variable $\bar{y}$, determining the brightness (Y) value of green color, has the highest level of contribution near 540nm as shown in Fig. 4.7. It is noted that the Y values after compensation with yellow dye **3** increased because in the vicinity of 540nm the transmittance after compensation was higher as shown in Table 4.3. The Y values of the color filters with Co-PC dyes (**1c**, **2c**) were lower than those with other metals as in the case of transmittance, but their color gamut expanded thanks to the increased y values. They exhibited more bluish green colors because of the decreased x values.

Table 4.4 The coordinate values corresponding to the CIE 1931 chromaticity diagram and the color difference values of the pigment-based and dye-based color filters.

Spin-coated dyes	Y	x	y	$\triangle E_{ab}$
1a	55.67	0.206	0.55	1.88

1b	58.98	0.215	0.546	6.95
1c	48.51	0.190	0.589	13.03
2a	54.13	0.194	0.545	1.45
2b	56.25	0.203	0.532	0.93
2c	49.46	0.181	0.607	2.15
3	93.28	0.433	0.515	1.04
1a+3	60.62	0.309	0.537	2.61
1b+3	61.24	0.303	0.539	8.08
1c+3	51.37	0.236	0.564	16.73
2a+3	59.56	0.308	0.526	2.20
2b+3	60.14	0.299	0.519	1.87
2c+3	55.70	0.260	0.585	3.46
Pigment	57.86	0.244	0.504	0.85

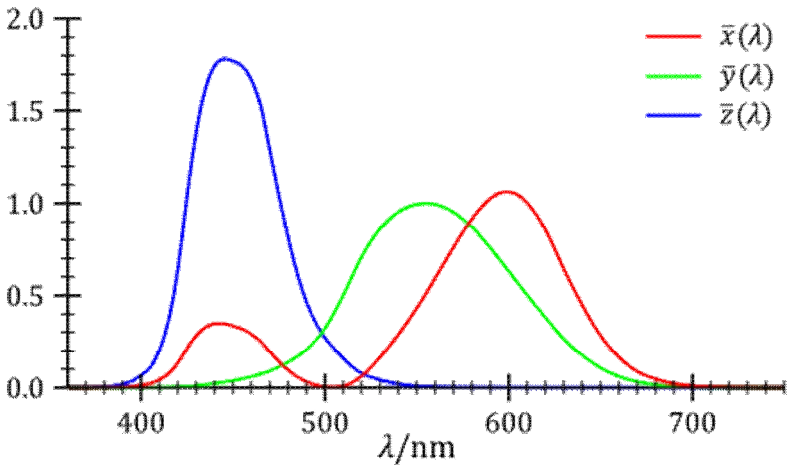

Figure 4.7 The CIE 1931 XYZ color matching functions.

4.3.3.2 Thermal stability of dye-based color filters

In order to estimate the thermal stability of color filters, the ΔE_{ab} values resulting from post-baking were measured as shown in Table 4.4. The ΔE_{ab} values of the color filters should be less than 3 after heating for one hour at 230 °C for commercial applications **[9]**. The ΔE_{ab} values of the dye-based color filters except **1b** and **1c** were smaller than 3, which means that their thermal stability is sufficient to be applied for LCD color filters. The difference of thermal stability resulting from structural difference were reflected so as that the color filters with β-position substituted PC dyes (**2a~c**) showed smaller ΔE_{ab}

than those of color filters with α-position substituted PC dyes (**1a~c**). In general, the thermal stabilities of the color filters with Co-PC dyes, deduced from the ΔE_{ab} values, were lower than other metal PC dyes, which accords with the results of TGA analysis. The yellow compensating dye, benzoperylene diimide **3**, showed a good ΔE_{ab} value of 1.04 when solely spin coated, but exhibited bigger ΔE_{ab} values to some degree when blended with green PC dyes. These results are considered to mean that although the thermal stabilities of the individual dyes are superb, their color difference values can increase due to the enhanced migration of dye molecules when blended with each other and added to an industrial solvent and binder. Nevertheless, the dyes **1a**, **2a**, and **2b** showed sufficient thermal stability when spin coated to color filters with or without dye **3**, although the ΔE_{ab} values of the dye-based color filters with them were slightly higher than that of the pigment-based color filter.

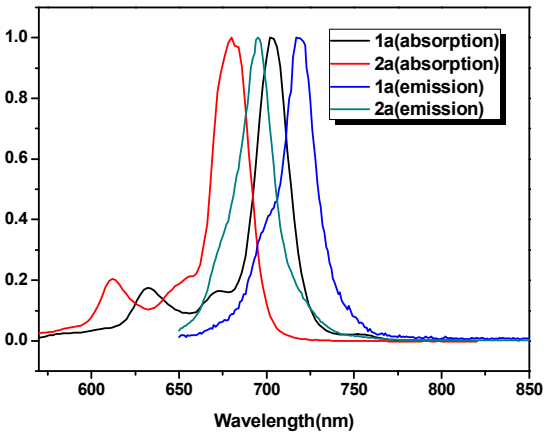

Figure 4.8 Normalized absorption and fluorescence spectra of the synthesized dyes, **1a** and **2a**, in PGMEA (5×10^{-6}mol litre^{-1}).

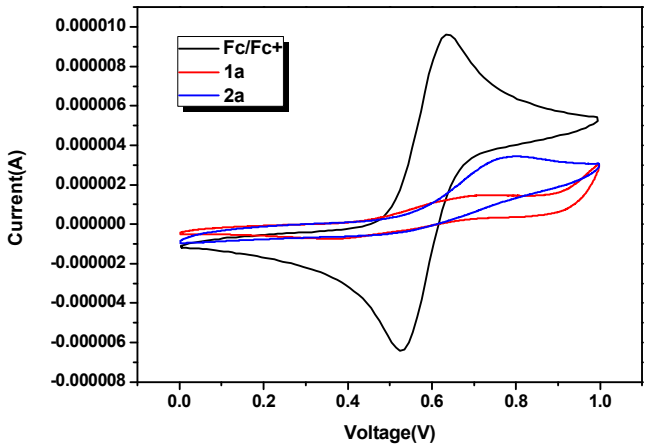

Figure 4.9 Cyclic voltammetry curves of ferrocene/ferrocenium (Fc/Fc^{+}), **1a** and **2a** in CH_2Cl_2.

Table 4.5 Optical and electrochemical properties of the synthesized dyes, **1a** and **2a**.

[a] Measured in 5×10^{-6}mol litre^{-1} of PGMEA solutions at room temperature.

[b] Measured in CH_2Cl_2 containing 0.1mol litre^{-1} of tetrabutylammonium tetrafluoroborate ($TBABF_4$) electrolyte (working electrode: glassy carbon; counter electrode: Pt; reference electrode: Ag/Ag^+; calibrated with Fc/Fc^+ as an internal reference and converted to NHE by addition of 630mV).

[c] Estimated from intersection wavelengths between absorption and emission spectra.

dye	absorption[a]	emission[a]	Oxidation potential data[b]		
	λ_{max}	λ_{max}	E_{ox} (vs NHE)	$E_{0\text{-}0}$[c]	E_{ox}-$E_{0\text{-}0}$ (vs NHE)
1a	702nm	717nm	0.554V	1.744V	-1.190V
2a	680nm	695nm	0.644V	1.802V	-1.158V

4.4 Conclusions

The six PC dyes and a benzoperylene dye were synthesized and applied for dye based color filters. The synthesized dyes were highly soluble in industrial solvents, PGMEA and uniformly spin coated to glass substrates without severe aggregation. The various properties of PC dyes for the color filters were influenced by the positions of the bulky substituents. The β-position substituted PC dyes were superior in the absorption range, color strength and thermal stability, but inferior in solubility to the α-position substituted ones. The prepared dye-based color filters exhibited excellent transmittance due to the smaller particle size of the dye molecules suppressing light scattering. In addition, they expressed similar or larger color gamuts in spite of the much lower colorant contents in the inks, due to a much higher tinctorial strength compared to the pigment-based color filter. When the yellow compensating dye **3** was mixed in the color filters, the half-band width of the transmittance peak decreased due to its absorption. In addition, the maximum transmittance and the brightness(Y) of the coordinate values increased due to its fluorescence, which led to a vivid green color.

In conclusion, the phthalocyanine and benzoperylene dyes were successfully applied to the LCD color filters and showed superior optical

properties than conventional pigment-based color filters. Some dyes were also sufficient in thermal stability, and hence, showed potential for use in high-definition displays.

4.5 References

[1] K. Tsuda, *Displays*, 1993, **14**, 115.

[2] R. W. Sabnis, *Displays*, 1999, **20**, 119.

[3] K. Takanori, N. Yuki, N. Yuko, Y. Hidemasa, W. B. Kang, P. G. Pawlowski, *Jpn J Appl Phys.*, 1998, **37**, 1010.

[4] D. Y. Na, I. B. Jung, S. Y. Nam, C. W. Yoo, Y. J. Choi, *J Korean Inst Electr Electron Mater Eng.*, 2007, **20**, 450.

[5] T. Sugiura. *J Soc Inf Disp.*, 1993, **1**, 177.

[6] M. S. Aĝritaş, *Dyes Pigm.*, 2007, **74**, 490.

[7] G. Cheng, X. Peng, G. Hao, V. O. Kennedy, I. N. Ivanov, K. Knappenberger, T. J. Hill, M. A. J. Rodgers and M. E. Kennedy, *J. Phys. Chem. A*, 2003, **107**, 3503.

[8] A. Erdoĝmuş and T. Nyokong, *Dyes Pigm.*, 2010, **86**, 174.

[9] J. Choi, C. Sakong, J. H. Choi, C. Yoon, J. P. Kim, *Dyes Pigm.*, 2011, **90**, 82.

[10] W. Eberhardt, M. Hanack, *Synthesis*, 1997, 95.

[11] C. C. Leznoff, S. M. Marcuccio, S. Greenberg, A. B. P. Lever, K. B. Tomer, *Can. J. Chem.*, 1985, **63**, 623.

[12] R. D. George, A. W. Snow, J. S. Shirk, W. R. Barger, *J. Porphyr. Phthalocyan.*, 1998, **2**, 1.

[13] A. W. Snow, in: K. M. Kadish, K. M. Smith, R. Guilard (Eds.), Porphyrin Handbook, Phthalocyanines: Properties and Materials, Academic Press, New York, 2003, vol. 17.

[14] G. Seybold, G. Wagenblast, *Dyes Pigm.*, 1989, **11**, 303.

[15] J. Mark, M. J. Stillman, *J. Am. Chem. Soc.*, 1994, **116**, 1292.

[16] M. Durmus, T. Nyokong, *Inorg. Chem. Commun.*, 2007, **10**, 332.

[17] H. Li, T. J. Jensen, F. R. Fronczek, M. G. H. Vicente, *J. Med. Chem.*, 2008, **51**, 502.

[18] H. Zollinger, *Color Chemistry*, VCH, Weinheim, 1987.

[19] Y. J. Hwang, D. M. Shin, *Mol. Cryst. Liq. Cryst*., 2007, **472**, 25.

[20] C. H. Giles, D. G. Duff, R. S. Sinclair. *Rev Prog Coloration*, 1982, **12**, 58.

[21] S. Das, R. Basu, M. Minch, P. Nandy, *Dyes Pigm.*, 1995, **29**, 191.

[22] Z. Chunlong, M. Nianchun, L. Liyun, *Dyes Pigm.*, 1993, **23**, 13.

[23] W. Herbst, K. Hunger, Industrial organic pigments: production, properties, applications: Third edition. Willey-VCH. 1998.

[24] P. F. Gordon, P. Gregory, Organic chemistry in colour, Springer-Verlag, 1987.

[25] N. Kobayashi, *Bull. Chem. Soc. Jpn*., 2002, **75**, 1.

[26] S. Müller, K. Müllen, *Chem. Commun*., 2005, 4045.

[27] Y. D. Kim, J. P. Kim, O. S. Kwon, I. H. Cho, *Dyes Pigm.*, 2009, **81**, 45.

[28] T. Ohmi, *JSME Int J Ser B (Jpn Soc Mech Eng)*, 2004, **47**, 422.

[29] T. Takamatsu, S. Ogawa, M. Ishii, *Sharp Tech J*, 1991, **50**, 69.

[30] C. Sakong, Y. D. Kim, J. H. Choi, C. Yoon, J. P. Kim, *Dyes Pigm.*, 2011, **88**, 166.

[31] R. J. D. Tilley. Colour and optical properties of materials, John Wiley & Sons Inc, Chichester, 2000.

Chapter 5

Synthesis and Characterization of Novel Triazatetra benzcorrole Dyes for LCD Color Filter and Black Matrix

5.1 Introduction

Liquid crystal display (LCD) modules, which are widespread media in today's information age, are composed of a back light unit, a color filter (CF), and a thin-film transistor (TFT) board, with a liquid crystal between CF and TFT board. The CF, which converts the white backlight into various colored lights, consists of RGB (red, green, and blue) pixels, a black matrix (BM) for prevention of light leakage, an overcoat for improving the flatness of the pixel surface, and a column spacer to control the gap between cells [**1-4**].

Currently, various dye molecules are under extensive investigation for the manufacturing of RGB pixels and BM to improve the performance of LCD. The pigments, being used for the main colorants of RGB pixels, show superior

thermal and photo-chemical stabilities, but have low optical and chromatic properties due to their aggregation behavior **[5, 6]**. Dyes can be attractive alternatives to overcome this limitation due to the reduced light scattering resulting from the fact that they can be dissolved in the media and exist in molecular form. Recently, their superior optical properties for higher brightness have outweighed the inferior thermal stabilities because the LCD manufacturing process temperature has been decreasing [**7**]. The colorants for LCD BMs should not interfere with the electrical signals of TFT to be applied for color filter on array (COA) mode that CF is patterned right onto the TFT array. Therefore, extensive investigation is currently being performed on colorants with low dielectric constants such as dyes, so that LCD BMs can replace the carbon black with high dielectric constant [**8, 9**]. Recently, our group applied the phthalocyanine (PC) derivatives with high color strength and thermal stability to LCD CF and BM by improving their solubility **[10, 11]**. In this study, the novel triazatetrabenzcorrole (TBC) dyes were designed and synthesized through the ring contraction process of PC dyes. They exhibited more advantageous absorption peaks for LCD CF and BM than PC dyes, and enhanced solubility to the industrial solvents by the introduction of bulky axial substituents. For the above purpose, the thermal stability, optical properties, and solubility of the prepared dyes as the colorant materials for LCD CF and BM

were investigated according to their characteristic structures. In addition, the transmittance, color gamut, and dielectric constants of the spin-coated films with these dyes were examined.

5.2 Experimental

5.2.1 Materials and instrumentation

1,8-Diazabicyclo-7-undecene (DBU), 3(4)-nitrophthalonitrile, 2,5-bis-(1,1-dimethylbutyl)-methoxyphenol purchased from TCI, and 4-methylphenol, PBr_3, $CuCl_2$ purchased from Sigma-Aldrich were used as received. All the other reagents and solvents were of reagent-grade quality and obtained from commercial suppliers. Transparent glass substrates were provided by Paul Marienfeld GmbH & Co. KG. Commercial pigment-based CF and acrylic binder DW1 were supplied by NDM Inc.

^1H NMR spectra were recorded on a Bruker Avance 500 spectrometer at 500MHz using chloroform-d and TMS, as the solvent and internal standard, respectively (Seoul National University National Center for inter-University Research Facilities). Matrix Assisted Laser Desorption/Ionization Time Of Flight (MALDI-TOF) mass spectra were collected on a Voyager-DE STR

Biospectrometry Workstation with a-cyano-4-hydroxy-cynamic acid (CHCA) as the matrix. Absorption and transmittance spectra were measured using a HP 8452A spectrophotometer. Fluorescence spectra were measured using a Shimadzu RF-5301PC spectrofluorometer. Elemental analysis was carried out with a Flash EA 1112 CNH analyzer. Cyclic voltammetry was performed using a three-electrode cell and a VersaSTAT 3-100. Chromatic characteristics of the spin-coated films were analyzed on a Scinco color spectrophotometer. Dielectric constants were measured using Edward E306 thermal evaporator and Agilent 4294A precision impedance analyzer. Thermogravimetric analysis (TGA) was conducted under nitrogen at a heating rate of 10 °C min-1 using a TA Instruments Thermogravimetric Analyzer 2050. The thickness of the spin-coated film was measured using a Nano System Nanoview E-1000. Field emission scanning electron microscopy (FE-SEM) images of spin-coated films were taken by JSM-840A microscope.

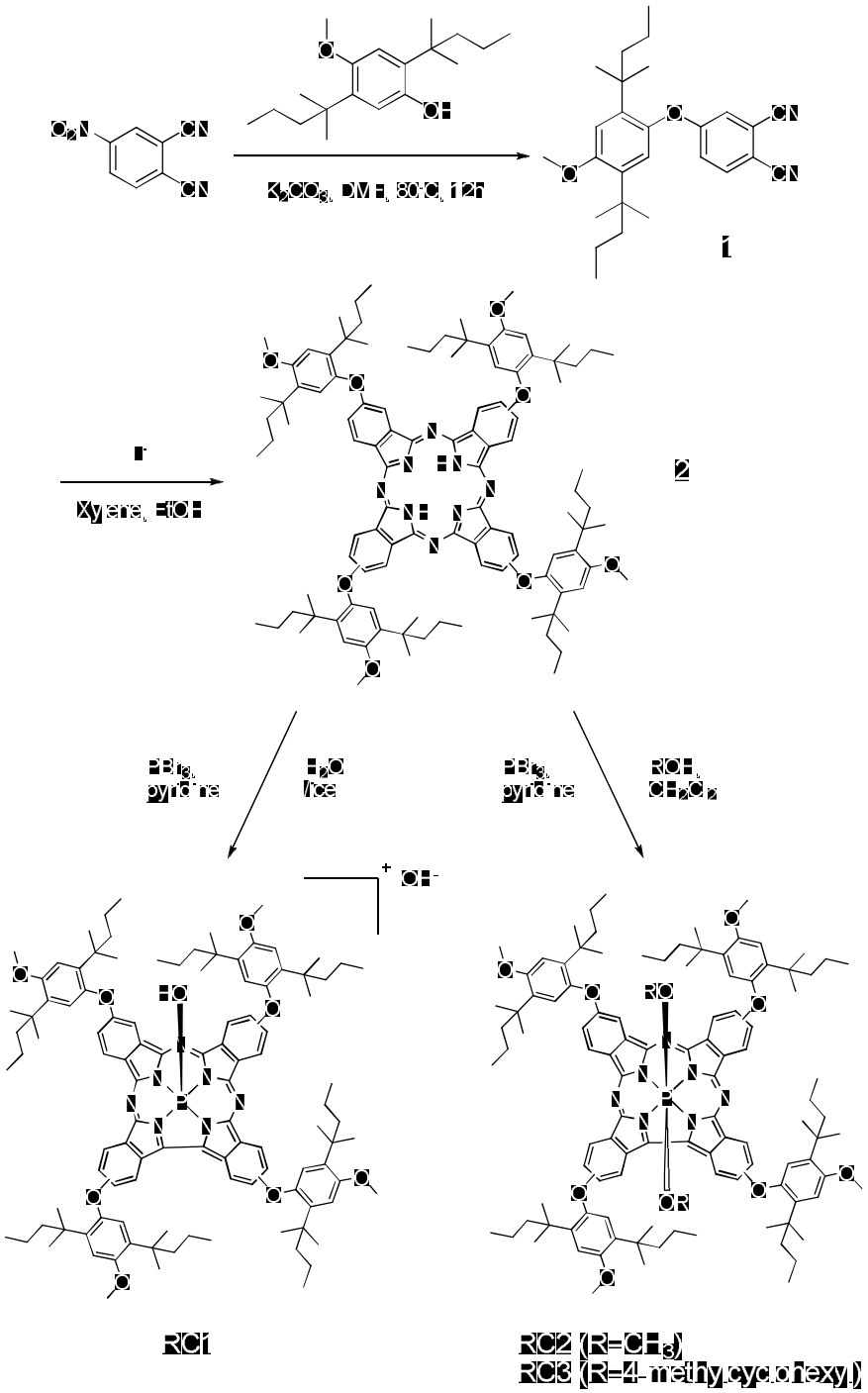

Scheme 5.1 Synthesis of triazatetrabenzcorrole dyes.

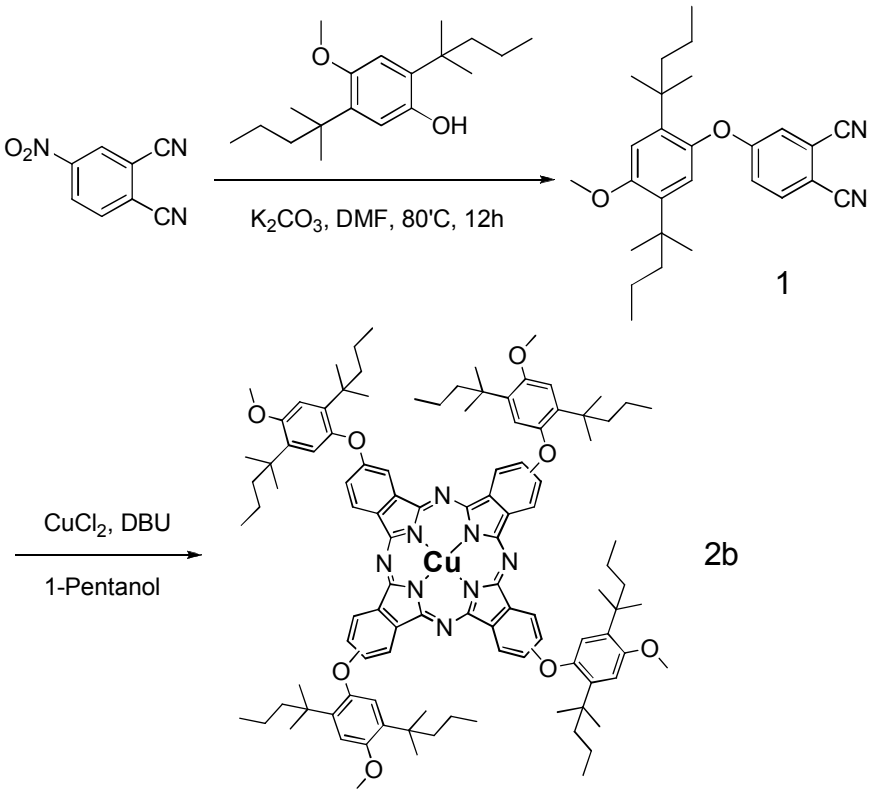

Scheme 5.2 Synthesis of phthalocyanine dye.

5.2.2 Synthesis

2(3)-Tetrakis(2,5-Bis(1,1-dimethylbutyl)-4-methoxyphenoxy)-phthalocyanine (**2**) was synthesized according to the previously reported procedures **[11]**, 2(3)-Tetrakis(2,5-Bis(1,1-dimethylbutyl)-4-methoxyphenoxy)-phthalocyaninatocopper(II) (**2b**) and N,N'-Bis(2,6-diisopropylphenyl)-5-

phenylbenzoperylene-2,3,8,9-tetracarboxdiimides (**3**) were synthesized according to the procedures reported elsewhere [**10**].

5.2.2.1 Hydroxyphosphorus(V)2(3)-Tetrakis(2,5-Bis(1,1-dimethylbutyl)-4-methoxyphenoxy)-triazatetrabenzcorrole Hydroxide (RC1)

2 (1.24g, 0.74mmol) was placed in a 100 mL flask equipped with a condenser and gas inlet adapter and dissolved in 20 mL of pyridine. An amount of PBr_3 (9.0 g, 33.0 mmol) was added and the resulting solution heated to 120 °C and stirred for 2 h. After 2 h, approximately 3/4 of the solvent was allowed to evaporate under a flow of argon. The mixture was then poured into a water/ice bath and the resulting suspension filtered to give a green solid. The solid was purified on a silica gel column using 1/6 ethyl acetate/hexane as the eluent. The bright green band was collected and concentrated producing **RC1** as a bright green solid (0.45 g, 35%). MALDI-TOF MS : m/z 1725.0 (100%, $[M+OH]^+$); Found: C, 75.07; H, 8.15; N, 5.75. Calc. for C108H138N7O10P: C, 75.19; H, 8.06; N, 5.68.

5.2.2.2 Dimethoxyphosphorus(V)2(3)-Tetrakis(2,5-Bis(1,1-dimethylbutyl)-4-methoxyphenoxy)-triazatetrabenzcorrole (RC2)

2 (1.24g, 0.74mmol) was placed in a 100 mL flask equipped with a condenser and gas inlet adapter and dissolved in 30 mL of pyridine. An amount of PBr_3 (9.0 g, 33.0 mmol) was added and the resulting solution heated to 120 °C and stirred for 2 h. After 2 h, the volume of the reaction mixture was reduced by vacuum distillation to 1-2 mL and then treated with a 50/50 solution of CH_2Cl_2/MeOH for 2 h. The resulting green solid was dissolved in CH_2Cl_2 and filtered to remove excess pyridinium bromide as a white crystalline solid. The filtrate was reduced in volume under reduced pressure and loaded onto a silica gel column for purification with 1/7 ethyl acetate/hexane as the eluent. The bright green band to elute was collected and dried under vacuum to give **RC2** as a bright green solid (0.75 g, 58%). MALDI-TOF MS : m/z 1752.4 (100%, $[M^+]$); Found: C, 75.17; H, 8.20; N, 5.65. Calc. for C110H142N7O10P: C, 75.35; H, 8.16; N, 5.59.

5.2.2.3 Di(4-methylcyclohexoxy)phosphorus(V)2(3)-Tetrakis(2,5-Bis(1,1-dimethylbutyl)-4-methoxyphenoxy)-triazatetrabenzcorrole (RC3)

2 (1.24g, 0.74mmol) was placed in a 100 mL flask equipped with a condenser and gas inlet adapter and dissolved in 30 mL of pyridine. An amount

of PBr_3 (9.0 g, 33.0 mmol) was added and the resulting solution heated to 120 °C and stirred for 2 h. After 2 h, the volume of the reaction mixture was reduced by vacuum distillation to 1-2 mL and then treated with a 50/50 solution of CH_2Cl_2/4-methylcyclohexanol for 12 h. The resulting green solid was dissolved in CH_2Cl_2 and filtered to remove excess pyridinium bromide as a white crystalline solid. The filtrate was reduced in volume under reduced pressure and loaded onto a silica gel column for purification with CH_2Cl_2 as the eluent. The second bright green band to elute was collected and loaded onto a silica gel column for purification again with 3/40 ethyl acetate/hexane as the eluent. The first bright green band to elute was collected and dried under vacuum to give **RC3** as a shiny bright green solid (0.78 g, 55%). MALDI-TOF MS : m/z 1917.8 (100%, $[M^+]$); Found: C, 76.11; H, 8.56; N, 5.13. Calc. for $C_{122}H_{162}N_7O_{10}P$: C, 76.41; H, 8.52; N, 5.11.

5.2.3 Preparation of dye-based inks and spin-coated films

Dye-based ink for a CF and BM was composed of the propylene glycol methyl ether acetate (PGMEA) (2.8g), acrylic binder (2.0g), and dye (0.07g). The prepared dye-based inks were coated on a transparent glass substrate using a MIDAS System SPIN-1200D spin coater. The coating speed was initially 100

rpm for 10 s, which was then increased to 600 rpm and kept constant for 20 s. The wet dye-coated glasses were then dried at 80 °C for 20 min, prebaked at 150 °C for 10 min, and postbaked at 230 °C for 1h. After each step, the coordinate values of the dye-coated glasses were measured.

5.2.4 Investigation of solubility

Solubility of the synthesized dyes in propylene glycol methyl ether acetate (PGMEA) were examined to determine the effects of peripheral and axial substituents. The prepared dyes were added to the solvents at various concentrations, and the solutions were sonicated for 5 min using an ultrasonic cleaner ME6500E. The solutions were left to stand for 48 h at room temperature, and checked for precipitation to determine the solubility of the dyes.

5.2.5 Measurement of spectral and chromatic properties

Absorption spectra of the synthesized dyes and transmittance spectra of pigment-based and dye-based CFs were measured using a UV-vis spectrophotometer. Fluorescence spectrum of the synthesized dyes were measured using a Shimadzu RF-5301PC spectrofluorometer. Chromatic values

were recorded on a color spectrophotometer (Scinco colormate).

5.2.6 Measurement of dielectric properties

The prepared dye-based inks were coated on a aluminum substrate using a MIDAS System SPIN-1200D spin coater. The coating speed was initially 100 rpm for 10 s, which was then increased to 800 rpm and kept constant for 20 s. Aluminum electrodes were deposited by Edward E306 thermal evaporator and capacitances were measured by Agilent 4294A precision impedance analyzer.

5.2.7 Measurement of thermal stability

Thermal stability of the synthesized dyes was evaluated by TGA. The prepared dyes were heated to 110 °C and held at that temperature for 10 min to remove residual water and solvents. The dyes were then, heated to 220 °C and held at that temperature for 30 min to simulate the processing thermal conditions of CF manufacturing. The dyes were finally heated to 400 °C to determine their degradation temperature. The temperature was raised at the rate of 10 °C min-1 under nitrogen atmosphere.

To check the thermal stability of the dyes in spin-coated films, the

fabricated spin-coated glasses were heated in a forced convection oven (OF-02GW Jeiotech Co., Ltd.). The color difference values (ΔE_{ab}) before and after heating were measured on a color spectrophotometer (Scinco colormate) in CIE L'a'b' mode.

5.3 Results and Discussion

5.3.1 Synthesis

The novel three TBC phosphorus compounds with enhanced solubility and broadened absorption peak were designed and synthesized as shown in Scheme 5.1. Each precursor of metal-free PC (**1**) was synthesized through a nucleophilic aromatic substitution reaction between nitro phthalonitriles and phenols with the functional groups having affinity with the industrial solvent, PGMEA, and its structure was confirmed by ^{1}H NMR [**12**]. The metal-free PC (**2**) was synthesized by a cyclotetramerization reaction of the precursors and purified via column chromatography [**13**]. The PCs synthesized from monosubstituted phthalonitriles can theoretically have constitutional isomers, and their properties were observed without further attempts to separate these isomers in this work [**14**]. The TBC phosphorus compounds were synthesized via a ring-

contraction reaction mediated by PBr_3 in pyridine in which a meso-nitrogen atom is extruded from an appropriate metal-free PC precursor. In order to ensure a good yield of TBC, the pyridine must be carefully distilled over CaH_2, and the phthalocyanine starting material must be dried in a heated (50 °C) vacuum oven for several hours immediately prior to use [**15**]. After the ring-contraction reaction, the TBC compound **RC1** was successfully precipitated by quenching with an ice/water mixture. Purification by silica gel chromatography was carried out by using ethyl acetate/hexane solution as the eluent, rather than ROH/CH_2Cl_2 solution, to avoid any axial ligand exchange with alcohols. The TBC compounds **RC2** and **RC3** were synthesized by quenching with an appropriate ROH/CH_2Cl_2 mixture. The structures of synthesized TBCs were confirmed by MALDI-TOF spectroscopy and elemental analysis.

Table 5.1 Solubility of the synthesized dyes at 20 °C in PGMEA.

Synthesized dyes	Solubility (g/100ml)
2b	**6**
RC1	**9**

RC2	**9**
RC3	**10**

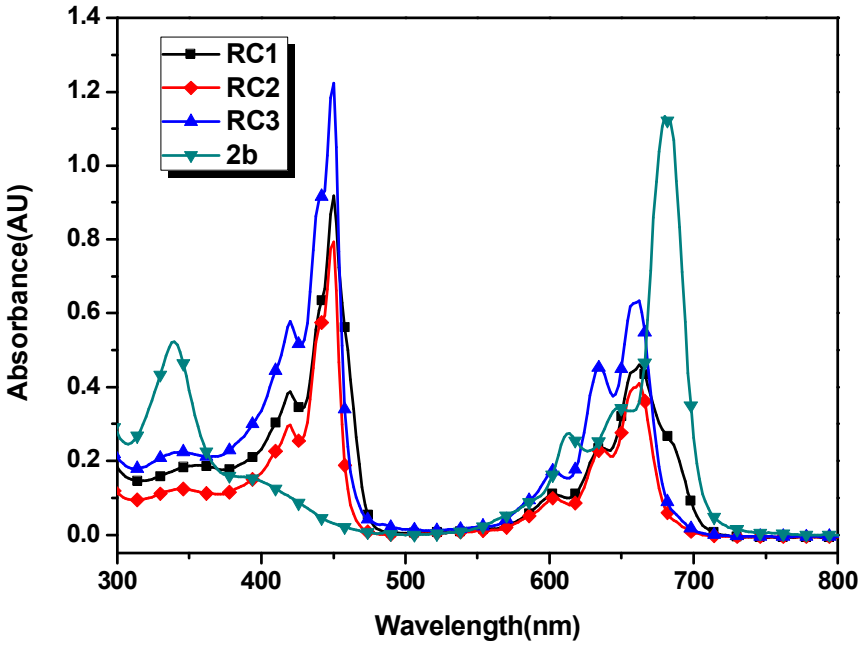

Figure 5.1 Absorption spectra of the synthesized dyes in PGMEA (5×10^{-6}mol liter^{-1}).

5.3.2 Characterization of dyes

5.3.2.1 Solubility of dyes

For dyes to be successfully applied as colorants for LCD CF or BM, they should exhibit high solubility in industrial solvents. Regardless of the compatibility with binders, dye molecules should dissolve more than 5wt% in industrial solvents to have the desired optical properties [**10,11,16**]. Especially, to prevent the reaggregation behavior between the dye molecules after the post baking process, bulky substituents should be introduced and indeed such molecules are therefore normally also better soluble in organic solvents. Such a reaggregation between molecules is believed to be the primary cause of the decline of transmittance of LCD CFs. The solubility data of the synthesized dyes in industrial solvent, PGMEA, are listed in Table. 5.1. In the case of PC dye **2b**, as found in the previous work, the bulky functional groups substituted at the peripheral positions caused steric hindrance to reduce intermolecular aggregation and the ether linkages in its structures enhanced its miscibility with PGMEA [**10**]. However, the introduction of bulky axial ligands was considerably more effective in hindering the intermolecular π-π stacking

between phthalocyanine hetero cycles [**17-22**]. The **RC1~3** dyes, with bulky axial ligands at the phosphorus atom, showed considerably higher solubility than PC dye **2b** with only peripheral substituents in PGMEA. In particular, **RC3** exhibited the highest solubility contributed by the bulkiest axial substituent, the methylcyclohexoxy group. The increased solubility can be advantageous for the **RC1~3** series to show excellent optical properties as the colorant materials for LCD.

Table 5.2 Absorption spectra of the synthesized dyes in PGMEA (5×10^{-6}mol liter^{-1}).

Synthesized dyes	λ_{max} (nm)	ε_{max} (L mol-1 cm-1)
RC1	**450, 662**	**184000, 92000**
RC2	**450, 662**	**159000, 82000**
RC3	**450, 662**	**245000, 127000**
2b	**340, 680**	**105000, 227000**

5.3.2.2 Spectral properties of dyes

The UV-vis absorption spectra of PC dye **2b** and TBC dyes **RC1~3** are shown in Fig. 5.1 and the corresponding data are listed in Table 5.2. As reported elsewhere, the absorption peaks of TBC compounds **RC1~3** had a red-shifted Soret band and blue-shifted Q-band compared to the corresponding PC dye **2b** [**23-25**]. These traits can be extremely beneficial for dyes **RC1~3** to be applied as colorants of green CF and BM of an LCD.

For dye-based LCD CF, the green dyes should strongly absorb the range above 630 nm [**10**]. The absorption peaks of the three synthesized TBC dyes started from 600nm and showed extremely strong and sharp maxima in the range of 650~680 nm as shown in Fig. 5.1. In addition, the growth and bathochromic shift of the Soret bands induced from the conversion from PC compounds to TBC compounds is extremely crucial for these TBC compounds to exhibit vivid green colors. This very strong and sharp absorption at 450 nm cut off the transmittance before 480 nm, replacing the role of the yellow compensating dyes, as shown in Fig. 5.4 [**10, 26**]. As reported in our previous work, the synthesis of stable yellow dye with strong absorption is very difficult because, in general, the stability and color strength of dye molecules often increase with increasing size of the aromatic system, which inevitably causes a bathochromic shift in their absorption [**27**]. However, the synthesized TBC dyes **RC1~3** can eliminate the addition of yellow compensating dye, which can

simplify the manufacturing process, omitting the need to consider the content ratio, compatibility, and thermal deterioration accompanied with the blending of a green main dye and yellow compensating dye.

For dye-based LCD BM, the dyes should have absorptions that are as strong and broad as possible in the entire visible region [**11**]. The synthesized TBC dyes exhibited additional strong absorption in the visible range induced from the growth and bathochromic shift of the Soret band, which made their absorption peaks closer to those of the panchromatic dyes. The drawback of PC dyes, as possible candidates for dye-based LCD BM, is their absorption deficiency from 450 nm to 600 nm due to the wide gap between the Soret band and the Q-band [**11**]. On the other hand, the synthesized TBC dyes **RC1~3** can easily prevent light leakage in the visible range since they have a narrower gap between the Soret band and the Q-band. In particular, the bathochromic shift of the Soret band of the prepared dyes **RC1~3** was about 110 nm, which was more than that of the general TBC compounds [**23-25**]. Such a bathochromic shift of the Soret band is likely to be the result of the destabilization of the HOMO - 1 (a2u) orbital caused by the removal of a meso-nitrogen atom [**15**]. The Q-bands of the synthesized dyes **RC1~3** were hypsochromic shifted about 18 nm compared to PC dye **2b**, comparable to those of common TBC compounds [**23-25**]. The molar extinction coefficients of dyes **RC1~3** increased in the order of

RC2 < **RC1** < **RC3**, whereas the absorption maxima (λ_{max}) of the dyes were identical as expressed in Table 5.2. In particular, the molar extinction coefficient of **RC3** was even higher than that of PC dye **2b**.

5.3.2.3 Thermal stability of dyes

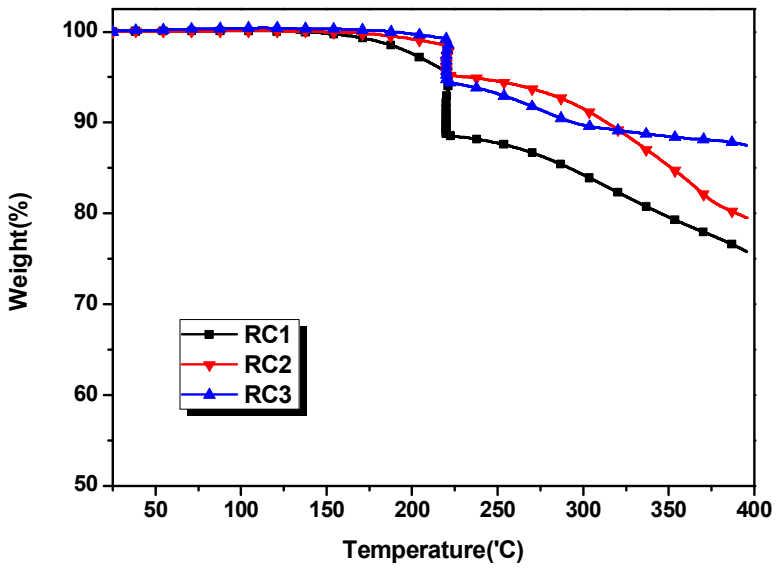

Figure 5.2 TGA analysis of the synthesized dyes (isothermal 30 min at 220 °C).

The dye molecules should have strong intermolecular interactions and form compact aggregates in order to have high thermal stabilities [**28-30**]. The PC

dyes, as the precursor of the TBC dyes as the main colorants for green CFs and BM, are known to be generally very stable. In particular, they have high thermal stability since they consist of extensive aromatic planar and symmetric systems which lead to stacking like rolls of coins [**31-33**]. The synthesized TBC dyes **RC1~3** mostly maintained the superior stability of the PC dyes. However, their stabilities were somewhat deteriorated due to the axial substituents at phosphorus inducing the decreased π-π stacking interaction. While the peripheral substituents of **RC1~3** are also bulky enough to cause steric hindrance, having the terminal alkoxy group was found to relieve the deterioration of thermal stability [**11, 34**]. The high molecular weight and polar substituents of the synthesized TBC dyes are advantageous for intermolecular interactions, such as van der Waals force and dipole-dipole interaction [**35**]. In order to use dyes as CFs, they should be able to endure a temperature of 220 °C (which is the conventional highest temperature in the LCD manufacturing process) without significant weight loss [**36, 37**]. As shown in Fig. 5.2, dyes **RC2** and **RC3** were stable at the TGA analysis, showing less than 5% weight loss after 30 min at 220 °C. However, the weight loss of **RC1** was relatively larger since the distortion of the **RC1** molecule was induced by the axial substituent introduced asymmetrically as illustrated in Fig. 5.3. In addition, the hydroxyl axial group of **RC1** is believed to be chemically less stable than the

alkoxy axial group of the other dyes. The **RC3** dye showed greater weight loss than **RC2** at the isothermal period, but appeared more stable as the temperature increased.

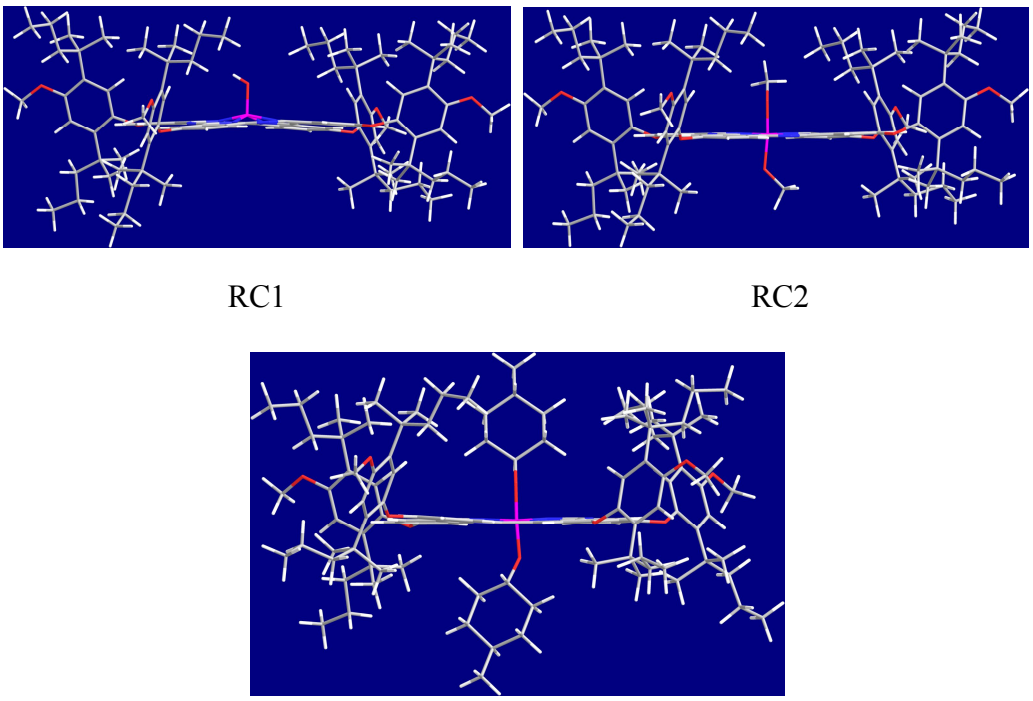

Figure 5.3 Geometry-optimized structures of the synthesized dyes.

5.3.2.4 Geometry optimization and electrochemistry of dyes

Geometry optimizations of the synthesized dyes were carried out using Gaussian 09 software. They were calculated with DFT on a B3LYP/6-31+G (d,p) level. The calculated results were in accord with the solubility and thermal stability data of the prepared dyes. The synthesized TBC dyes **RC1~3** have axial substituents, introduced perpendicular to the main body as illustrated in Fig. 5.3, believed to be effective to prevent their π-π stacking. This anti-aggregation effect was expressed well as their solubilities in Table 5.1. The influence of the axial substituent gave **RC3** maximum solubility since this methyl cyclohexyl axial group was geometrically even bulkier than other groups. The main body of **RC1** was distorted more than that of **RC2** and **RC3**, as illustrated in Fig. 5.3, leading to a lower thermal stability.

The oxidation potential data of TBC dyes **RC1~3** are listed in Table 1S and are deduced from normalized absorption, fluorescence spectra, and cyclic voltammetry curves shown in Fig. 1S and Fig. 2S. The overall electrochemical behavior of the three TBC dyes **RC1~3** appeared similar, as shown in Fig. 2S, suggesting that the influence over their redox potential induced from the axial ligand difference is negligible. The negative values for E_{ox} and E_{ox}-$E_{0\text{-}0}$ of **RC1~3** were greater than those of common PC dyes, impliying that **RC1~3** are easier to oxidize and more difficult to reduce than PC dyes. This is consistent with the notion that the corroles, in general, help stabilize a higher oxidation

state [**15**].

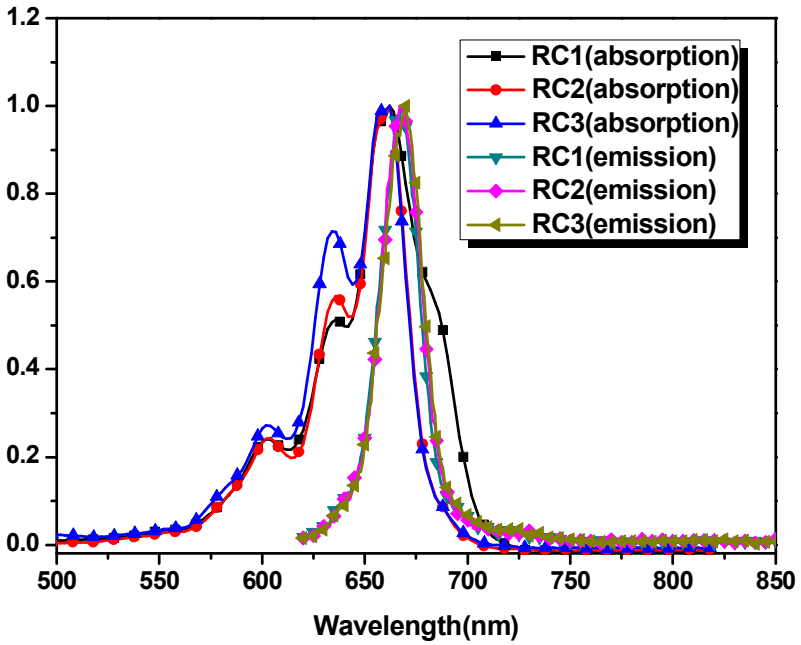

Figure 5.1S Normalized absorption and fluorescence spectra of the synthesized dyes, in PGMEA (5×10^{-6}mol liter^{-1}).

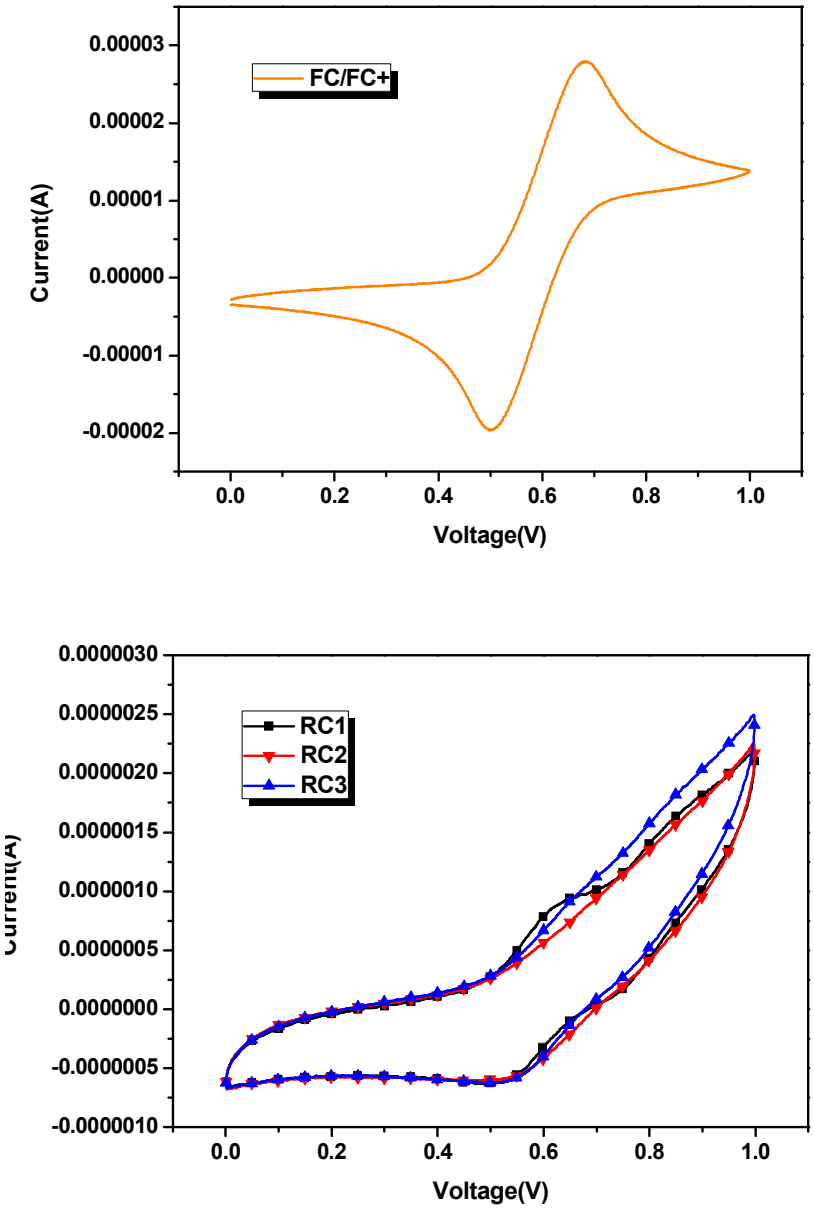

Figure 5.2S Cyclic voltammetry curves of ferrocene/ferrocenium (Fc/Fc^{+}) and the synthesized dyes in CH_2Cl_2.

dye	absorption[a]	emission[a]	Oxidation potential data[b]		
	λ_{max}	λ_{max}	E_{ox} (vs NHE)	$E_{0\text{-}0}$[c]	E_{ox}-$E_{0\text{-}0}$ (vs NHE)
RC1	662nm	668nm	0.654V	1.86V	-1.206V
RC2	662nm	667nm	0.642V	1.87V	-1.228V
RC3	662nm	670nm	0.648V	1.86V	-1.212V

Table 5.1S Optical and electrochemical properties of the synthesized dyes.

[a] Measured in 5×10^{-6}mol litre^{-1} of PGMEA solutions at room temperature.

[b] Measured in CH_2Cl_2 containing 0.1mol litre^{-1} of tetrabutylammonium tetrafluoroborate ($TBABF_4$) electrolyte (working electrode: glassy carbon; counter electrode: Pt; reference electrode: Ag/Ag^+; calibrated with Fc/Fc^+ as an internal reference and converted to NHE by addition of 630mV).

[c] Estimated from intersection wavelengths between absorption and emission spectra.

5.3.3 Characterization of spin-coated films

5.3.3.1 Spectral and chromatic properties of spin-coated films for LCD CFs

The transmittance spectra of spin-coated TBC dyes **RC1~3** are shown in Fig. 5.4, and the corresponding data are listed in Table 5.3. These transmittance spectra were compared to the spectrum of the mixture of PC dye **2b** and the yellow compensating dye **3**, and the spectrum of the pigment-based CF. The spin-coated films with TBC dyes **RC1~3** exhibited outstanding transmittance from 490 nm to 580 nm, advantageous to be used as LCD green CFs. In order to achieve a high brightness (Y) for the green color (the most important index for high quality LCD CF), the square shaped high transmittance spectrum is ideal. The reason why the transmittance spectra of **RC1~3** are closer to this ideal transmittance is mainly attributed to their absorption spectra. Firstly, the Soret bands of the absorption peaks of **RC1~3**, compared to the spectrum of yellow compensating dye **3** [**26**], were sharper and slightly hipsochromic shifted, leading to the steep-shaped transmittance peak and the increase of transmittance in the 490-510 nm region. In addition, the undesirable shoulder before the main transmittance disappeared because of the higher molar extinction coefficients of their Soret bands. Secondly, TBC dyes **RC1~3**

showed a declined aggregation peak in front of the Q-band, resulting from higher solubility, and their Q-bands were slightly less hipsochromic shifted compared to common TBC compounds [**38, 39**]. These factors led to the increased transmittance in the 560-580 nm region. Lastly, **RC1~3** with decreased aggregating tendency had smaller particle sizes in the media leading to less light scattering, resulting in an overall rising trend of transmittance [**35, 40**]. In particular, **RC2** exhibited 93.25% of the highest maximum transmittance at 510 nm. **RC3** cut off the undesirable transmittance most clearly because of the highest molar extinction coefficients.

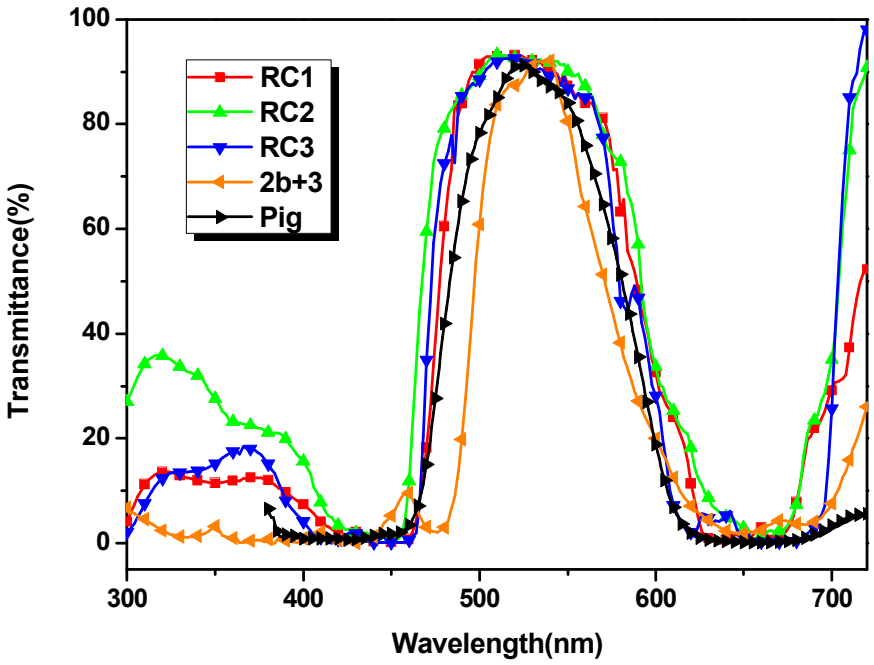

Figure 5.4 Transmittance spectra of the pigment-based and dye-based color filters.

Table 5.3 Transmittance of the pigment-based and dye-based color filters.

Spin-coated dyes	λ_{max} (nm)	Maximum transmittance (%)

RC1	**514**	**93.18**
RC2	**510**	**93.25**
RC3	**520**	**92.59**
2b+3	**538**	**92.24**
Pigment	**522**	**91.30**

Table 5.4 The coordinate values corresponding to the CIE 1931 chromaticity diagram and the color difference values of the pigment-based and dye-based color filters.

Spin-coated dyes	**Y**	**x**	**y**	**ΔE_{ab}**
RC1	**60.33**	**0.279**	**0.516**	**4.90**
RC2	**62.84**	**0.298**	**0.509**	**2.95**
RC3	**62.29**	**0.275**	**0.523**	**3.03**
2b+3	**60.14**	**0.299**	**0.519**	**1.87**
Pigment	**57.86**	**0.244**	**0.504**	**0.85**

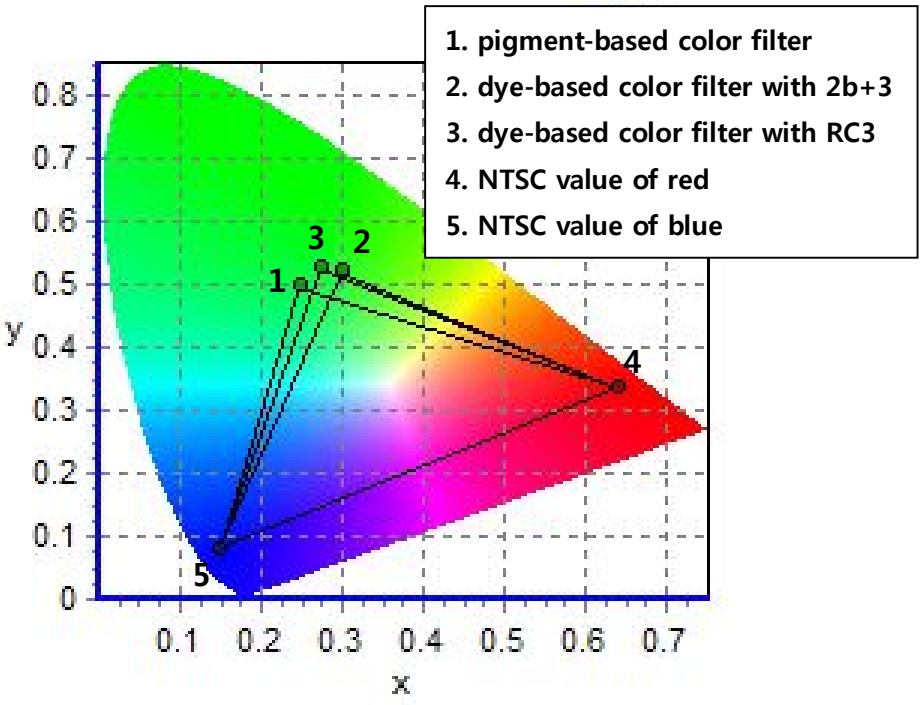

Figure 5.5 CIE 1931 chromaticity diagram of the pigment-based and dye-based color filters.

The coordinate values of the spin-coated dye-based CFs are compared with a pigment-based CF as shown in Table 5.4 and Fig. 5.5. The all dye-based CFs are so efficient that they showed similar or larger color gamuts in spite of the much lower colorant contents in the inks due to the much higher tinctorial strength [**10, 16**]. The TBC dyes **RC1~3** showed a superior brightness (Y) value

compared to PC dye **2b** and the pigment-based CF owing to the higher transmittance in the green region. Especially, **RC2** exhibited 62.84 of the highest brightness value. **RC3** showed the widest color gamut with the highest y value. Judging from this result, the transmittance and brightness of **RC3** can increase further since the amount of **RC3** in the color ink can be reduced for obtaining the same color strength.

5.3.3.2 Dielectric properties of spin-coated films for LCD BMs

The synthesized TBC dyes **RC1~3** have excellent optical properties to be applied for LCD BM since the gap between the Soret band and Q-band is narrow. In recent years, the dielectric properties of the colorants have been considered very important for satisfactory application to COA mode, in which CF is patterned right onto the TFT array. Accordingly, colorants with low dielectric constants such as dyes are under extensive investigation for LCD BMs since the conventional carbon black-based BM with high dielectric constant interferes with the electrical signals of TFT [**8, 9**]. The demanded dielectric constant with the current commercialized thickness of BM (1-1.5 μm) is smaller than 7, whereas the dielectric constant of the carbon black-based BM is larger than 20 [**41**]. The dielectric constants of the TBC dyes **RC1~3** spin-

coated on the aluminum substrate are listed in Table 5.5. Their dielectric constants were calculated according to the following equation. The symbol C refers to capacitance (F), ε_0 refers to dielectric constant under vacuum (8.854×10^{-14} Fcm^{-1}), t refers to thickness (cm), and A refers to the area of the electrode (cm^2).

$$\varepsilon_r \text{ (dielectric constant)} = C/\varepsilon_0 \times t/A$$

The dielectric constants of the spin-coated films with the TBC dyes of **RC1~3** were less than 7 and satisfactory for industrial application, owing to the low dielectric character of the dye molecules. In particular, **RC3** showed the lowest dielectric constant of 3.33 at 10 kHz frequency. The dielectric constants of the spin-coated films decreased as the applied frequency increased due to the lag in the charge transfer of the dye molecule caused by the rapid change in the external electronic field [**40**].

Table 5.5 Dielectric constants of the dye-based black matrices.

Spin-coated dyes	**t/A**	**Frequency (kHz)**	**Capacitance (pF)**	**Dielectric constant**
RC1	**0.46**	**1**	**0.94**	**4.88**
		10	**0.88**	**4.57**

RC2	**0.63**	**1**	**0.55**	**3.91**
		10	**0.51**	**3.63**
RC3	**0.44**	**1**	**0.72**	**3.58**
		10	**0.67**	**3.33**

5.3.3.3 Thermal stability and FE-SEM images of spin-coated films

The practical thermal stability of spin-coated CFs and BMs needs to be discussed with color difference (ΔE_{ab}) values as expressed in Table 5.4 and Table 5.6 since it is affected by the compatibility with industrial solvents and binders as well as the inherent thermal stability of dye molecules [**10**]. The criterion of sufficient thermal stability for commercial applications was that the ΔE_{ab} values of the spin-coated films should be less than 3 after heating for one hour at 230 °C [**16**]. However, the baking temperature decrease in the LCD manufacturing process is easing this criterion for sufficient thermal stability. Under this criterion, the spin-coated TBC dyes **RC1~3** exhibited somewhat less thermal stability compared to the PC dye or pigment-based CF as shown in Table 5.4. This is because of the relatively reduced aggregating tendency of axially substituted dyes **RC1~3**, which coincides with the result of solubility

discussion. Such a reduced aggregating tendency of **RC1~3** made their particle size smaller than that of PC dye **2b** on the spin-coated films as illustrated in FE-SEM images in Fig. 5.6. This smaller dye aggregate size leads to superior solubility and optical property which are in a trade-off relationship with thermal stability to some degree. As reported in a previous paper, the substituents hindering intermolecular π-π stacked interaction induced smaller dye aggregate sizes in the FE-SEM images, which in turn reduced the drop of transmittance when the dye contents were increased [**42**]. However, the thermal stability of dyes improves as the dye aggregate size increases in general [**28-30**]. As illustrated in Fig. 5.6, the dye aggregate size decreased as the axial substituents became bulkier in the order of **RC1** > **RC2** > **RC3**. However, the ΔE_{ab} value of **RC1** appeared to be the largest, probably due to the distortion of the main body and the weak stability of the hydroxyl group. Therefore, the replacement of such hydroxyl group into the alkoxy group is believed to make the TBC dye more stable.

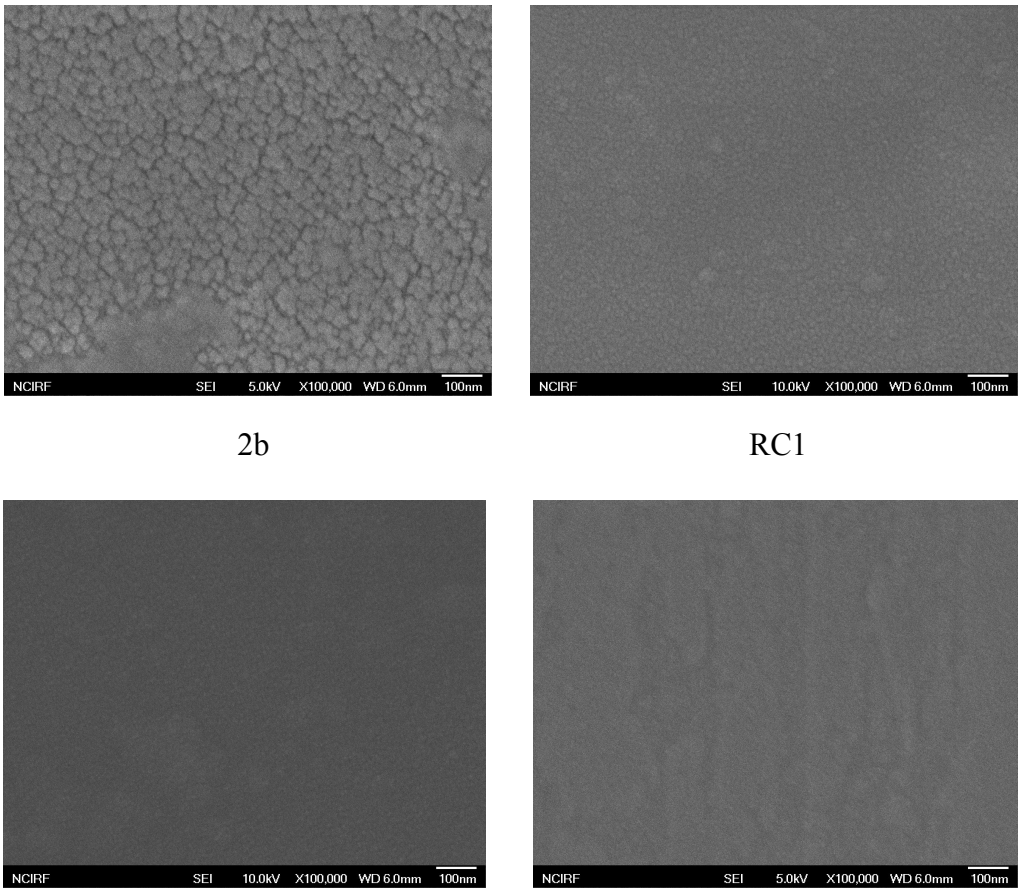

Figure 5.6 The FE-SEM images of the spin-coated films.

Under the most recent LCD manufacturing process baking condition, the films spin-coated with TBC dyes **RC1~3** exhibited improved thermal stability as shown in condition **a** of Table 5.6. Especially, **RC2** and **RC3** exhibited

sufficient thermal stability for commercial application. In this condition, the coordinate value y was somewhat increased and the brightness (Y) was somewhat decreased due to the reduced dye degradation. The thermal stability of spin-coated film can also be improved by slowing down the spin-coating speed. The films spin-coated with **RC1~3** exhibited improved thermal stability under the condition **b** which had the reduced rpm (100 rpm for 5 s, 300 rpm for 20 s) of spin-coating as shown in Table 5.6. The improvement of thermal stability, namely the decrease of the ΔE_{ab} value, in this condition was contributed to by the growth of the film thickness resulting from the reduced spin-coating speed. Such a growth of film thickness raised the coordinate value y, but resulted in reduced brightness (Y).

Table 5.6 The coordinate values corresponding to the CIE 1931 chromaticity diagram and the color difference values of the spin-coated films in reformed conditions.

Spin-coated dyes	**Y**	**x**	**y**	**ΔE_{ab}**
RC1[a]	**60.13**	**0.282**	**0.521**	**3.16**
RC2[a]	**62.79**	**0.294**	**0.510**	**1.75**

RC3[a]	**62.21**	**0.277**	**0.534**	**1.98**
RC1[b]	**60.05**	**0.278**	**0.526**	**3.83**
RC2[b]	**62.27**	**0.293**	**0.521**	**2.66**
RC3[b]	**61.56**	**0.275**	**0.554**	**2.60**

[a] Prebaked for 10 min at 90 °C and postbaked for 30 min at 200 °C.

[b] Spin-coated with reduced rpm (100 rpm for 5 s, 300 rpm for 20 s).

5.4 Conclusions

The three novel TBC phosphorus dyes were successfully synthesized and applied for dye-based LCD CF and BM. They were synthesized via a ring-contraction reaction in which a meso-nitrogen atom is extruded from an appropriate metal-free PC precursor. On account of this meso-nitrogen extrusion, the absorption peaks of the synthesized dyes had a red-shifted Soret band and a blue-shifted Q-band compared to the PC dyes, which can be extremely beneficial for application as colorants of green CF and BM of LCD. In addition, these dyes exhibited superior solubility to the industrial solvents by introducing the bulky axial substituents at the phosphorus atom.

The synthesized dyes were dissolved in industrial solvent-binder composites and spin-coated on the glass or aluminum substrate. In terms of dye-based LCD green CF, the strong and bathochromic shifted Soret bands of the prepared dyes effectively replaced the role of the yellow compensating dye. The spin-coated films exhibited a square shaped ideal transmittance spectrum, leading to excellent brightness contributed by the smaller particle size as illustrated in the FE-SEM images. In terms of dye-based LCD BM, the prepared dyes were advantageous for panchromatic absorption since the gap between their Soret band and Q-band was narrow. In addition, the spin-coated films exhibited low dielectric constants satisfactory for application to the COA mode. They showed slightly inferior thermal stability compared to the PC dye, but could be improved under reformed conditions.

5.5 References

[1] Tsuda K. Colour filters for LCDs. Displays 1993;14:115-24.

[2] Sabnis RW. Color filter technology for liquid crystal displays. Displays 1999;20:119-29.

[3] Castellano JA. Handbook of display technology. UK: Academic Press Inc; 1992.

[4] Diest K, Dionne JA, Spain M, Atwater HA. Tunable color filters based on metal-insulator-metal resonators. Nano Lett 2009;9:2579-83.

[5] Kudo T, Nanjo Y, Nozaki Y, Yamaguchi H, Kang WB, Pawlowski G. Polymer optimization of pigmented photoresists for color filter production. Jpn J Appl Phys 1998;37:1010-6.

[6] Kelley AT, Alessi PJ, Fornalik JE, Minter JR, Bessey PG, Garno JC, Royster TL. Investigation and application of nanoparticle dispersions of pigment yellow 185 using organic solvents. ACS Appl Mater Interfaces 2010;2:61-8.

[7] Sugiura T. Dyed color filters for liquid-crystal displays. J Soc Inf Disp 1993;1:177-80.

[8] Tani M, Ito S, Sakagawa M, Sugiura T. A photoresist for black matrix on TFT arrays. Soc Inform Display Digest 1997;28:969-72.

[9] Hirayama H, Hidaka K, Imai N, Ibaraki N. Integrated black matrix on TFT arrays composed on newly developed Bi-SiOx ceramic thin film. Soc Inform Display Digest 1997;28:180-3.

[10] Choi J, Kim SH, Lee W, Yoon C, Kim JP. Synthesis and characterization of thermally stable dyes with improved optical properties for dye-based LCD color filters. New J Chem 2012;36:812-8.

[11] Lee W, Yuk SB, Choi J, Jung DH, Choi S, Park J, Kim JP. Synthesis and characterization of solubility enhanced metal-free phthalocyanines for liquid

crystal display black matrix of low dielectric constant. Dyes Pigm 2012;92:942-8.

[12] Aĝritaş MS. Non-aggregating phthalocyanines with bulky 2,4-di-tert-butylphenoxy-substituents. Dyes Pigm 2007;74:490-3.

[13] Cheng G, Peng X, Hao G, Kennedy VO, Ivanov IN, Knappenberger K, Hill TJ, Rodgers MAJ, Kennedy ME. Synthesis, photochemistry, and electrochemistry of a series of phthalocyanines with graded steric hindrance. J Phys Chem A 2003;107:3503-14.

[14] Erdoĝmuş A, Nyokong T. Novel, soluble, FluXoro functional substituted zinc phthalocyanines; synthesis, characterization and photophysicochemical properties. Dyes Pigm 2010;86:174-81.

[15] Fox JP, Goldberg DP. Octalkoxy-substituted phosphorus(V)triazatetrabenzcorroles via ring contraction of phthalocyanine precursors. Inorg Chem 2003;42:8181-91.

[16] Choi J, Sakong C, Choi JH, Yoon C, Kim JP. Synthesis and characterization of some perylene dyes for dye-based LCD color filters. Dyes Pigm 2011;90:82-8.

[17] Li H, Jensen TJ, Fronczek FR, Vicente MGH. Syntheses and properties of a series of cationic water-soluble phthalocyanines. J Med Chem 2008;51:502-11.

[18] Oleinick NL, Antunez AR, Clay ME, Rihter BD, Kenney ME. New phthalocyanine photosensitizers for photodynamic therapy. Photochem Photobiol 1993;57:242–7.

[19] He J, Larkin HE, Li YS, Rihter BD, Zaidi SIA, Rodgers MAJ, Mukhtar H, Kenney ME, Oleinick NL. The synthesis, photophysical and photobiological properties and in vitro structureactivity relationships of a set of silicon phthalocyanine PDT photosensitizers. Photochem Photobiol 1997;65:581–6.

[20] Lee PPS, Ngai T, Huang JD, Wu C, Fong WP, Ng DKP. Synthesis, characterization, biodegradation, and in vitro photodynamic activities of silicon(IV) phthalocyanines conjugated axially with poly(epsilon-caprolactone). Macromolecules 2003;36:7527–33.

[21] Lee PPS, Ngai T, Cheng Y, Chi W, Ng DKP. Synthesis, characterization, and degradation of silicon(IV) phthalocyanines conjugated axially with poly(sebacic anhydride). J Polym Sci A Polym Chem 2005;43:837–43.

[22] Zhu YJ, Huang JD, Jiang XJ, Sun JC. Novel silicon phthalocyanines axially modified by morpholine: Synthesis, complexation with serum protein and in vitro photodynamic activity. Inorg Chem Commun 2006;9:473–7.

[23] Fujiki M, Tabei H, Isa KJ. New tetrapyrrolic macrocycle: .alpha.,.beta.,.gamma.-triazatetrabenzcorrole. J Am Chem Soc 1986;108:1532-6.

[24] Liu J, Zhang F, Zhao F, Tang Y, Song X, Yao G. Complexation of phosphorus(III) with a novel tetrapyrrolic phthalocyanine-like macrocyclic compound. Photochem Photobiol 1995;91:99-104.

[25] Li J, Subramanian LR, Hanack M. Studies on phosphorus phthalocyanines and triazatetrabenzcorroles. Eur J Org Chem 1998;12:2759-67.

[26] Choi J, Lee W, Sakong C, Yuk SB, Park JS, Kim JP. Facile synthesis and characterization of novel coronene chromophores and their application to LCD color filters. Dyes Pigm 2012;94:34-9.

[27] Zollinger H. Color Chemistry. 3rd ed. Weinheim: Wiley-VCH; 1987.

[28] Giles CH, Duff DG, Sinclair RS. The relationship between dye structure and fastness properties. Rev Prog Coloration 1982;12:58-65.

[29] Das S, Basu R, Minch M, Nandy P. Heat-induced structural changes in merocyanine dyes: X-ray and thermal studies. Dyes Pigm 1995;29:191-201.

[30] Chunlong Z, Nianchun M, Liyun L. An investigation of the thermal stability of some yellow and red azo pigments. Dyes Pigm 1993;23:13-23.

[31] Herbst W, Hunger K. Industrial organic pigments: production, properties, applications. 3rd ed. Weinheim: Wiley-VCH; 1998.

[32] Gordon PF, Gregory P. Organic chemistry in colour. Berlin: Springer-Verlag; 1987.

[33] Kobayashi N. Design, synthesis, structure, and spectroscopic and

electrochemical properties of phthalocyanines. Bull Chem Soc Jpn 2002;75:1-19.

[34] Hacıvelioğlu F, Durmuş M, Yeşilot S, Gürek AG, Kılıç A, Ahsen V. The synthesis, spectroscopic and thermal properties of phenoxycyclotriphosphazenyl-substituted phthalocyanines. Dyes Pigm 2008;79:14-23.

[35] Kim YD, Kim JP, Kwon OS, Cho IH. The synthesis and application of thermally stable dyes for ink-jet printed LCD color filter. Dyes Pigm 2009;81:45-52.

[36] Ohmi T. Manufacturing process of flat display. Jpn Soc Mech Eng 2004;47:422-8.

[37] Takamatsu T, Ogawa S, Ishii M. Color filter fabrication technology for LCDs. Sharp Tech J 1991;50:69-74.

[38] Durmus M, Nyokong T. The synthesis, fluorescence behaviour and singlet oxygen studies of new water-soluble cationic gallium (III) phthalocyanines. Inorg Chem Commun 2007;10:332-8.

[39] Li H, Jensen TJ, Fronczek FR, Vicente MGH. Syntheses and properties of a series of cationic water-soluble phthalocyanines. J Med Chem 2008;51:502-11.

[40] Tilley RJD. Colour and optical properties of materials. Chichester: John

Wiley & Sons Inc; 2000.

[41] Jung J, Park Y, Jaung JY, Park J. Synthesis of new single black pigments based on azo and anthraquinone moieties for LCD black matrix. Mol Cryst Liq Cryst 2010;529:88-94.

[42] Sakong C, Kim YD, Choi JH, Yoon C, Kim JP. The synthesis of thermally-stable red dyes for LCD color filters and analysis of their aggregation and spectral properties. Dyes Pigm 2011;88:166-73.

Chapter 6

The Influence of Aggregation Behavior of Novel Quinophthalone Dyes on Optical and Thermal Properties of LCD Color Filters

6.1 Introduction

Nowadays, dyes are employed in a wide range of high technology industries, such as displays [**1-5**], energy [**6-8**], bio [**9-11**] and digital printing [**12-14**]. Currently, various dye molecules are investigated for application to the color filters of a liquid crystal display (LCD) panel, whose quality influences the performance of an LCD display. The color filter, a key component which converts the white backlight into various colored lights, consists of RGB (red, green, and blue) pixels with pigments, a black matrix for prevention of light leakage, an overcoat for improving the flatness of pigments, and a column spacer for control of the gap between cells [**15,16**].

The pigments, being used as the main colorants of the RGB pixels, show

superior thermal and photo-chemical stability, but low optical and chromatic properties due to their aggregation behavior **[17,18]**. Dyes can be attractive alternatives to overcome this limitation because they dissolve in media and exist in molecular form, and this property can reduce light scattering. However, such advantages of the dyes can be effective only when they are compatible with the color resist, which consists of an industrial solvent, macromolecular binder, and various additives. If the structures of the dye molecules are not suitable for preventing intermolecular aggregation, the particle sizes of the dye can become bigger than those of the pigments. Also, if the structures are not sufficiently compatible with the binder and additives of the color resist, the dye molecules can re-aggregate after the baking process even though their structures are sufficiently soluble in the industrial solvents. Such problems have been pointed out as the major factors that deteriorate the optical property and thermal stability of dye-based LCD color filters [**19**]. Nevertheless, relatively little research has been carried out on these kinds of problems.

In this study, four novel yellow quinophthalone dyes were designed and synthesized to examine the relation between their molecular structures and aggregation behavior. In addition, the influence of the aggregation behavior on the properties of LCD color filters with the synthesized dyes was discussed thoroughly. The change of the dye aggregate size was observed by field

emission scanning electron microscopy (FE-SEM), and the spectral and thermal property of the dye molecules were examined. In addition, the transmittance, contrast ratio, and color difference values of spin-coated films with the synthesized dyes were investigated.

6.2 Experimental

6.2.1 Synthesis

6.2.1.1 2-methyl-8-quinolinylamine (1)

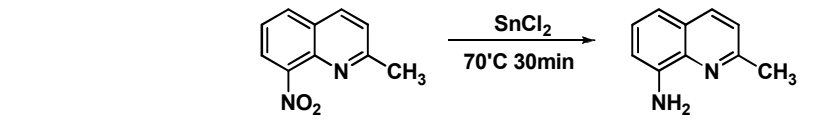
SnCl2
70'C 30min
1

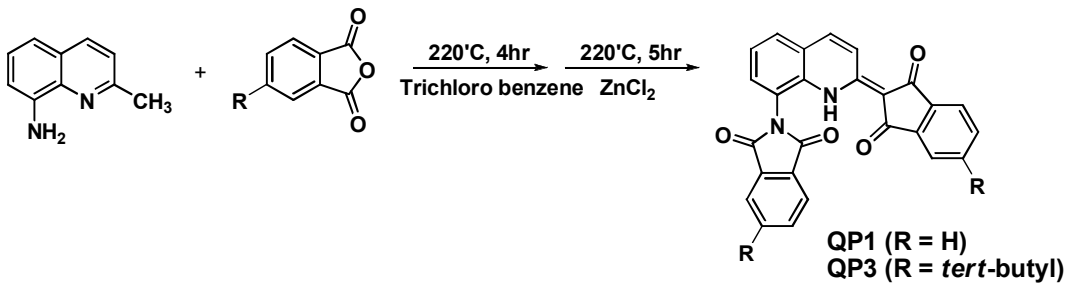
220'C, 4hr
220'C, 5hr
Trichloro benzene ZnCl2
QP1 (R = H)
QP3 (R = tert-butyl)

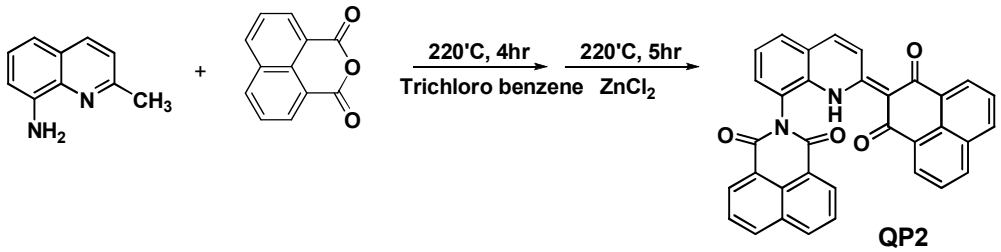
220'C, 4hr
220'C, 5hr
Trichloro benzene ZnCl2
QP2

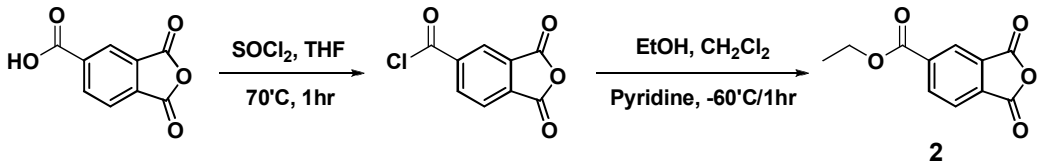
SOCl2, THF
70'C, 1hr
EtOH, CH2Cl2
Pyridine, -60'C/1hr
2

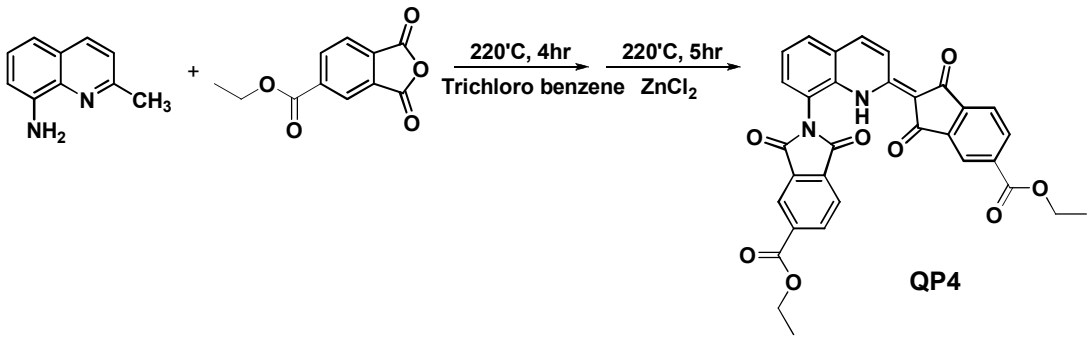
220'C, 4hr
220'C, 5hr
Trichloro benzene ZnCl2
QP4

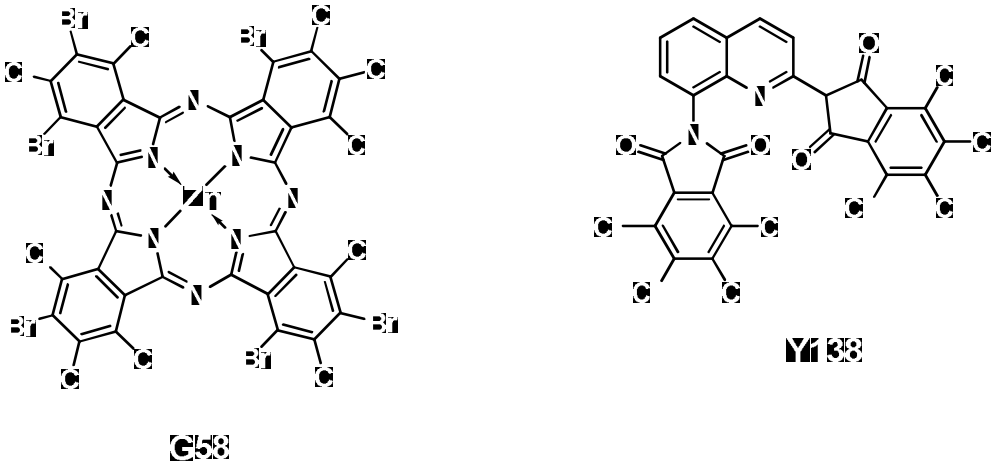

Scheme 6.1 Synthesis of quinophthalone dyes and structures of the prepared pigments.

8-Nitroquinaldine (1.88 g, 0.01 mol) was placed in a 100 mL flask equipped with a condenser and gas inlet adapter and dissolved in ethanol (20 mL). An amount of $SnCl_2$ (11.27 g, 0.05 mol) was added and the resulting solution heated to 70 °C and stirred for 0.5 h. After reaction, the mixture was cooled to room temperature, and then poured into distilled water / ice (300 mL). Sodium bicarbonate was carefully added to adjust the pH to between 7 - 8. The crude product was extracted by treating with ethyl acetate (700 mL) in a separatory funnel and washed several times with brine. To remove the remaining moisture,

the ethyl acetate solution of the crude product was dried with $MgSO_4$. After vacuum distillation, **1** was obtained as yellow oil, frozen to solid to be reacted for next step (1.30 g, 82%). ^{1}H NMR (500MHz, $CDCl_3$): δ = 2.70 (s, 3H), 4.95 (s, 2H), 6.89 (d, *J* = 7.5 Hz, 1H), 7.10 (d, *J* = 8.5 Hz, 1H), 7.24 (m, 2H), 7.94 (d, *J* = 8.5 Hz, 1H)

6.2.1.2 Trimellitic anhydride ethyl ester (2)

Trimellitic acid anhydride (1.92 g, 0.01 mol) was boiled with thionyl chloride (7.14 g, 0.06 mol) in THF (30 mL) for l h. The anhydride acid chloride was isolated by vacuum distillation of the solvent. The intermediate was then recrystallized from heptane giving rise to fine colorless needles.

Trimellitic anhydride acid chloride (6.32 g, 0.03 mol) and absolute ethanol (1.44 g, 0.045 mol) were dissolved in dry CH_2CI_2 (30 mL) and cooled to -60 °C (CO_2/acetone) under a dry N_2-atmosphere. Distilled pyridine (2.4 mL, 0.03 mol) was then added dropwise to the stirred mixture. After the addition was over, the solution was kept at -60 °C for 1 h, and then heated to room temperature, where it was stirred for a further 4 h. The reaction mixture was washed with water and dried over Na_2SO_4. After distillation of the solvent the residue was recrystallized from n-heptane to give **2** as a white solid (5.75 g,

87%) [**20**]. Mp > 95 °C; ^{1}H NMR (500MHz, $CDCl_3$): δ = 1.38 (t, *J* = 20.5 Hz, 3H), 4.41 (q, *J* = 17.5 Hz, 2H), 7.78 (d, *J* = 13.0 Hz, 1H), 8.21 (s, 1H), 8.42 (d, *J* = 8.5 Hz, 1H)

6.2.1.3 N-[2-(2,3-dihydro-1,3-dioxo-1H-inden-2-yl)-8-quinolyl]phthalimide (QP1)

1 (1.58 g, 0.01 mol) was placed in a 100 mL flask equipped with a condenser and gas inlet adapter and dissolved in trichlorobenzene (40 mL). Phthalic anhydride (1.48 g, 0.01 mol) was added and the resulting solution heated to 220 °C and stirred for 4 h. The mixture was then added with phthalic anhydride (1.48 g, 0.01 mol) again with $ZnCl_2$ (0.45 g, 0.003 mol) and heated under reflux further for 5 h. After reaction, the mixture was cooled to room temperature, and then poured into n-hexane (1000 mL) to be precipitated. The resulting suspension was filtered, washed with 1% aqueous NaOH several times and dried in vacuum oven for 24 h. The crude product was dissolved in $CHCl_3$, filtered again and the filtrate was evaporated to remove the solvent. The solid was purified on a silica gel column using 1.25/1 ethyl acetate/hexane as the eluent. The bright orange band was collected and concentrated producing **QP1** as a bright orange solid (2.18g, 52%). Mp > 320 °C (decomp.); ^{1}H NMR

(500MHz, $CDCl_3$): δ = 7.47 (d, *J* = 7.0 Hz, 1H), 7.50 (t, *J* = 9.0 Hz, 1H), 7.52 (d, *J* = 5.5 Hz, 2H), 7.63 (d, *J* = 7.0 Hz, 2H), 7.68 (d, *J* = 7.0 Hz, 1H), 7.80 (d, *J* = 7.5 Hz, 1H), 7.93 (t, *J* = 8.5 Hz, 2H), 8.09 (d, *J* = 5.0 Hz, 1H), 8.11 (t, *J* = 11.5 Hz, 2H), 8.64 (d, *J* = 10.0 Hz, 1H); MALDI-TOF MS: m/z 418.99 (100%, $[M + H^+]$); Found: C, 74.41; H, 3.42; N, 6.73. Calc. for $C_{26}H_{14}N_2O_4$: C, 74.64; H, 3.37; N, 6.70.

6.2.1.4 N-[2-(2,3-dihydro-1,3-dioxo-1H-phenalen-2-yl)-8-quinolyl]1,8-naphthalimide (QP2)

QP2 was synthesized in the same manner with **QP1** using **1** (1.58g, 0.01mol) and 1,8-naphthalic anhydride (1.98g, 0.01mol) twice and obtained as a yellow solid (2.07g, 40%). Mp > 250 °C (decomp.); ^1H NMR (500MHz, $CDCl_3$): δ = 7.61 (d, *J* = 7.5 Hz, 1H), 7.68 (d, *J* = 8.0 Hz, 2H), 7.79 (d, *J* = 5.0 Hz, 2H), 7.82 (t, *J* = 7.5 Hz, 2H), 7.90 (t, *J* = 9.5 Hz, 2H), 8.01 (t, *J* = 10.5 Hz, 1H), 8.09 (d, *J* = 8.5 Hz, 1H), 8.29 (d, *J* = 8.0 Hz, 2H), 8.43 (d, *J* = 8.0 Hz, 1H), 8.66 (d, *J* = 7.5 Hz, 2H), 8.74 (d, *J* = 7.0 Hz, 1H), 9.68 (d, *J* = 9.5 Hz, 1H); MALDI-TOF MS: m/z 519.32 (100%, $[M + H^+]$); Found: C, 78.71; H, 3.42; N, 5.53. Calc. for $C_{34}H_{18}N_2O_4$: C, 78.76; H, 3.50; N, 5.40.

6.2.1.5 4-tert-butyl-N-[2-(5-tert-butyl-2,3-dihydro-1,3-dioxo-1H-inden-2-yl)-8-quinolyl]phthalimide (QP3)

QP3 was synthesized in the same manner with **QP1** using **1** (1.58g, 0.01mol) and 4-*tert*-butylphthalic anhydride (2.04g, 0.01mol) twice and obtained as a bright orange solid (2.92g, 55%). Mp > 320 °C (decomp.); ^{1}H NMR (500MHz, $CDCl_3$): δ = 1.32 (s, 9H), 1.48 (s, 9H), 7.49 (d, *J* = 7.5 Hz, 1H), 7.52 (s, 1H), 7.57 (s, 1H), 7.59 (d, *J* = 8.0 Hz, 1H), 7.61 (d, *J* = 8.0 Hz, 1H), 7.78 (d, *J* = 8.0 Hz, 1H), 7.94 (t, *J* = 7.5 Hz, 1H), 8.03 (d, *J* = 7.0 Hz, 1H), 8.06 (d, *J* = 8.5 Hz, 1H), 8.14 (d, *J* = 7.0 Hz, 1H), 8.65 (d, *J* = 8.0 Hz, 1H), 14.20 (d, *J* = 8.5 Hz, 1H); MALDI-TOF MS: m/z 531.11 (100%, [M + H^+]); Found: C, 76.43; H, 5.72; N, 5.18. Calc. for $C_{34}H_{30}N_2O_4$: C, 76.96; H, 5.70; N, 5.28.

6.2.1.6 N-[2-(2,3-dihydro-1,3-dioxo-1H-inden-2-yl ethyl ester)-8-quinolyl]phthalimide ethyl ester (QP4)

QP4 was synthesized in the same manner with **QP1** using **1** (1.58g, 0.01mol) and **2** (2.20g, 0.01mol) twice and obtained as a bright orange solid (2.87g, 51%). Mp > 320 °C (decomp.); ^{1}H NMR (500MHz, $CDCl_3$): δ = 1.38 (t, *J* = 8.0 Hz, 3H), 1.48 (t, *J* = 8.0 Hz, 3H), 4.38 (q, *J* = 7.5 Hz, 2H), 4.52 (q, *J* =

7.0 Hz, 2H), 7.56 (d, *J* = 6.0 Hz, 1H), 7.59 (d, *J* = 7.5 Hz, 1H), 7.68 (d, *J* = 7.5 Hz, 1H), 7.86 (d, *J* = 8.0 Hz, 1H), 8.13 (s, 1H), 8.15 (s, 1H), 8.20 (t, *J* = 7.5 Hz, 1H), 8.23 (d, *J* = 8.5 Hz, 1H), 8.63 (d, *J* = 9.5 Hz, 1H), 8.67 (d, *J* = 10.0 Hz, 1H), 8.76 (d, *J* = 4.5 Hz, 1H), 14.47 (s, 1H); MALDI-TOF MS: m/z 563.03 (100%, $[M + H^+]$); Found: C, 68.14; H, 3.99; N, 5.01. Calc. for $C_{32}H_{22}N_2O_8$: C, 68.32; H, 3.94; N, 4.98.

6.2.2 Materials and instrumentation

8-Nitroquinaldine, trimellitic acid anhydride, $ZnCl_2$ purchased from TCI, and phthalic anhydride, 1,8-naphthalic anhydride, 4-tert-butylphthalic anhydride, $SOCl_2$, $SnCl_2$ purchased from Sigma-Aldrich were used as received. All the other reagents and solvents were of reagent-grade quality and obtained from commercial suppliers. Transparent glass substrates were provided by Paul Marienfeld GmbH & Co. KG. Commercial pigment-based color filter and acrylic binder were supplied by LG chem ltd.

^1H NMR spectra were recorded on a Bruker Avance 500 spectrometer at 500MHz using chloroform-d and TMS, as the solvent and internal standard, respectively. Matrix Assisted Laser Desorption/Ionization Time Of Flight (MALDI-TOF) mass spectra were collected on a Voyager-DE STR

Biospectrometry Workstation with α-cyano-4-hydroxycinnamic acid (CHCA) as the matrix. Absorption and transmittance spectra were measured using a HP 8452A spectrophotometer. Elemental analysis was carried out with a Flash EA 1112 CNH analyzer. Chromatic characteristics of the spin-coated films were analyzed on a Scinco color spectrophotometer. Contrast ratios of the spin-coated films were analyzed on a Zonetech color contrast tester. Thermogravimetric analysis (TGA) was conducted under nitrogen at a heating rate of 10 °C min-1 using a TA Instruments Thermogravimetric Analyzer 2050. The thickness of the spin-coated film was measured using a Nano System Nanoview E-1000. FE-SEM images of spin-coated films were taken by JSM-840A microscope.

6.*2.3 Preparation of color inks and dye-based color filters*

Three organic color inks were prepared with different concentration (0.19 mmol, 0.22 mmol, 0.25 mmol) of synthesized dyes, propylene glycol methyl ether acetate (PGMEA) (2.8g) and acrylic binder (2.0g). The prepared dye-based inks were coated on a transparent glass substrate using a MIDAS System SPIN-1200D spin coater. The coating speed was initially 100 rpm for 10 s, which was then increased to 600 rpm and kept constant for 20 s. The wet dye-

coated glasses were then dried at 60 °C for 20 min, prebaked at 90 °C for 10 min, and postbaked at 200 °C for 30 min. After each step, the coordinate values of the dye-coated glasses were measured to calculate color difference values. All spin coated dye-based color filters were 1.6μm thick.

6.2.4 Measurement of spectral and chromatic properties

Absorption spectra of the synthesized dyes and transmittance spectra of dye-based color filters were measured using a UV-vis spectrophotometer. Chromatic values of dye-based color filters were recorded on a color spectrophotometer (Scinco colormate). Contrast ratios of dye-based color filters were expressed as relative ratio (Y_{max}/Y_{min}) between maximum brightness (Y_{max}) and minimum brightness (Y_{min}) using Zonetech color contrast tester.

6.2.5 Measurement of thermal stability

Thermal stability of the synthesized dyes was evaluated by TGA. The prepared dyes were heated to 110 °C and held at that temperature for 10 min to remove residual water and solvents. The dyes were then, heated to 220 °C and

held at that temperature for 30 min to simulate the processing thermal conditions of color filter manufacturing. The dyes were finally heated to 400 °C to determine their degradation temperature. The temperature was raised at the rate of 10 °C min^{-1} under nitrogen atmosphere.

To check the thermal stability of the dyes in color filters, the fabricated spin-coated glasses were heated in a forced convection oven (OF-02GW Jeiotech Co., Ltd.). The color difference values (ΔE_{ab}) before and after heating were measured on a color spectrophotometer (Scinco colormate) in CIE L*a*b* mode.

6.3 Results and Discussion

6.3.1 Synthesis

Dyes **QP1~4** were prepared through the synthetic routes illustrated in Scheme 6.1 and the overall characterization of dye structures were carried out by ^{1}H-NMR spectroscopy, MALDI-TOF spectroscopy and elemental analysis. Each precursor of the quinophthalone dyes, 8-aminoquinaldine (**1**), was obtained through a reduction of 8-nitroquinaldine with $SnCl_2$ and its structure was confirmed by ^{1}H NMR spectroscopy. Dyes **QP1** and **QP3** were synthesized

by the reaction between 8-aminoquinaldine and two moles of phthalic anhydride or 4-*tert*-butylphthalic anhydride [**21**]. The formation of the imide ring in the product by reaction of the primary amino group with an equivalence of phthalic anhydride is faster than the formation of the phthalone ring [**22**]. Therefore, equivalent moles of phthalic anhydride with $ZnCl_2$ were added again after imidization. Dye **QP2**, synthesized with naphthalic anhydride, which is bulkier than phthalic anhydride, were obtained in lower yield because of steric hindrance. Dye **QP4** was synthesized by the reaction between 8-aminoquinaldine and trimellitic anhydride ethyl ester (**2**), which has a solvent-friendly substituent. The structure of trimellitic anhydride ethyl ester (**2**), synthesized via esterification of the intermediate acid chloride from trimellitic acid anhydride, was confirmed by ^{1}H NMR spectroscopy. The synthesized dyes **QP1~4** have N–H···O intramolecular hydrogen bonding between the NH groups and the O atoms. In particular, **QP3** and **QP4** were considered to have stronger intramolecular hydrogen bonding than **QP1** and **QP2** since the proton peaks of their NH groups were located at a lower field, as confirmed by ^{1}H NMR spectroscopy (14.20, 14.47 ppm) [**23,24**]. The protons of these NH groups appeared as doublet peaks because of tautomerism.

6.3.2 Characterization of the synthesized dyes

6.3.2.1 Geometry optimization of the synthesized dyes

Geometry optimization of the synthesized dyes was carried out using Gaussian 09 software. They were calculated with DFT on a B3LYP/6-31+G (d,p) level. The synthesized yellow dyes **QP1~4** have the twisted phthalic anhydride or naphthalic anhydride at the quinoline molecule, as shown in Fig. 6.1, which can improve solubility and prevent intermolecular π-π stacking. However, the dihedral angles between the quinoline molecule and the substituents vary according to the substituent structure. Although the dihedral angles of **QP1, QP3, QP4** are comparable (65.30°, 64.81°, 64.06°), that of **QP2** is much bigger (89.54°) as shown in Fig. 6.1 since its naphthalic anhydride is bulkier than the phthalic anhydride of the other three dyes. This difference can be the major reason for the lowest thermal stability of **QP2**. Dyes **QP1~4** in Fig. 6.1 have hydrogen atoms at the nitrogen of quinolines, that implies the state of N–H···O intramolecular hydrogen bonding is more stable.

QP1 QP2

QP3 QP4

Figure 6.1 Geometry-optimized structures of the synthesized dyes.

6.3.2.2 Spectral properties of the synthesized dyes

The UV-vis absorption spectra of quinophthalone dyes **QP1~4**, measured as 10^{-5}M in PGMEA, are shown in Fig. 6.2 and the corresponding data are listed in Table 6.1. Although their spectra have similar shapes with double absorption maxima (λ_{max}), **QP3** and **QP4** showed higher molar extinction coefficients than the other two dyes. Their higher molar extinction coefficients are considered to

be induced by their increased transition dipole moment due to the additional substituents on the phthalic anhydride moiety. The bulky tert-butyl group of **QP3** prevents intermolecular aggregation and the ethyl ester group of **QP4** promotes miscibility with PGMEA. In particular, the λ_{max} values of **QP3** and **QP4** were relatively bathochromic-shifted, and hence these dyes showed very strong and sharp absorptions just before 500 nm. This absorption behavior can be ideal for a yellow compensating dye to be used in LCD color filters [**25**]. Overall, the spectral property of **QP3** is especially excellent since its spectrum showed a steeper gradient before 500 nm and a smaller absorption shoulder after 500 nm than the spectrum of **QP4**. In contrast, **QP2** showed the smallest molar extinction coefficient and its absorption peak was the least sharp and the most hypsochromically-shifted, making it the least ideal as a yellow compensating dye. Such differences in shape and strength of the absorption peaks can result from the structural factors. Namely, **QP2** has two distinct naphthalic structures at the quinoline body and its solubility is much lower than the others.

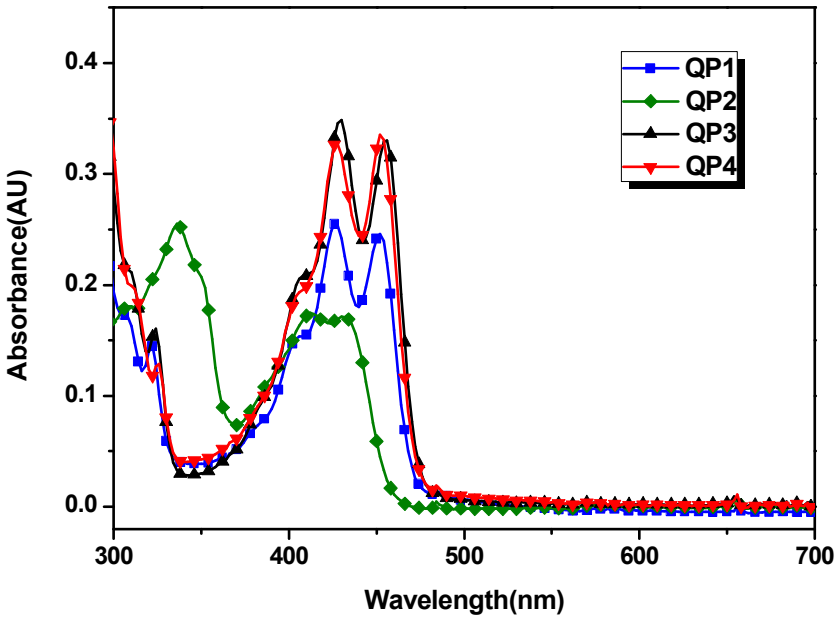

Figure 6.2 Absorption spectra of the synthesized dyes in PGMEA (10^{-5}mol liter^{-1}).

Dyes	λ_{max} (nm)	ε (L mol^{-1} cm^{-1})
QP1	426; 452	25,000
QP2	412; 430	17,000

QP3	**430; 456**	**35,000**
QP4	**428; 452**	**34,000**

Table 6.1 Absorption spectra of the synthesized dyes in PGMEA (10^{-5}mol liter^{-1}).

6.3.2.3 Thermal stability of the synthesized dyes

The dye molecules should have strong intermolecular interactions and form compact aggregates to have high thermal stability [**26-28**]. Quinophthalone derivatives are known to exhibit satisfactory thermal stability since they have hydrogen bonding sites and intermolecular π-π stacked interactions induced from polycyclic aromatic structures [**29**]. To be used in color filters, the colorants should lose a minimum amount of weight at 200 ~ 250 ℃ by TGA, which is the highest temperature conventionally used in the LCD manufacturing process [**30**]. The TGA graph shown in Fig. 6.3 estimated the thermal stability of dyes **QP1~4** by examining their isothermal weight losses at 220 ℃. The isothermal weight loss increased as **QP1** < **QP3** < **QP4** < **QP2** and **QP1**, **QP3**,

QP4 exhibited sufficient thermal stability for use in LCD color filters, showing less than 5% weight loss after 30 min at 220 °C. Dye **QP2** exhibited the worst thermal stability, showing more than 5% weight loss and initiation of degradation first near 250 °C. In contrast, dye **QP1** exhibited excellent thermal stability, showing very little weight loss until 300 °C, since it does not have additional substituents, which lead to the easier intermolecular aggregation. Although **QP2** does not have additional substituents either, it showed insufficient thermal stability since its naphthalic structures are twisted perpendicular to the quinoline body, as illustrated in Fig. 6.1, which discourages intermolecular interactions [**31-33**].

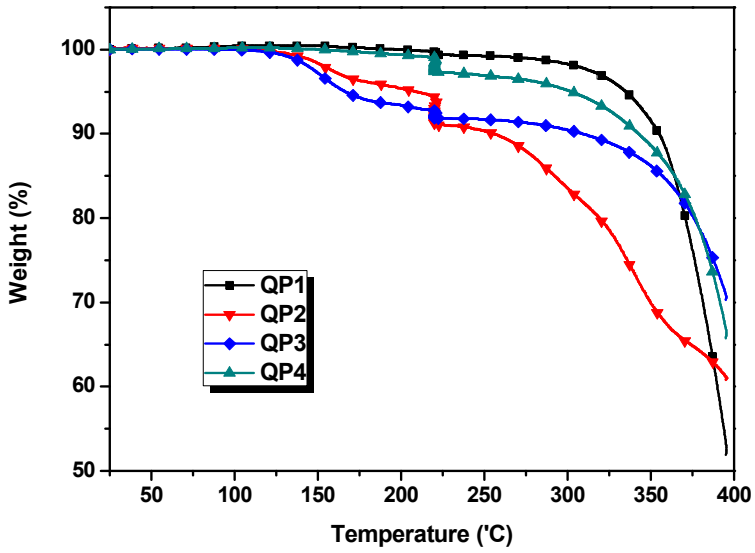

Figure 6.3 TGA analysis of the synthesized dyes (isothermal 30 min at 220 °C).

6.3.3 Aggregation behavior of dyes in color filters

6.3.3.1 Field emission scanning electron microscopy study (FE-SEM)

Whether the dye molecules form aggregates on the color filter substrate considerably influences the optical property and thermal property of the color filters [**19**]. Such aggregation tendency is related with the solution stability of the synthesized dyes in an industrial solvent. The dyes **QP3** and **QP4** exhibited

semipermanent solution stability in PGMEA because of their additional substituents, which improve solubility. Such tendency also influenced on the aggregate size of the dye molecules after spin-coating, as illustrated in Fig. 6.4. The dyes **QP3** and **QP4** showed much smaller aggregate sizes than **QP1** and **QP2** at 0.22 mmol in the pre-baked state. In the FE-SEM images, **QP1** showed aggregate sizes of about 100~500 nm; **QP2** about 300~1000 nm; whereas, **QP3** and **QP4** showed extremely small aggregate sizes even under 100,000× magnification. The film uniformity of **QP4** appeared to be a bit coarser than that of **QP3** since **QP4** has carboxylate substituents, which are believed to promote intermolecular hydrogen bonding.

If the dye molecules lack compatibility with the components of the color resist, they can be re-aggregated with the evaporation of the solvents after the baking process, even though they have good solubility in the industrial solvents. This is the critical problem of some dyes that can replace the conventional pigments used in LCD color filters. As illustrated in Fig. 6.4, the film uniformity of even **QP3** and **QP4** became coarser with the development of aggregation after 3 cycles of the postbaking processes at 200 ℃. Therefore, the compatibility of dyes to the components of the color resist as well as their solubility to the industrial solvent should be considered when designing color filter dye molecules.

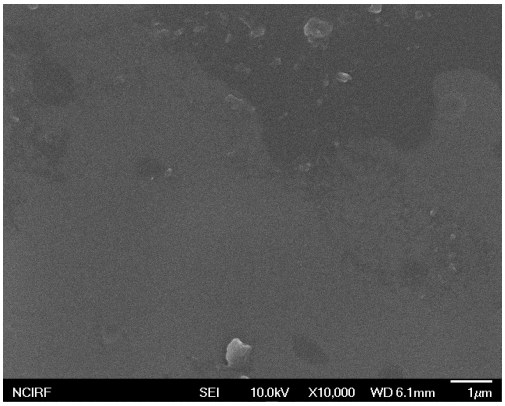

QP1 (prebake)

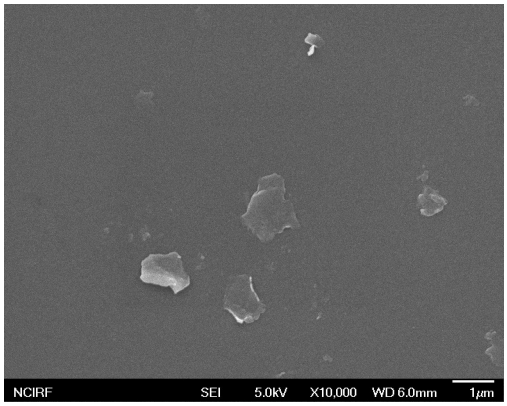

QP2 (prebake)

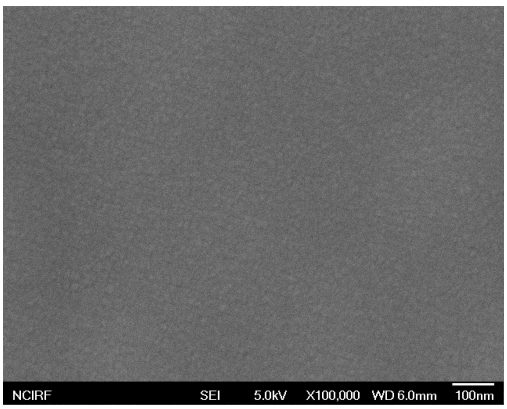

QP3 (prebake)

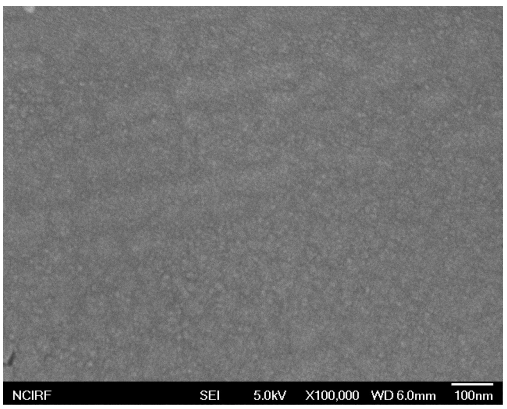

QP4 (prebake)

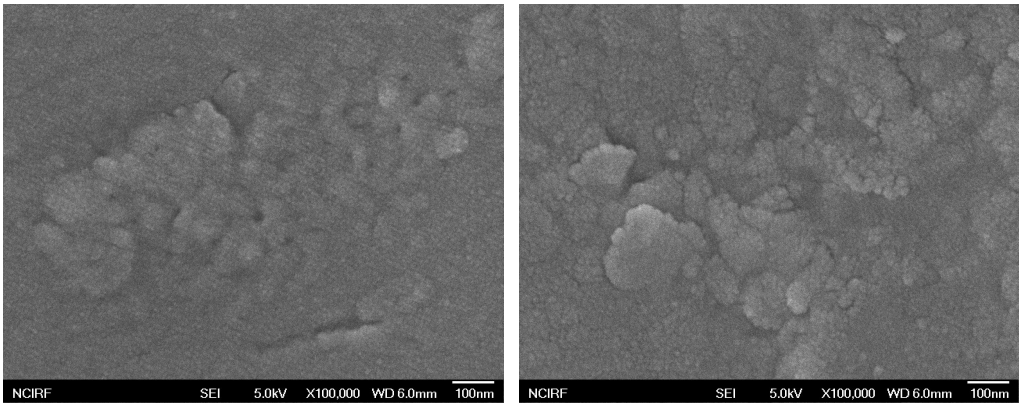

QP3 (post bake 3 times) QP4 (post bake 3 times)

Figure 6.4 The FE-SEM images of the spin-coated films.

6.*3.3.2 Aggregation-optical property relationship*

The transmittances of dye-based color filters with the synthesized dyes after postbaking once are shown according to the dye content in the color inks in Fig. 6.5. When the dye content in the color inks was increased, the absorption peaks were strengthened and broadened, which led to decreased transmittances under 500 nm. However, the transmittances above 500 nm varied according to the aggregation behavior, which is influenced by the dye structure. The dyes **QP3** and **QP4** which have sufficient solubility to PGMEA because of their additional

substituents had little influence on the transmittances of the color filters above 500 nm in spite of the increased dye content. In contrast, the transmittances of the color filters above 500 nm using dyes **QP1** and **QP2** with insufficient solubility extensively decreased, and new absorption bands were formed. These decreased transmittances were due to the light scattering by the larger aggregate sizes of **QP1** and **QP2**, as illustrated in the FE-SEM images. Such a dye aggregation tendency also affects the ground state of the dyes, leading to the formation of additional absorption bands [**34-36**]. In particular, the transmittance of the color filter using **QP2**, which showed the biggest aggregate size in the FE-SEM images, was dramatically decreased with increasing dye content. In the case of **QP3** and **QP4**, the development of the new absorption bands was negligible because these dyes had a much lower aggregation tendency.

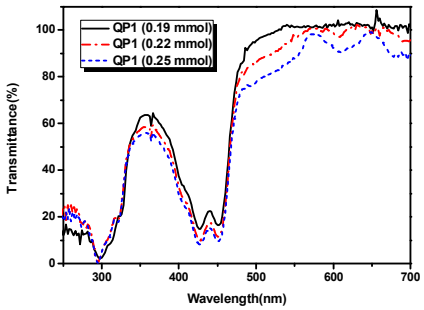

QP1

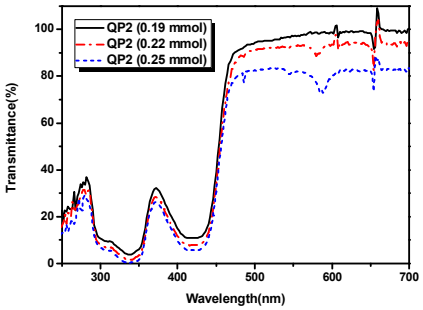

QP2

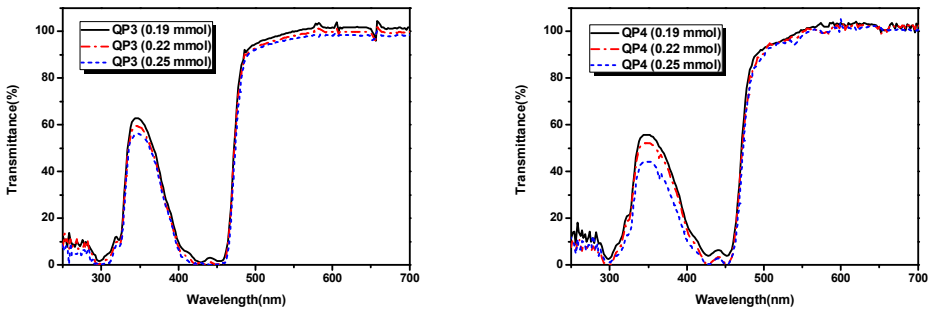

QP3 QP4

Figure 6.5 The transmittance variations of dye-based color filters according to the dye content in the color inks.

Subsequently, the variation of transmittance of the color filter according to the degree of baking was analyzed. The graph of the variation of transmittance according to the number of postbaking processes at 200 ℃ for dye content of 0.19 mmol is represented in Fig. 6.6. The transmittances of the color filters above 500 nm of **QP1** and **QP2** decreased as the number of baking times increased, making these dyes undesirable as yellow compensating dyes. In the case of **QP1**, the transmittance around 500 nm was seriously reduced whereas the transmittance around 600 nm was barely changed. In the case of **QP2**, the

overall transmittance above 450 nm decreased significantly. Basically, since these dyes have low solution stability and high aggregation tendency, their molecules are also believed to show a high re-aggregation tendency with the evaporation of the solvent as the baking process is repeated. Such a re-aggregation behavior makes the particle sizes of **QP1** and **QP2** bigger than those shown in Fig. 6.4, which hinders the transmission of the LCD module's back light.

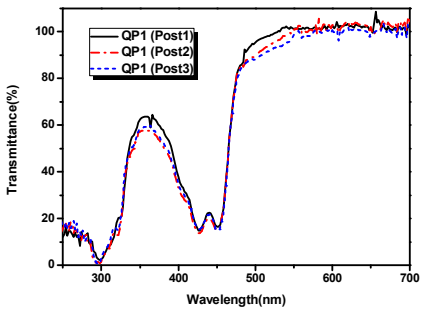

QP1

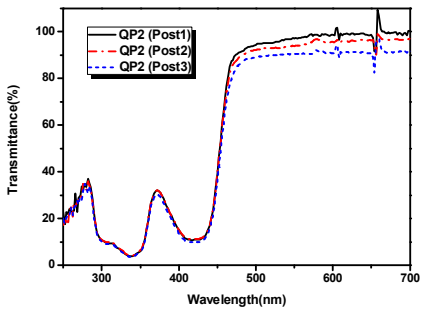

QP2

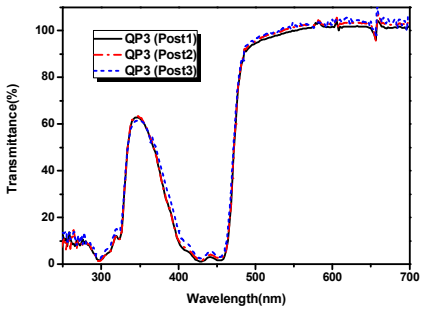

QP3

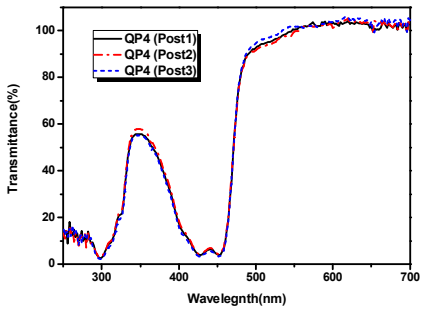

QP4

Figure 6.6 The transmittance variations of dye-based color filters according to the degree of baking.

The color filters with dyes **QP3** and **QP4**, which have a lower aggregation tendency than **QP1** and **QP2**, showed different transmittance change in the same experiment. The transmittances of the color filters spin-coated with these dyes showed little change or even increased slightly as the baking process was repeated. In general, some percentage of dye molecules are sublimated or degraded as heat treatment is repeated, decreasing the color strength but increasing the transmittance [**33**]. In other words, although the color filters with dyes **QP1** and **QP2** showed the decreased transmittance with the growth of particle sizes of the dyes as the baking process was repeated due to the lack of the solution stability, the color filters using **QP3** and **QP4** with relatively low aggregation tendency did not show such drop of transmittance since the sublimation or degradation is believed to trade off against such transmittance decreasing factors. As illustrated in Fig. 6.4, **QP3** and **QP4** deteriorated the film uniformity of the color filters rather than generate huge aggregates after the repeated baking processes, due to the migration of the dye molecules.

Colorants	Replacement ratio	Composition (G58/Y138/dye)	CR relative to Pigment (before PB)	CR relative to Pigment (after PB)	Relative CR through PB
G58+Y138	**0%**	**72/28/0**	**-**	**-**	**91.3%**
G58+QP3	**100%**	**76.5/0/23.5**	**108.1%**	**98.1%**	**82.8%**
G58+QP3	**50%**	**74/13/13**	**95.6%**	**99.8%**	**95.3%**
G58+QP4	**100%**	**76.5/0/23.5**	**115.6%**	**87.5%**	**69.1%**
G58+QP4	**50%**	**72/14/14**	**102.6%**	**98.6%**	**87.8%**

Table 6.2 The relative contrast ratios of dye-based and pigment-based color filters.

The re-aggregation behavior or the film uniformity deterioration at the surface of a dye-based color filter according to the postbaking process can be expressed more clearly by measuring the contrast ratio. The contrast ratio, indicated as the relative ratio (Y_{max}/Y_{min}) between maximum brightness (Y_{max}) and minimum brightness (Y_{min}), can be higher by increasing Y_{max} or by decreasing Y_{min} [**37**]. The relative contrast ratios of green color filters are given in Table 6.2, when the yellow pigment (Y138), which compensates the main

green pigment (G58), is replaced with yellow dye **QP3** or **QP4**, respectively. Since the molar extinction coefficient of dyes **QP3** and **QP4** were bigger than that of Y138, the amount of yellow colorant could be reduced in the same color coordinate values. It is noted that, before the postbaking, the contrast ratios of the dye-based color filters were higher than that of the pigment-based color filter consisting of G58 and Y138, except for only one sample. This is mainly because the synthesized dyes dissolve in the media and exist in molecular form, which induces lower light scattering and results in higher Y_{max}. However, after the postbaking, all the dye-based color filters showed lower contrast ratios compared to the pigment-based color filter. Judging from the previous results, this is due to the formation of surface aggregates or the deterioration of film uniformity induced by heat treatment. Such behavior causes light scattering at the surfaces of the color filters, which in turn induces the phase differences of the back light to increase light leakage. Accordingly, the light leakage triggers the increase of Y_{min}, which lowers the contrast ratio [**38**]. In particular, in the case where Y138 was replaced by 100% dye **QP4**, although the contrast ratio of the dye-based color filter relative to that of the pigment-based one before postbaking reached 115.6%, the value after postbaking strikingly decreased to 87.5%. In the rightmost column of Table 6.2, all contrast ratios of the color filters decreased after postbaking. Consequently, the aggregation of dye

molecules can be the main reason for the deterioration of the optical property of a dye-based color filter, but it can be controlled to some degree according to the structure of the dye molecules.

6.3.3.3 *Aggregation-thermal stability relationship*

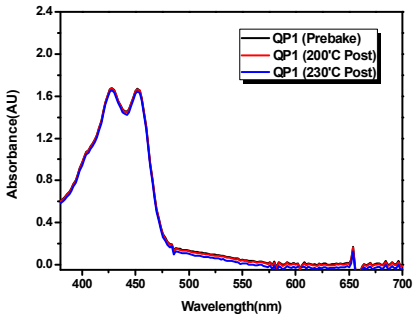

QP1

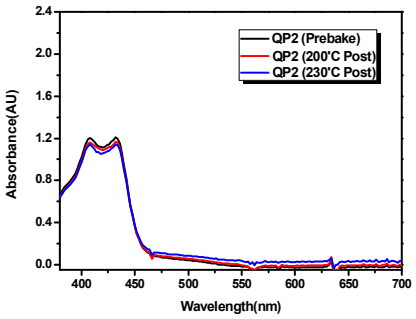

QP2

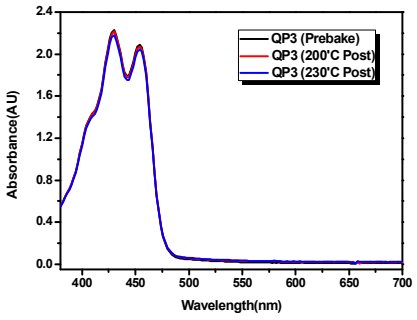

QP3

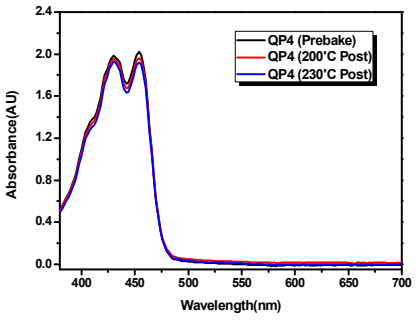

QP4

Figure 6.7 The change of the absorption peaks of dye-based color filters with increasing postbaking temperature.

Dyes	PB1	PB2	PB3
QP1	0.45	3.04	5.89
QP2	3.31	6.20	9.18
QP3	0.56	2.74	2.77
QP4	1.62	2.04	2.37

Table 6.3 The color difference values of dye-based color filters when the postbaking process was conducted for 1, 2, and 3 times respectively.

In order to examine the degradation temperature of the chromophores of synthesized dyes spin-coated onto the substrate, the change of the absorption peaks of the dye-based color filters with increasing postbaking temperature was analyzed. The graphs of the absorption peaks changed very little around the

wavelengths of absorption maxima, as shown in Fig. 6.7. This result suggests that the chromophores of the synthesized dyes in the dye-based color filters degraded very little up to 230 °C postbaking temperature.

The practical thermal stability of spin-coated color filters needs to be discussed with the color difference (ΔE_{ab}) values expressed in Table 6.3, since it is affected by the compatibility of the synthesized dyes with industrial solvents and binders as well as the inherent thermal stability of the dye molecules [**39**]. Judging from the above results, the change of these color difference values of the prepared color filters below 230 °C is most likely to be caused by the re-aggregation or the migration of dye molecules rather than the degradation of chromophores. The color difference values of the prepared color filters when the postbaking process (prebaked at 90 °C for 10 min and postbaked at 200 °C for 30 min) was conducted for 1, 2, and 3 times respectively are presented in Table 6.3. Although **QP1** and **QP2** exhibited high color difference values of 5.89 and 9.18 respectively after the 3 times of postbaking, **QP3** and **QP4** exhibited lower values of 2.77 and 2.37 respectively, which are applicable for LCD color filters. The criterion of sufficient thermal stability for commercial applications was that the ΔE_{ab} values of the spin-coated films should be less than 3. As shown in Table 6.3, the color difference values of **QP1** and **QP2** greatly increased compared to **QP3** and **QP4** as the baking process was

repeated. As stated in the previous section, it was considered that these dyes with low solution stability had high aggregation tendency and tended to easily re-aggregate and migrate with evaporation of the solvent as the baking process was repeated. Such re-aggregation and migration of dye molecules reduced the film uniformity, and hence the coordinate value of any arbitrary point on the film was changed, which led to the greatly increased color difference values. In particular, even though **QP1** showed the lowest color difference value after one-time postbaking, since its inherent thermal stability is the highest among the prepared dyes as shown in TGA graph, its color difference value started to exceed those of **QP3** and **QP4** after the two repeats of postbaking due to its higher aggregation tendency. Dye **QP2**, which has the lowest inherent thermal stability and the highest aggregation tendency, showed the highest color difference values at the all stages of postbaking. Dyes **QP3** and **QP4** with relatively low aggregation tendency showed color difference values under 3 even after three repeats of postbaking. Although they also showed some degree of re-aggregation in accordance with the FE-SEM images and contrast ratio data, it is noted that the increase of their color difference values rapidly saturated. Consequently, as in the case of optical property, the aggregation of dye molecules can be the main reason for the deterioration of the thermal stability of a dye-based color filter, but the degree of deterioration can be

reduced by the modification of the dye structure.

6.4 Conclusions

Four novel yellow quinophthalone dyes were designed and synthesized to examine the influence of aggregation behavior on the properties of LCD color filters. They showed different UV-vis absorption spectra according to their characteristic structures, and two of them exhibited excellent spectral properties, making them suitable as yellow compensating dyes. Their thermal stabilities depended on their aggregation tendency and their structural factors which were analyzed by geometry optimization. The transmittances of the dye-based color filters decreased as the dye contents in color inks increased, but the degree of decrease was much severe in the cases of the dyes with higher aggregation tendency. Similarly, when the color filters were postbaked repeatedly, the transmittances decreased severely in the cases of the dyes with higher aggregation tendency. In the measurement of the contrast ratio of the color filters, the re-aggregation behavior and film uniformity deterioration at the surfaces of the color filters according to the baking process were expressed clearly. Although the contrast ratios of dye-based color filters were higher than that of pigment-based one before postbaking, the values of the dye-based filters

after postbaking greatly decreased below that of pigment-based one. In the measurement of color difference values, which express the thermal stability of color filters, the values of the dyes with higher aggregation tendency increased remarkably as the baking process was repeated. This was also due to the re-aggregation and migration of the dye molecules with evaporation of the solvent. Consequently, the aggregation of dye molecules can be the main reason for the deterioration of the optical and thermal properties of dye-based color filters, but the degree of deterioration can be reduced by the modification of the dye structure.

6.5 References

[1] Hu Z, Xue M, Zhang Q, Sheng Q, Liu Y. Nanocolorants: a novel class of colorants, the preparation and performance characterization. Dyes Pigm 2008;76:173-8.

[2] Koo HS, Chen M, Pan PC, Chou LT, Wu FM, Chang SJ, et al. Fabrication and chromatic characteristics of the greenish LCD colour-filter layer with nanoparticle ink using inkjet printing technique. Displays 2006;27:124-9.

[3] Sugiura T. Dyed color filters for liquid-crystal displays. J Soc Inf Disp 1993;1:177-80.

[4] Sabnis RW. Color filter technology for liquid crystal displays. Displays 1999;20:119-29.

[5] Tsuda K. Color filters for LCDs. Displays 1993;14:115-24.

[6] O'Regan B, Grätzel M. A low-cost, high-efficiency solar cell based on dyesensitized colloidal TiO_2 films. Nature 1991;353:737-40.

[7] Bai Y, Cao Y, Zhang J, Wang M, Li R, Wang P, et al. High-performance dyesensitized solar cells based on solvent-free electrolytes produced from eutectic melts. Nat Mater 2008;7:626-30.

[8] Kim S, Lee JK, Kang SO, Ko J, Yum JH, Fantacci S, et al. Molecular engineering of organic sensitizers for solar cell applications. J Am Chem Soc 2006;128:16701-7.

[9] Dolmans DE, Fukumura D, Jain RK. Photodynamic therapy for cancer. Nat Rev Cancer 2003;3:380-7.

[10] Zhou L, Zhou JH, Dong C, Ma F, Wei SH, Shen J. Water-soluble hypocrellin a nanoparticles as a photodynamic therapy delivery system. Dyes Pigm 2009;82:90-4.

[11] Gorman SA, Bell AL, Griffiths J, Roberts D, Brown SB. The synthesis and properties of unsymmetrical 3,7-diaminophenothiazin-5-ium iodide salts: potential photosensitisers for photodynamic therapy. Dyes Pigm 2006;71:153-60.

[12] Calvert P. Inkjet printing for materials and devices. Chem Mater 2001;13:3299-305.

[13] Yang Y, Naarani V. Improvement of the lightfastness of reactive inkjet printed cotton. Dyes Pigm 2007;74:154-60.

[14] Hladnik A, Muck T. Characterization of pigments in coating formulations for high-end ink-jet papers. Dyes Pigm 2002;54:253-63.

[15] Castellano JA. Handbook of display technology. UK: Academic Press Inc; 1992.

[16] Diest K, Dionne JA, Spain M, Atwater HA. Tunable color filters based on metal-insulator-metal resonators. Nano Lett 2009;9:2579-83.

[17] Takanori K, Yuki N, Yuko N, Hidemasa Y, Kang WB, Pawlowski PG. Polymer optimization of pigmented photoresists for color filter production. Jpn J Appl Phys 1998;37:1010-6.

[18] Na DY, Jung IB, Nam SY, Yoo CW, Choi YJ. The rheological behavior and dispersion properties of millbase for LCD colorfilters. J Korean Inst Electr Electron Mater Eng 2007;20:450-5.

[19] Sakong C, Kim YD, Choi JH, Yoon C, Kim JP. The synthesis of thermally-stable red dyes for LCD color filters and analysis of their aggregation and spectral properties. Dyes Pigm 2011;88:166-73.

[20] Reinecke H, Campa J, Abajo J, Kricheldorf HR, Schwarz G. LC-poly(ester-amide-imide)s derived from trimellitic acid and 4-aminobenzoic acid. Polymer 1996;37:3101-9.

[21] Ullmann. Encyclopedia of industrial chemistry. 5th ed. Weinheim: Wiley-VCH; 1993.

[22] Faulkner EB, Schwartz RJ. High performance pigments. Weinheim: Wiley-VCH; 2009.

[23] Skrabal P, Zollinger H. Mechanism of azo coupling reactions: part XXXV. pH dependence and ortho/para ratio in coupling reactions of aminohydroxynaphthalenesulfonic acids. Dyes Pigm 1988;9:201-7.

[24] Mizuguchi J, Senju T. Solution and solid spectra of quinacridone derivatives as viewed from the intermolecular hydrogen bond. J Phys Chem B 2006;110:19154-61.

[25] Choi J, Lee W, Sakong C, Yuk SB, Park JS, Kim JP. Facile synthesis and characterization of novel coronene chromophores and their application to LCD color filters. Dyes Pigm 2012;94:34-9.

[26] Giles CH, Duff DG, Sinclair RS. The relationship between dye structure and fastness properties. Rev Prog Coloration 1982;12:58-65.

[27] Das S, Basu R, Minch M, Nandy P. Heat-induced structural changes in merocyanine dyes: X-ray and thermal studies. Dyes Pigm 1995;29:191-201.

[28] Chunlong Z, Nianchun M, Liyun L. An investigation of the thermal stability of some yellow and red azo pigments. Dyes Pigm 1993;23:13-23.

[29] Herbst W, Hunger K. Industrial organic pigments: production, properties, applications. 3rd ed. Weinheim: Willey-VCH; 1998.

[30] Choi SH, Kil GH, Kim NR, Yoon C, Kim JP, Choi JH. Preparation of red dyes derived from diketo-pyrrolo-pyrrole based pigment and their properties for LCD color filters. Bull Korean Chem Soc 2010;31:3427-30.

[31] Ma YS, Wang CH, Zhao YJ, Yu Y, Han CX, Qiu XJ, Shi Z. Perylene diimide dyes aggregates: Optical properties and packing behavior in solution and solid state. Supramol Chem 2007;19:141-9.

[32] Würthner F, Thalacker C, Diele S, Tschierske C. Fluorescent J-type aggregates and thermotropic columnar mesophases of perylene bisimide dyes. Chem Eur J 2001;7:2245-52.

[33] Choi J, Sakong C, Choi JH, Yoon C, Kim JP. Synthesis and characterization of some perylene dyes for dye-based LCD color filters. Dyes Pigm 2011;90:82-8.

[34] Kobayashi T. J-Aggregates. Singapore: World Scientific; 1996.

[35] Mishra A, Behera RK, Behera PK, Mishra BK, Behera GB. Cyanines during the 1990s: a review. Chem Rev 2000;100:1973-2011.

[36] Eisfeld A, Briggs JS. The J- and H-bands of organic dye aggregates. Chem

Phys 2006;324:376-84.

[37] Lin CC. Effects of contrast ratio and text color on visual performance with TFT-LCD. Int J Ind Ergon 2003;31:65-72.

[38] Singh R, Unni KNN, Solanki A, Deepak. Improving the contrast ratio of OLED displays: An analysis of various techniques. Opt Mater 2012;34:716-23.

[39] Choi J, Kim SH, Lee W, Yoon C, Kim JP. Synthesis and Characterization of Thermally Stable Dyes with Improved Optical Properties for Dye-based LCD Color Filters. New J Chem 2012;36:812-8.

Summary

Several series of red, yellow, and green thermally stable dyes with high solubility were synthesized and spin-coated to be applied for dye-based LCD color filters. Their characteristics were investigated compared with those of the commercial pigments and some of them were also applied to the dye-based LCD black matrix. Since the particle size of dyes is smaller than that of pigments, the prepared dye-based color filters had superior optical performance than the pigment-based color filter while it showed a similar thermal resistance to the pigment-based one.

In order to improve the optical performance of red color filters, several perylene dyes were designed and synthesized. Among them, dyes with bulky functional substituents at the bay and terminal positions were highly soluble in cyclohexanone, the industrial solvent currently used in the pigment dispersion method. The prepared color filters with these dyes exhibited superior spectral properties due to the smaller particle size of the dyes. However, their thermal stability varied with the dye structures, and only the dyes mono-substituted at the bay position had sufficient thermal stability.

In order to used as high performance yellow compensating dyes, novel

coronene derivatives were synthesized from N,N'-bis(2,6-diisopropylphenyl)-1,7-dibromoperylene-3,4,9,10-tetracarboxdiimide via a one-step reaction. The suggested synthetic route is the simplest and most economical among the methods to extend the aromatic systems along the short molecular axis of perylene. The synthesized molecules exhibited superior stability and color strength as yellow chromophores. They were characterized by significant hypsochromic shifts of the absorption compared to perylene tetracarboxdiimide and high fluorescence quantum yields.

In order to improve the optical performance of green color filters, several phthalocyanine dyes were designed and synthesized. The solubility, spectral properties, and thermal stability of the prepared six phthalocyanine dyes varied depending on their isomeric structures and core metals. They were dissolved in industrial solvent–binder composites and spin coated with yellow compensating coronene dye into dye-based LCD color filters. The prepared color filters exhibited superior optical properties compared to conventional pigment-based ones due to the fluorescence of coronene dye and less light scattering resulting from the smaller particle size of the phthalocyanine dyes.

Three novel triazatetrabenzcorrole dyes were synthesized via a ring-contraction reaction to be applied as colorants for dye-based color filter and black matrix. The absorption peaks of the synthesized dyes showed a red-

shifted Soret band and a blue-shifted Q-band compared to phthalocyanine dyes, and this can be extremely beneficial when applied for liquid crystal display color filter and black matrix. These dyes exhibited enhanced solubility in the industrial solvents by the introduction of bulky axial substituents. The spin-coated films prepared with these dyes exhibited superior optical and chromatic properties compared to the phthalocyanine-based or pigment-based ones for green color filter, even without the addition of a yellow compensating dye. In addition, they showed satisfactory dielectric properties for the black matrix of color filter on array mode.

Four novel yellow quinophthalone dyes were designed and synthesized in order to examine the influence of aggregation behavior on the optical and thermal properties of liquid crystal display color filters. When the synthesized dyes were spin-coated onto a glass substrate, re-aggregation or migration of the dye molecules were shown in the field emission scanning electron microscopy images after the baking processes. These behaviors of dye molecules can be the main reason for the deterioration of the optical and thermal properties of dye-based color filters, but the degree of deterioration could be reduced by the modification of the dye structures.

초 록

평판디스플레이의 발전에 따라 LCD는 기존의 CRT TV를 대체하고 있으며, 컴퓨터 모니터, 디지털 카메라, 휴대전화 등의 다양한 분야에 사용되어 인간과 기계사이의 인터페이스역할을 하고 있다. LCD로 화상을 표시하는 컴퓨터나 평판 TV 등은 LCD 모듈을 사용하는데 이는 빛을 발하는 backlight unit과 화상을 구현하는 액정 패널(panel)로 구성되어 있으며 컬러필터는 이러한 액정 패널의 한 부분이다. 컬러필터는 backlight의 백색광을 적, 녹, 청 3색의 빛으로 변환하여 이를 적절히 혼합함으로써 컬러를 구현하는 광학부품으로 LCD 모듈 제작에서 가격 비중이 가장 높고 다양한 기술이 집적되어 있어 이를 개발하는 것은 경제적, 기술적으로 매우 큰 의미를 지닌다고 할 수 있겠다. 현재 LCD 컬러필터 제조에 사용되는 색소재료인 안료는 내열성, 내광성, 내화학성 등 내구성은 매우 우수하지만, 입자 거동에 의해 발생하는 광산란에 의하여 휘도와 명암비가 떨어지고 색상이 탁하다는 근본적인 한계점이 있다. 반면 염료는 분자 거동에 의해 색순도, 투과도 등의 분광특성에서는 우수한 장점이 있지만, 열에 대한 안정성이 안료에 비해 떨어지기 때문에 액정 배향막 공정 중에서 RGB 고유의 색상을 유지하기 힘

들며, 내광성, 내화학성 등의 내구성도 약하다는 단점을 갖고 있다. 따라서, 액정디스플레이의 색상 특성을 향상시키기 위한 방안으로 염료를 도입하기 위해서는 근본적인 단점인 내열성, 내광성, 내화학성 등 내구성이 우선적으로 개선되어야 한다. 더불어 컬러레지스트의 주용매에 대한 용해도가 높고 잉크의 기타 조제들과 상용성이 우수한 염료의 개발이 필요하다. 따라서 본 연구에서는 고휘도, 고명암비를 갖는 LCD 컬러필터 제조를 위해 기존의 제작 공정인 포토리소그라피법에 적용 가능한 고성능 염료를 개발하고자 하였다. 개발하고자 하는 염료는 RGB 해당 영역에서 높은 투과율을 나타내고 공정 용매에 높은 용해도를 가지며 컬러필터에서 요구하는 내구성을 만족하여야 한다.

컬러필터 적색 영역에서의 광학 특성 향상을 위해 8종의 perylene 염료들이 합성되었고 그들 중 말단기와 bay 위치에 bulky functional기를 지닌 염료들이 공정 용매인 cyclohexanone에 높은 용해도를 보였다. 또한 이러한 염료들로 spin-coating된 컬러필터들은 안료보다 작은 입자 크기에 힘입어 더 우수한 광학적 특성을 보였다. 그러나 내열 특성은 염료 별 구조에 따라 다른 경향을 나타내었으며 bay position의 한쪽 부분만 치환된 구조들만이 상용 안료에 준하는 안정성을 확보하였다.

고성능 황색 보정 염료 개발을 위해 2종의 신규 coronene과

benzoperylene 염료들이 one-step 반응에 의해 합성되었다. 새로 제안된 합성 경로는 perylene 본체에서 단축 방향으로 aromatic system을 확장하는 매우 간단하고 효율적인 방법이다. 또한 합성된 황색염료들은 일반적인 황색염료들의 한계인 낮은 몰흡광계수와 안정성을 극복하였다. 합성된 염료들은 perylene 전구체에 비해 훨씬 단파장화한 흡수파장과 높은 형광성을 가진다.

컬러필터 녹색 영역에서의 광학 특성 향상을 위해 6종의 phthalocyanine 염료들이 합성되었다. 합성된 녹색 염료들은 이성질체 구조와 중심금속에 따라 용해도, 색특성, 내열성에서 차이를 보인다. 이러한 녹색 염료들에 앞서 개발한 황색 염료들을 조합하여 100% 염료형 LCD 컬러필터를 제조하였으며, 황색염료들의 형광특성과 녹색염료들의 작고 고른 입자크기에 힘입어 상용 안료형 컬러필터에 비해 우수한 광학특성을 나타내었다.

색상 보정이 필요 없는 녹색 컬러필터와 LCD black matrix로의 활용을 위하여 3종의 triazatetrabenzcorrole 염료들이 ring-contraction 반응에 의해 합성되었다. 합성된 염료들은 흡수peak에서 phthalocyanine 전구체에 비하여 장파장화하고 증진된 Soret-band와 단파장화한 Q-band를 보이며 이는 녹색 컬러필터와 black matrix로 활용되기에 매우 이상적이다. 또한 이 염료들은 중심금속에 도입된 bulky axial 치환기로 인하여 공정 용매에 더욱 향상된

용해도를 보인다. 이 염료들로 spin-coating된 컬러필터는 phthalocyanine 염료형 컬러필터에 비해서도 광학특성이 우수하며 black matrix에 활용될 시 만족스러운 낮은 유전율을 보인다.

염료분자의 aggregation 거동이 LCD 컬러필터의 광학적, 내열적 특성에 미치는 영향을 분석하기 위해서 4종의 신규 quinophthalone 염료들이 합성되었다. 합성된 염료들로 제조한 컬러필터를 반복해서 baking 처리하면 표면에서 재응집되며 균일성이 깨지는 현상이 FE-SEM으로 관측되었다. 이러한 재응집 현상은 염료형 컬러필터의 광학적, 내열적 특성을 저하시키는 주요 원인이 되나 염료구조의 개선을 통하여 저하 정도를 최소화할 수 있음을 나타내었다.

주요어: 액정디스플레이(LCD), 컬러필터, 블랙 매트릭스, 광식각 공정, 퍼릴렌 염료, 코로닌 염료, 프탈로시아닌 염료, 트리아자테트라벤즈코롤 염료, 퀴노프탈론 염료, 투과도, 색 재현범위, 명암비, 내열성, 분자간 회합

학번: 2008-20692

List of Publications

Original Papers

1. **Jun Choi**, Chun Sakong, Jae-Hong Choi, Chun Yoon, Jae Pil Kim, "Synthesis and characterization of some perylene dyes for dye-based LCD color filters", *Dyes and Pigments*, **2011**, 90, 82-88.

2. Woosung Lee, Sim Bum Yuk, **Jun Choi**, Dong Hyun Jung, Seung-Hoon Choi, Jongseung Park, Jae Pil Kim, "Synthesis and characterization of solubility enhanced metal-free phthalocyanines for liquid crystal display black matrix of low dielectric constant", *Dyes and Pigments*, **2012**, 92, 942-948.

3. **Jun Choi**, Woosung Lee, Chun Sakong, Sim Bum Yuk, Jong S. Park, Jae Pil Kim, "Facile synthesis and characterization of novel coronene chromophores and their application to LCD color filters", *Dyes and Pigments*, **2012**, 94, 34-39.

4. **Jun Choi**, Se Hun Kim (equally contributed), Woosung Lee, Chun Yoon, Jae Pil Kim, "Synthesis and characterization of thermally stable dyes with improved optical properties for dye-based LCD color filters", *New J. Chem.*, **2012**, 36, 812-818.

5. **Jun Choi**, Woosung Lee, Jin Woong Namgoong, Tae-Min Kim, Jae Pil Kim, "Synthesis and characterization of novel triazatetrabenzcorrole dyes for LCD color filter and black matrix", *Dyes and Pigments*, **2013**, 99, 357-365.

6. **Jun Choi**, Se Hun Kim, Woosung Lee, Jae Bok Chang, Jin Woong Namgoong, Young Hoon Kim, Sang Hun Han, Jae Pil Kim, "The influence of aggregation behavior of novel quinophthalone dyes on optical and thermal properties of LCD color filters", *Dyes and Pigments*, **2014**, 101, 186-195.

7. Woosung Lee, Sim Bum Yuk, **Jun Choi**, Hae Jung Kim, Hyun Woo Kim, Se Hun Kim, Boeun Kim, Min Jae Ko, Jae Pil Kim, "The effects of the number of anchoring groups and *N*-substitution on the performance of phenoxazine dyes in dye-sensitized solar cells", *Dyes and Pigments*, **2014**, 102, 13-21.

8. Woosung Lee, **Jun Choi**, Se Hun Kim, Jong S. Park, Jae Pil Kim, "Analysis and characterization of dye-based black matrix film of low dielectric constant containing phthalocyanine and perylene dyes", *Journal of Nanoscience and Nanotechnology*, accepted.

9. Woosung Lee, **Jun Choi**, Jin Woong Namgoong, Se Hun Kim, Jae Pil Kim, "Effects of five-membered heterocyclic bridges and ethoxyphenyl substitution on the performance of phenoxazine-based dye-sensitized solar cells", *Dyes and Pigments*, accepted.

10. Se Hun Kim, **Jun Choi** (equally contributed), Chun Sakong, Woosung Lee, Boeun Kim, Min Jae Ko, Dong Hoe Kim, Kuk Sun Hong, Jae Pil Kim, "The effect of the number, position, and shape of methoxy groups on the performance of triphenylamine donors in dye-sensitized solar cells", submitted.

감사의 글

서울대학교 재료공학부 박사과정을 졸업하기까지 부족하나마 오늘날의 제가 있게 해주신 저의 부모님과 하나밖에 없는 동생, 항상 제 곁에서 힘이 되어준 올해 결혼을 앞둔 여자친구에게 이 작은 결실을 바칩니다.

또한 저를 6년 동안 지도해주신 김재필 교수님과, 많은 조언 및 도움을 아끼지 않은 연구실 선후배님들께 감사의 마음을 전합니다.

2014년 1월

최 준